University Medical School of Naples
"Federico II"

Department of Neuroscience, Reproductive and Odontostomatologic Sciences

Director: Prof. Lucio Annunziato

Spatial and temporal patterns of postsynaptic genes and proteins expression by multiple receptors targeting agents: unraveling the impact of multitargeting approach on dopamine-glutamate mediated synaptic plasticity

Doctoral candidate: Dr. Carmine Tomasetti

PhD Program in Neuroscience, XXVI Cycle
Doctoral School of Molecular Medicine

Tutor:
Prof. Andrea de Bartolomeis

Coordinator:
Prof. Lucio Annunziato

Academic Year: 2012-2013

Introduction.

Schizophrenia is a complex disorder affecting nearly 1% of the general population. A large amount of evidence suggests that schizophrenia is caused by aberrant synaptic plasticity and metaplasticity. Perturbation of regular dendritic spines architecture and function has been described in the disease [1,2] [3]. Multiple neurotransmitter systems have been implicated in schizophrenia pathophysiology, and strong evidence points out abnormalities in dopamine, glutamate, and serotonin neurotransmission [4,5]. Signaling pathways activated by these neurotransmitters converge on the postsynaptic density (PSD), which is considered as a structural and functional multi-protein crossroad. PSD is an electron-dense thickening localized under postsynaptic membranes, which comprises several hundred proteins and particularly characterizes large excitatory glutamatergic synapses [6]. PSD proteins are distributed in highly organized macromolecular complexes that process, integrate, and converge synaptic signals to the nucleus [7]. Overall, PSD proteins are involved in synaptic plasticity and dendritic spines architecture. Rearrangements in PSD protein multimers at synaptic spines, occurring with precise stimulus-related spatiotemporal patterns, are currently supposed to underlie synaptic plasticity-related events, such as long-term potentiation (LTP) and long term depression (LTD) [8,9].

According to the biological functions of PSD in humans, a recent study demonstrated that mutations in 199 human PSD genes (the 14% of all PSD genes) are implicated in more than two hundred diseases [10]. The 50% of these diseases are primary nervous system disorders, including neurological, psychiatric, and developmental disorders [10]. Moreover, a large part of those mutations may principally affect cognitive and learning processes, as well as emotion/affective behaviors and social interaction. Therefore, according to this view, emerging evidence is accumulating that implicates PSD proteins

dysfunctions in major psychiatric disorders in which cognitive/behavioral and social processes are impaired, such as schizophrenia and autism spectrum disorders. Based on the NMDA receptor hypofunction hypothesis of schizophrenia [11], several studies have found abnormalities in PSD proteins in brain regions where NMDA receptors are localized, as well as gene-association studies have revealed increased risk for schizophrenia in patients with mutations in genes affecting NMDA functions (for a review, see [12]). Moreover, several molecular defects in PSD components and in PSD-related proteins have been found in postmortem brains of schizophrenia patients, mostly in regions implicated in the pathophysiology of the disease [13,14]. Thus, PSD alterations may contribute to the synaptic derangements in schizophrenia [9]. Consistent with the putative role of PSD proteins in schizophrenia, several studies have implicated glutamatergic PSD components in the molecular mechanisms of action of antipsychotic drugs. Though primarily acting on dopamine transmission, evidence exists that antipsychotics may also modulate glutamate-related targets, in particular the N-Methyl-D-Aspartate receptor (NMDAR)-interacting molecules of the PSD [15,16]. Indeed, different antipsychotic drugs have been shown to modulate glutamate-related molecules in PSD [17-19,15,20,21]. Therefore, PSD proteins have been proposed as a target for antipsychotic action [22]. Antipsychotics may affect glutamatergic neurotransmission at multiple levels, and they may regulate dendritic spines formation and synaptogenesis [23,24], as well as the expression, trafficking, and functioning of PSD-related molecules [20,25-27].

I. Dopamine and glutamate circuitries nexus: a pathophysiology integrated model of psychosis

Dopamine and glutamate systems are the most important neurotransmission circuitries implicated in the pathogenesis of psychosis. Their manifold interconnections, even with the other neurotransmission systems, control cognitive, behavioral and motor processes. Thus, from the loss of balance in the complex interplay among these systems could originate the variety of expression of psychotic disorders, such as schizophrenia or bipolar disorder.

In specific brain areas, which have been implicated in the pathophysiology of psychosis (i.e prefrontal cortex, corpus striatum, and nucleus accumbens), dopamine and glutamate signaling pathways converge on responsive neural populations, such as the striatal medium-sized spiny GABAergic neurons (MSNs) or the cortical GABAergic interneurons, where they interact at postsynaptic level. Deciphering the molecular mechanisms that control the postsynaptic dopamine-glutamate interplay may be crucial to our understanding of the dysfunctions implicated in psychosis, as well as for the development of new therapeutic strategies.

The diverse actions of dopamine are mediated by at least five distinct subtypes of dopamine receptors (DARs), which belong to the G-proteins coupled receptors (GPCRs). Two D1-like receptor subtypes (D1 and D5 receptors) couple to the G protein G_s and activate adenylyl cyclase. The D2-like receptors (D2, D3, and D4 receptors) inhibit adenylyl cyclase and activate K^+ channels [28].

On the other hand, glutamate functions are mediated by both ionotropic and metabotropic receptors. The widely distributed ionotropic glutamate receptors are ion channels activated by glutamate and may be divided in subtypes according to postsynaptic currents: N-Methyl-D-Aspartate Receptors (NMDARs), 2-amino-3-(5-

methyl-3-oxo-1,2-oxazol-4-yl)propanoic acid receptors (AMPARs) and kainate receptors (reviewed in [29]).

Metabotropic Glutamate Receptors (mGlu receptors) belong to the seven transmembrane passages receptors superfamily and exert their cellular effects by activating G-protein-dependent pathways [30,31]. According to their transductional pathways, mGlu Receptors can be divided in three groups: group I (mGlu1 and mGlu5 receptors subtypes), whose stimulation leads to Phospholipase C – inositol 1,4,5-trisphosphate (PLC-IP3)-Ca^{2+} pathway activation and increases intracellular calcium; group II (mGlu2 and mGlu3 receptors subtypes) and group III (mGlu4, mGlu6, mGlu7, and mGlu8 receptors subtypes), whose stimulation decreases intracellular calcium concentrations by inhibiting adenylyl cyclase.

Both dopamine and glutamate receptors, indeed, may impact calcium-dependent intracellular signals (reviewed in [32-34]) that are key triggers of the molecular mechanisms underpinning synaptic plasticity, which include both activity dependent gene transcription and long-term neural adaptations [35].

Amongst the wide variety of postsynaptic effectors that control calcium intracellular signals are the postsynaptic density (PSD) scaffolding proteins, which play a crucial role in the complex postsynaptic architecture of excitatory synapses (for a review, see [36]), where the most part of signal transduction events take part that lead to the dopamine-glutamate-mediated synaptic plasticity.

I.1. Dopamine-glutamate hypothesis of psychosis

Over thirty years in psychotic disorders basic investigation have moved the attention from unidirectional models of pathogenesis to multidirectional and integrated ones.

Abnormal dopamine and glutamate functions, as well as abnormal development of dopaminergic and glutamatergic neurons, have been implicated in the pathophysiology of the major psychotic disorders, such as schizophrenia and bipolar disorder [37-39,22,40,41], but the underlying mechanisms are still elusive. Both prefrontal cortex (PFC) and striatum—which have been reported as dysfunctional in psychosis—receive dopaminergic and glutamatergic inputs converging on specific neural populations. The MSNs of striatum, indeed, receive dopaminergic projections from the substantia nigra and ventral tegmental area (VTA) of the midbrain, as well as they receive glutamatergic projections from the PFC [42]. On the other hand, dopamine afferents arising from VTA and glutamate afferents arising from hippocampus, thalamus, amygdala and other cortical areas commonly target both the pyramidal neurons and the GABA interneurons of prefrontal cortex (reviewed in [43]).

Several studies demonstrated that manipulations of both dopamine and glutamate systems may mimic several symptoms of psychotic disorders [44-46]. For instance, drugs affecting glutamatergic system may reproduce negative and cognitive symptoms of schizophrenia, whereas dopamine agonists principally reproduce certain positive symptoms, such as delusions and hallucinations [45].

Based on the evidence that NMDAR-blocking drugs (such as phencyclidine) could induce psychotic manifestations by impacting dopamine neurotransmission, some authors have proposed that a NMDAR dysfunction could be a primary step in the pathogenesis of psychotic disorders, leading to a subsequent—or concurrent—dopaminergic dysfunction (Figure 1) [47-49].

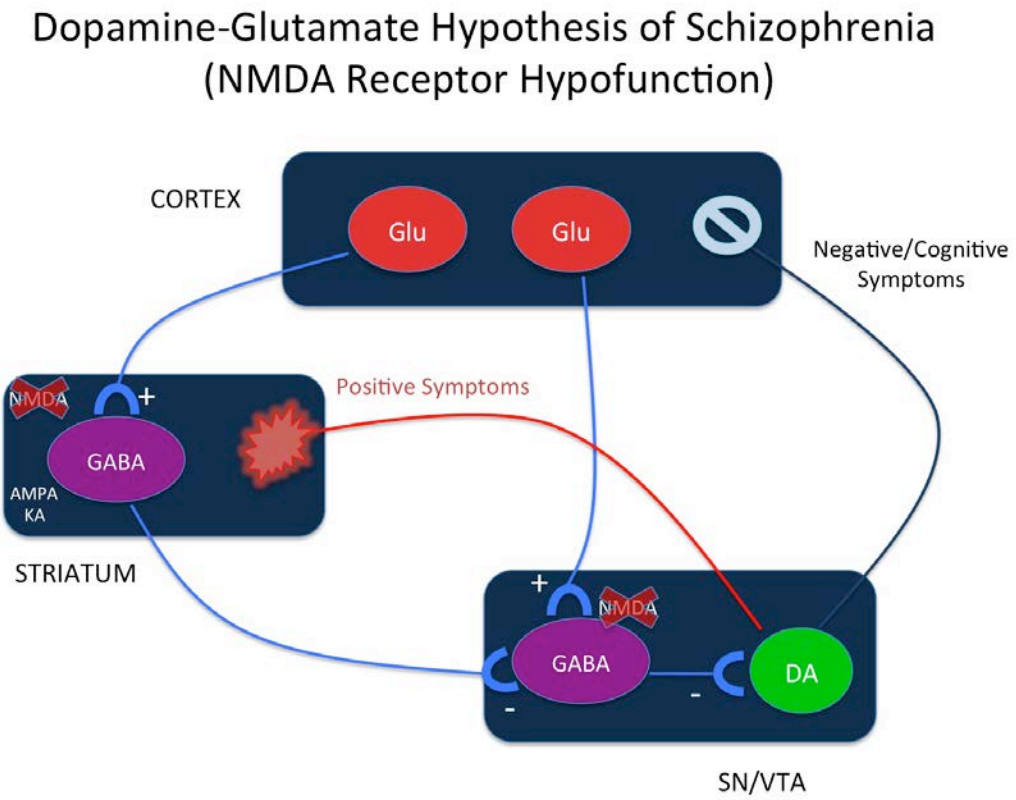

Figure 1. NMDA receptor hypofunction hypothesis of schizophrenia.
NMDA receptors may be pathologically hypofunctional in schizophrenia. Glutamate projections from cortex to VTA normally control mesolimbic dopamine release by tonic inhibition. The hypoactivity of NMDA receptors on VTA neurons would cause mesolimbic dopamine hyperactivity, which is correlated to positive symptoms. Moreover, cortical glutamaetrgic projections also normally boost dopamine mesocortical secretion, via intermediate GABA striatal interneurons. The NMDA dysfunction would reduce the tonic mesocortical dopoamine release, thereby determining cortical dopamine hypoactivity and subsequent negative and cognitive symptoms of schizophrenia.

I.2. Dopamine and glutamate signaling pathways converge on responsive GABAergic neurons in both cortex and striatum

Several studies demonstrated that dopamine and glutamate receptors co-localize on the same neurons in PFC and striatum, thus posing the basis for their molecular postsynaptic interactions. In the PFC, glutamatergic and dopaminergic afferents have been described to converge on the same dendritic spines of excitatory pyramidal neurons, principally in layer V, forming the so-called “synaptic triads” [50]. D1-like dopamine receptors have been shown to localize, with prevalent postsynaptic distribution, at dendritic synapses, [51] where also D2-like dopamine receptors are

located, the D2 receptor subtypes (D2Rs) having a preferential localization at layer V, whereas the D4 receptor subtypes (D4Rs) being broadly distributed [52]. NMDARs and dopamine receptors (DARs) have been described to co-localize in the same postsynaptic spines, providing the base for their subcellular interaction at synapses (Fig. 1) [53]. The dendritic spines of PFC pyramidal neurons are also enriched with group I and group II mGlu receptors, which have essential roles both in controlling dopamine release as well as in modulating glutamate influences [54-56]. Nonetheless, both dopamine and glutamate receptors have been reported to co-distribute in GABAergic cortical interneurons [52,54,57].

In the striatum, D1-like receptors localize mostly on GABAergic MSNs (i.e. the striatal output neurons), preferentially at postsynaptic level, whereas D2-like receptors are located both at presynaptic level—acting as autoreceptors on dopaminergic terminals and as regulators on glutamatergic afferents—and at postsynaptic level on MSNs (for a review, see [58]). Ionotropic glutamate receptors (NMDARs, AMPARs and kainate receptors) largely co-localize with dopamine receptors in striatum, both at presynaptic level on dopaminergic and glutamatergic afferents and at postsynaptic level on MSNs, where they control excitatory currents [59-62]. On the other hand, there is a growing interest for metabotropic glutamate receptors distribution in the striatum in recent years, because of their close interaction with dopamine receptors. The two group I mGlu receptors, indeed, have different localizations in dopaminergic striatal synapses, the mGlu1a receptors being primarily presynaptic with regulatory effects, whereas the mGlu5 receptors being essentially postsynaptic with prominent synaptic plasticity functions [63]. Moreover, mGlu1 receptors seem to segregate principally in striatonigral MSNs, which are enriched with D1-like dopamine receptors (the “direct” pathway), whereas mGlu5 receptors are mostly located on striatopallidal MSNs, which are characteristically enriched with D2-like receptors (the “indirect” pathway) [64]. Group

II and III mGlu receptors share no less importat roles than group I mGlu receptors. They are, indeed, broadly distributed in dopaminergic and glutamatergic striatal terminals, and contribute to regulate dopamine receptors function. Nonetheless, they are largely present on GABAergic and cholinergic striatal interneurons [32].

Therefore, glutamate and dopamine systems interact at multiple levels and their signaling interplays both in cortical and subcortical structures, thus generating an entangled modulatory system that likely is the neuroanatomical substrate for the pathophysiology of psychotic disorders (Figure 2). However, the reciprocal influence of dopamine and glutamate signaling in the neurons where their transductional pathways respectively interact relies on a complex interconnection of intracellular calcium-dependent networks, whose molecular components are still largely elusive.

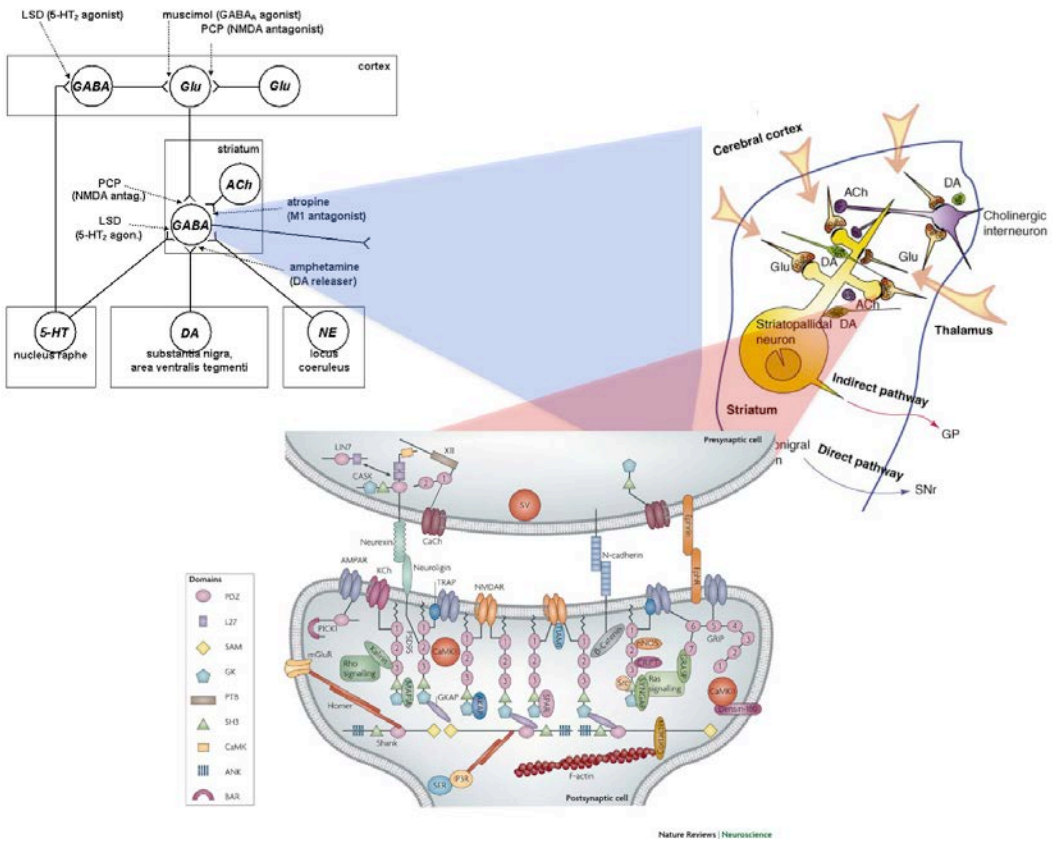

Figure 2. GABA interneurons elaborate multiple neurotransmission signals through a complex subsynaptic ultrastructure called Postsynaptic Density.

II. Dopamine-glutamate post-synaptic crossroads: the calcium-dependent synaptic plasticity network

As aforementioned, in specific cerebral regions, such as prefrontal cortex and corpus striatum, dopamine and glutamate projections converge at GABAergic responsive neurons. These neurons integrate, through sophisticated intracellular mechanisms, the information originated by the activation of dopamine and glutamate receptors. Thus, dopamine and glutamate interact in PFC and striatum in order to influence neural excitability and to promote synaptic plasticity (Figure 3). The complex modulation of Ca^{2+} intracellular levels as well as the activation of calcium-dependent signaling molecules represent the key substrates for the establishment of synaptic plasticity induced by dopamine-glutamate interplay in both PFC and striatum [65,66]. Indeed, dopamine D1 and D2 receptors have opposite effects on excitability and calcium levels in neurons. D1 receptors (D1Rs) activate adenylyl cyclase and promote cyclic Adenosine Monophosphate (cAMP)-dependent protein kinase A (PKA) mechanisms, such as calcium-channels activation, whereas D2Rs reduce cAMP formation and PKA activity, thus having the final effect of inhibiting neural excitability (extensively reviewed in [67]). On the other hand, the stimulation of NMDARs leads to direct and indirect activation Ca^{2+}-dependent signaling proteins—such as the calcium-calmodulin-dependent kinase (CaMK) and the PKA—which are essential to synaptic rearrangements [68]. Likewise, mGlu receptors promote calcium-dependent processes through the PLC-IP3 pathway, which modulates intracellular calcium levels (reviewed in [32]).

Besides the differences existing between the molecular mechanisms that underlie calcium-dependent synaptic plasticity in cortical and striatal areas, several studies agree that dopamine signaling is critical to modulate glutamate-induced calcium oscillations

in order to promote a correct set up of synaptic plasticity mechanisms, such as in long-term depression (LTD) and long-term potentiation (LTP) [69,70].

Although a large part of the signaling cascades involved in calcium-dependent synaptic modulation of cortical and striatal dopamine-glutamate synapses have been extensively studied (e.g. adenylyl cyclase, cAMP, PKA, PLC-IP3 etc.), a great deal of evidence suggests a role for PSD scaffolding proteins, which appear as key determinants of the cross-talk between dopamine and glutamate postsynaptic pathways.

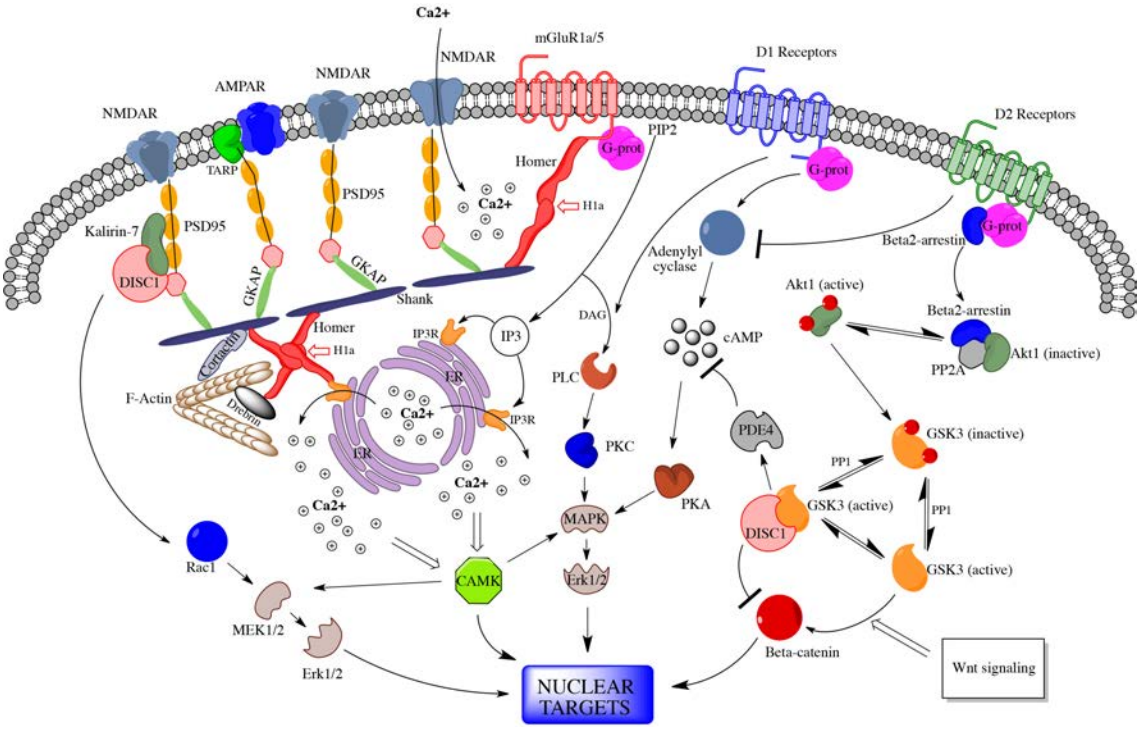

Figure 3. Complex interactions among transductional pathways in the PSD. PSD proteins elaborate and integrate multiple transductional pathways starting at different membrane receptors (i.e. glutamate, dopamine). Scaffolding proteins (Homer, Shank, PSD-95) provide physical connections among different receptors, such as ionotropic and metabotropic glutamate receptors, as well as they link these receptors to intracellular calcium stores. Dopamine receptors activate transductional pathways that tightly intermingle with glutamatergic ones, through the action of key PSD proteins, such as GSK3, which may participates in the elaboration of diverse signals (dopamine, glutamate, Wnt) and regulates neuronal survival and differentiation. All these transductional pathways converge in the end on appropriate nuclear targets via specific effectors, such as CaMK, MAPKs or Erk, in order to fine modulate long-term activity dependent neuronal rearrangements. *NMDAR*, N-methyl-D-aspartate glutamate receptor; *AMPAR*, α-amino-3-hydroxy-5-methyl-4-isoxazolepropionic acid glutamate receptor; *mGluR1a/5*, metabotropic glutamate receptor type 1a/5; *TARP*, transmembrane AMPA receptors regulating protein or stargazin; *PSD-95*, postsynaptic density protein 95kD; *DISC1*, disrupted in schizophrenia 1; *GSK3*, glycogen synthase kinase 3; *PDE4,* phosphodiesterase 4; *GKAP*, guanylate kinase associated protein; *H1a*, Homer1a immediate-early inducible protein; *PIP2*, phosphatydilinositol bisphosphate; *DAG*, diacylglycerol; *IP3*, inositol 1,4,5-trisphosphate; *cAMP*, cyclic adenosine monophosphate; *ER*, endoplasmic reticulum; *PLC*, phospholipase C; *PKC*, protein kinase C; *PKA*, protein kinase A; *CAMK*, calcium-calmodulin regulated kinase; *MAPKs*, mitogen-activated protein kinases; *Erk*, extracellular signal-regulated kinase; *MEK*, MAPK/Erk kinase; *Rac1*, Ras-related C3 botulinum toxin substrate 1.

II.1. Post-Synaptic Density Scaffolding Proteins

Post-Synaptic Density (PSD) is a specialized structure localized under the postsynaptic membrane at excitatory synapses with an approximate thickness of 30-60 nm and a diameter of 200-500 nm, and a complex structural anatomy [71]. Many proteins, such as ionotropic and metabotropic receptors, receptors-interacting proteins, enzymes, scaffolding and cytoskeletal proteins, constitute the complex lattice of the PSD [72]. PSD represents a powerful "triage center" where every message reaching the synapse is received, elaborated and routed to its own final destination. PSD proteins, indeed, seem to be involved in multiple processes, such as synaptic development and plasticity [73,74] and control of transductional pathways [75]. Thus, according to several observations, each molecular process putatively involved in postsynaptic dopamine-glutamate interplay should take necessarily place in the PSD, and thereby is controlled by PSD proteins [76]. Many PSD proteins (such as the dopamine- and adenosine 3',5' monophosphate (cAMP)-regulated phosphoprotein pf 32 kD (DARPP-32), CaMKII, Neuronal Calcium Sensor-1 (NCS-1), and calcyon) have essential roles in controlling and routing both dopamine and glutamate signalings. However, recent attention is focused on the so-called "scaffolding" proteins, which constitute an eclectic class of PSD proteins with multiple functions (Figure 4) [72].

A large number of studies pointed out the possible role of these proteins in the dopamine-glutamate intracellular crosslinking, and their implication in the pathophysiology of neuropsychiatric disorders originating from dysfunctions in these intricate connections [7,77-79]. Moreover, PSD scaffolding proteins seem to be essential for calcium-dependent plasticity at excitatory synapses [80].

Hereafter, we will describe the main PSD scaffolding proteins that have been implicated in dopamine-glutamate calcium-dependent plasticity, because of their direct connection with glutamate receptor functions in dopaminergic synapses: Homer, PSD95 and Shank.

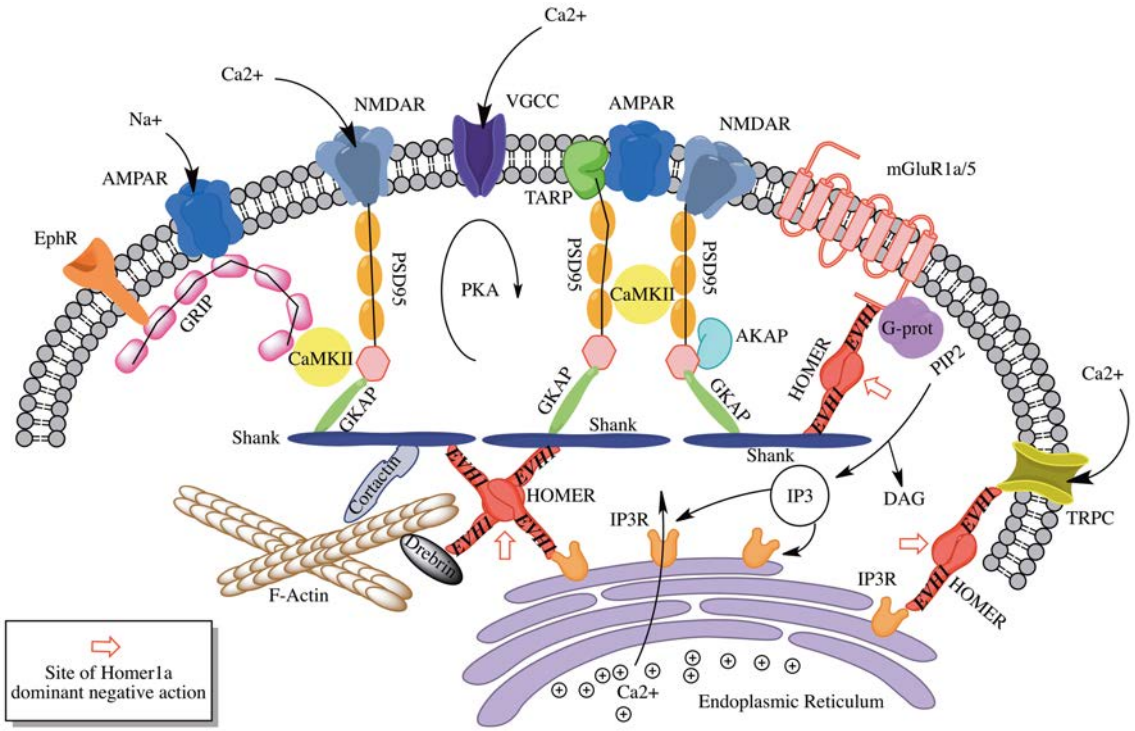

Figure 4. Postsynaptic scaffolding proteins dynamically organize calcium signaling network in neurons. Through multiple protein-protein interactions Homer long isoforms, PSD95 and Shank may crosslink transduction pathways starting at both ionotropic (*NMDAR, AMPAR*) and metabotropic (*mGlu1a/5*) glutamate receptors. Scaffolding proteins also provide complex interactions between membrane cation channels—such as voltage-gated calcium channels (VGCC) and transient receptor cation channels (*TRPC*)—with intracellular calcium stores. This network provides the fine-tuning of intracellular calcium signaling. Homer1a, the inducible short form of Homer1 proteins, may be induced by several stimuli. It acts as dominant negative by disassembling long Homers clusters, thereby rearranging the synaptic architecture. Thus, scaffolding proteins may reorganize postsynaptic structure in response to synaptic activity in order to establish short- and long-term neuroplastic changes. *EphR*=Ephrin receptor; *GRIP*=glutamate receptor interacting protein; *GKAP*=guanylate kinase associated protein; *CaMKII*=calcium/calmodulin dependent kinase II; *PKA*=protein kinase A; *TARP*=transmembrane AMPA receptors regulating protein; *IP3*=inositol 1,4,5-trisphosphate; *IP3R*= IP3 receptor; *DAG*=diacylglicerol; *PIP2*=phosphatidyl-inositol bisphosphate.

II.1.a. Homer family of proteins: multimodal adaptors at excitatory synapses

Homer proteins belong to the class of PSD scaffolding proteins, being mainly localized at glutamatergic excitatory synapses [81].

The Homer family comprises three principal members (Homer1, 2 and 3) and several isoforms and splicing variants, encoded by 12 known genes [82,83].

The multiple isoforms of Homer may be grouped in “long” (Homer1b/c, 2a/b, 3) and “short” proteins (Homer1a and Ania-3), according to the presence of a carboxy-terminal coiled-coil tail, which is absent in the short isoforms (for a review see: [36]).

Differently from long isoforms, which are constitutively expressed [82,84,83], Homer1a and Ania-3 are expressed in an immediate-early gene (IEG)-like fashion and induced by several synaptic activating stimuli [81,85].

Homer long isoforms may self-associate in multimeric complexes [86] by means of their coiled-coil terminals. Conversely, Homer1a and Ania-3 cannot multimerize and, when induced, they provide to disrupt the other complexes, acting as "dominant negative" thereby influencing synaptic plasticity [87-89].

Homer proteins can interact with many PSD proteins (Fig. 2), such as mGlu receptors, IP3 receptors, ryanodine receptors, transient receptor potential channels (TRPC), cytoskeletal proteins and the NMDAR-linked protein Shank [81,90,91,82,92,93,83,94]. Moreover, Homer long isoforms multimerization is involved in the control of glutamate-mediated postsynaptic adjustments [95,96] and in glutamatergic synapses development [97].

Conversely, Homer1a is induced by stimuli that modify the synaptic architecture, such as seizure, neurodevelopment, long-term potentiation, psychostimulant drugs [85,73,98,99].

The multimodal adaptor properties of Homer proteins implicate them in the multiple calcium-dependent processes underpinning synaptic plasticity at excitatory synapses [100]. Indeed, Homer proteins binding may allow the cross-talk between intracellular proteins that belong to the Ca^{2+} signaling network, comprising both ionotropic and metabotropic glutamate receptors as well as Ca^{2+}-modulators at intracellular stores, such as inositol 1,4,5-trisphosphate receptors (IP3Rs) and Ryanodine receptors (RyRs), in addition to calcium plasmamembrane channels [101-103]. Through this action of clustering, scaffolding and trafficking the most part of the core molecules belonging to the Ca^{2+}-dependent intracellular network, Homer proteins have a crucial role in

transducing extracellular stimuli to the nucleus as well as in producing concerted postsynaptic temporal and spatial patterns for efficient functional outputs (see [104]). Finally, recent evidence suggests that Homer long isoforms are implicated in an additional Ca^{2+}-independent pathway, which is triggered by the combined activation of NMDARs and mGlu receptors and involves the crosstalk between the NMDA receptor-associated protein PSD-95 and the mGlu1/5 receptors-associated protein Homer1b/c [105]. Therefore, given their multifunctional adaptor functions, it is conceivable that Homer proteins may have a significant role in the intracellular cross-linking between dopamine and glutamate pathways.

II.1.b. PSD95: the main PDZ scaffolding protein

PSD95 belongs to the membrane-associated guanylate kinases (MAGUKs), which are modular proteins composed of three N-terminal PDZ domains, followed by a src homology 3 (SH3) domain and a guanylate kinase (GK)-like region. The PDZ domain of PSD95 allows interaction with specific C-terminal Glu-(Ser/Thr)-Xxx-(Val/Ile) recognition motifs, which allow coupling of PSD95 with other signaling molecules (Fig. 2), such as Shank [106], as well as with both G-protein coupled receptors [74] and NMDA ionotropic glutamate receptors [107]. PSD95 interactions mediate stabilization and activity-dependent trafficking of NMDARs [108]. Indeed, early studies reported that, although showing a normal NMDARs localization, PSD95 mutant mice exhibit deficits in LTP, LTD and spatial learning, suggesting that PSD95 may play a crucial role in linking NMDARs to downstream effectors [109].

PSD95 is also indirectly linked to AMPARs though the interaction with another PSD protein, stargazin [110]. The bidirectional interconnection between PSD95 and stargazin mediates AMPARs targeting to synaptic membrane. Thus, it is possible that a

functional linking between NMDARs and AMPARs may occur through PSD95-stargazin complex.

PSD95 may target the phosphokinase A (PKA) to AMPARs via the interaction with the A-kinase anchoring protein (AKAP79). This linkage is necessary for the modulation of AMPA currents by PKA phosphorylation [111]. Moreover, PSD95 has been demonstrated to control also AMPARs surface expression through its own palmitoylation cycles [112].

All the latest studies agree that PSD95 plays a central role in the control of the Ca^{2+}-dependent network that is downstream of glutamate receptors [113,114], as well as in the signaling of Ca^{2+} and K+ channels that are responsible for synaptic excitability [115].

II.1.c. ProSAP/Shank family of proteins: major docking stations at PSD

The three members of the ProSAP/Shank family play a master role at the excitatory synapses. Shank proteins possess multiple domains that allow protein-protein interactions, such as ankyrin repeats, SH3, PDZ and SAM (sterile alpha motif) [116]. When Shank is efficiently targeted at synaptic sites through a PDZ-dependent mechanism, it may promote a regulation of synaptic shape and functions, via the interaction with Homer proteins [117]. Moreover, Shank proteins may bridge NMDARs and mGlu receptors via the interaction with GKAP (guanylate kinase-associated protein), and PSD95, thus likely integrating the signaling pathways starting at those two receptors (for review, see [9].

The docking functions of Shank may putatively allow an entangled coordination of calcium intracellular signaling by glutamate ionotropic and metabotropic receptors (Fig. 2), through the formation of a platform for the assembly of the other PSD protein

complexes [118]. Recent evidence, indeed, suggests that the huge homomultimeric sheets formed by Shank proteins may cluster with IP3Rs via Homer interaction, thereby controlling Ca^{2+} intracellular homeostasis [101,88].

III. Targeting the dopamine-glutamate interaction: role of PSD scaffold proteins in antipsychotic mechanisms of action, focus on Homer family

Among the wide range of molecular dysfunctions reported in psychosis, the unifying element seems to be the pervasive underlying calcium signaling abnormalities [119,120]. Dysfunctions in calcium homeostasis largely depends upon disruption of intracellular networks that provide connections among the principal signaling pathways implicated in schizophrenia—i.e. dopamine and glutamate. A major role in these interactions is played by PSD scaffolding proteins, which have been extensively implicated in the pathophysiology of psychotic disorders as well as in the mechanisms of action of antipsychotics, and that could represent valuable candidates for new therapeutic strategies based on a dopamine-glutamate integrated targeting.
Particular attention is being payed to Homer family proteins, which perform master organizing functions in the PSD network, by interconnecting the downstream pathways starting at both ionotropic and metabotropic glutamate receptors, as well as by linking these pathways to the intracellular machinery that controls Ca^{2+} oscillations.

III.1. *Homer proteins modulation by dopaminergic and glutamatergic stimuli*

Several studies have demonstrated that the expression of transcript encoding for both long and short Homer isoforms may be affected by psychotomimetic drugs modulating

either dopaminergic or glutamatergic receptors (Figure 5). Both acute methamphetamine and cocaine administration may induce *Homer1a* mRNA in the neocortex of saline-pretreated rats [121]. Also, increased long Homer protein amount in the nucleus accumbens has been described after acute cocaine administration [122]. Consistent with the role of Homers as scaffold proteins at the crossroad of dopamine and glutamate system, drugs acting at NMDARs, such as the non-competitive inhibitor PCP, may increase *Homer1a* mRNA expression in rat PFC prelimbic region and in primary auditory cortex two hours after treatment, as well as it may decrease *Homer1a* mRNA expression in retrosplenial cortex and dentate gyrus twenty-four hours after treatment [123]. Similarly to PCP, the NMDAR non-competitive antagonist ketamine may induce *Homer1a* mRNA in the ventral striatum and in the core and the shell of the nucleus accumbens when acutely administered at subanaesthetic doses [124]. Both PCP and ketamine are NMDAR non-competitive antagonists known to cause psychotic symptoms in humans and to exacerbate psychotic symptoms in schizophrenia patients [125,126]. Moreover, PCP and ketamine are believed to mimic NMDARs hypofunction (NRH), which is considered a valuable and heuristic pharmacological model of schizophrenic symptoms [14].

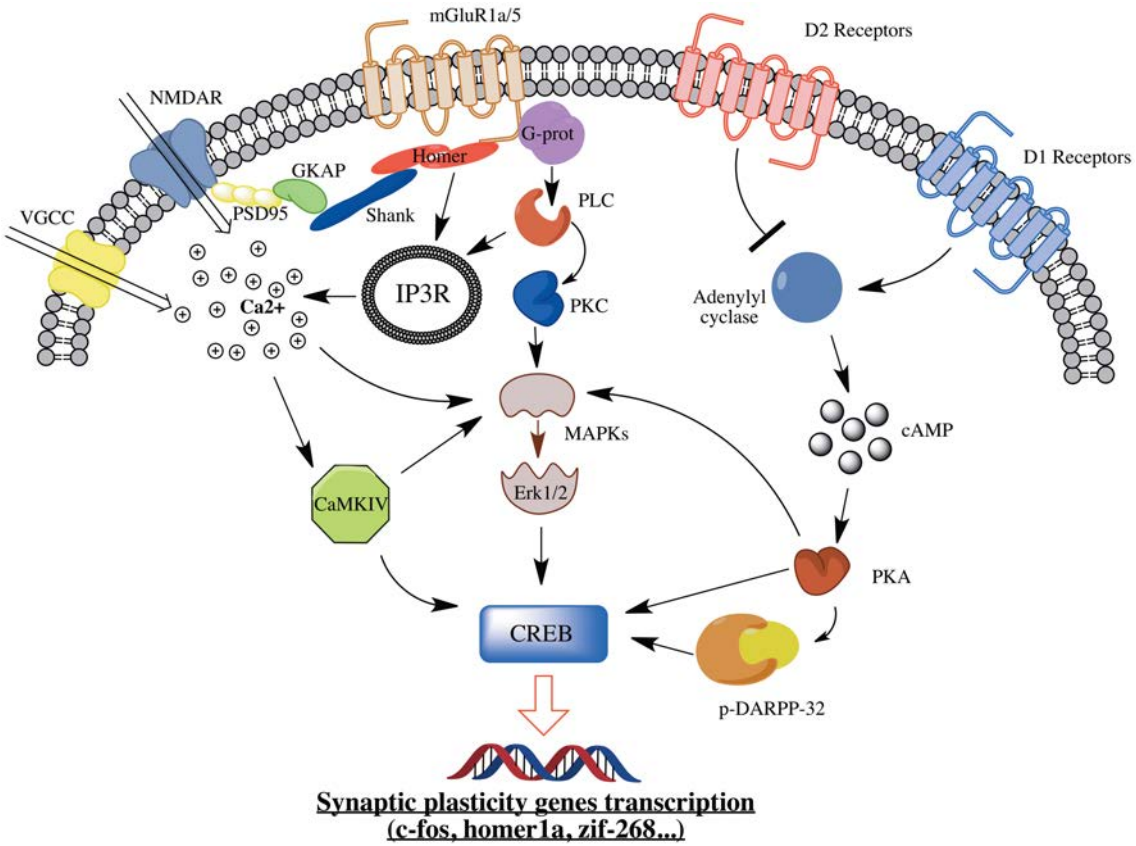

Figure 5. Dopamine-glutamate postsynaptic interaction. Dopamine and glutamate receptors may activate calcium-dependent and calcium-independent pathways that interact at multiple levels in the postsynaptic density. Postsynaptic scaffolding proteins (Homer, Shank, PSD95) represent key components of this cross-talk, as well as they may modulate both calcium-dependent and calcium-independent downstream cascades. The transductional pathways converge on effector molecules (*MAPK-Erk1/2-CREB*) that activate the transcription of genes responsible for synaptic plasticity (e.g *c-fos*, *homer1a*, *zif-268*). *GKAP*=guanylate kinase associated protein; *CaMKIV*=calcium/calmodulin dependent kinase IV; *PKA*=protein kinase A; *PLC*=phospholipase C; *PKC*=protein kinase C; *IP3R*=inositol 1,4,5-trisphosphate receptor; *MAPK*=mitogen-activated kinases; *Erk1/2*=extracellular signal-regulated kinase; *cAMP*=cyclic adenosine monophosphate; *pDARPP-32*=dopamine- and cyclic AMP-regulated phophoprotein of 32kD; *CREB*=cyclic AMP response element-binding.

III.2. Homer in the pathophysiology of psychotic disorders

Given its role in activity-dependent synaptic rearrangements, Homer gene and protein expression changes in response to dopaminergic and glutamatergic stimuli have been considered as fine-tuned mechanisms to preserve synaptic homeostasis [127]. Thus, growing evidence has been provided that Homer proteins dysfunctions might be involved in the pathophysiology of neuropsychiatric disorders implicating defects in synaptic platicity, such as schizophrenia [128,129] (Table 1). The deletion of *Homer1* gene has been demonstrated to induce behavioral and neurochemical abnormalities

relevant to animal models of schizophrenia, including altered performances in sensory, motor, social, and learning/memory tests [130,79]. *Homer1* knockout (KO) mice show altered food reward and reinforcement, altered antipsychotic-sensible sensorimotor gating, increased motor activation and attenuated habituation of motor activity when exposed to a novel environment. These mice also have increased sensitivity to the locomotor-activating effects of MK-801 or methamphetamine, decreased extracellular glutamate content in the nucleus accumbens and increased content in the PFC, as well as blunted increase in PFC extracellular glutamate after cocaine stimulation [79]. However, long and short *Homer1* variants are differently involved in PFC glutamate neurotransmission and in development of behaviors relevant to schizophrenia. Actually, a recent study demonstrated that the adeno-associated virus (AAV)-mediated restoration of either *Homer1a* or *Homer1c* in *Homer1* KO mice may differently affect synaptic functions and consequent behaviors [131]. *Homer1c* restoration in the PFC of *Homer1* KO mouse reverses aberrant working memory and sensorimotor function, locomotor hyperactivity in response to a novel environment, sensitivity to cocaine, and PFC glutamate content [131]. By contrast, the AAV-mediated restoration of *Homer1a* has been demonstrated to only reverse alterations in emotional reactivity in mutant animals [131]. Notably, these behavioral and neurochemical alterations have been found worsened by dopamine-function enhancers, such as cocaine and methamphetamine, and were prevented or attenuated by D2 receptor antagonist agents, such as haloperidol. Consistent with preclinical findings, several clinical studies have implicated *Homer* genes in schizophrenia pathophysiology. An early study found a significant association between a Single Nucleotide Polymorphism (SNP) within intron 4 of *Homer1* gene and schizophrenia [132]. However, this result was not replicated in an extended sample by the same authors [132].

More recently, an association between *Homer1* gene polymorphisms and clinical psychopathology assessments in schizophrenia has been demonstrated. Two *Homer1* polymorphisms (rs2290639, which is an intronic polymorphism, and rs4704560, which is a mutation in the 5'-flanking region of *Homer1* gene, and could be considered as a potential promoter polymorphism) have been associated with scores on Positive and Negative Syndrome Scale (PANSS, a rating scale for symptoms severity assessment in schizophrenia) subscales at baseline. Namely, the rs2290639 variant was significantly associated with scores on PANSS total, positive, and global psychopathology subscales, whereas the rs4704560 variant was significantly associated with scores on PANSS negative subscale [133].

Also, a putative role for *Homer2* gene in schizophrenia susceptibility has been suggested. Actually, the rs2306428 polymorphic variant has been strongly associated with the disease [134].

The role of Homer proteins in synaptic plasticity has stimulated further studies on their involvement in neuropsychiatric diseases in which molecular processes underlying cognition are considered dysfunctional, such as ASD. *Homer1* gene has been recognized as a novel autism-risk gene in a single nucleotide variant (SNV) analysis of blood samples from 290 unrelated non-syndromic autism cases and 300 ethnically-matched controls [135]. Several rare and potentially damaging variants have been identified in the autism population that co-segregate with the disorder and affect functionally relevant protein regions or regulatory sequences [135]. Intriguingly, the interaction between long Homer isoforms and mGluR5 is strongly diminished in *Fmr1* KO mice, a model of Fragile X Syndrome (an inherited cause of intellectual disability and autism) [136]. In this model, the genetic deletion of *Homer1a* may restore the long Homer-mGluR5 interaction and correct altered phenotypes, thus suggesting a potential Homer-related mechanism of mGluR5 dysfunction in this autism-related disease [137].

In summary, Homer proteins are key proteins of the PSD, involved in postsynaptic glutamatergic signaling and in dopamine-glutamate cross-talk. Long Homers act as scaffolding proteins, bridging glutamate receptors with their intracellular effectors. Short Homers disrupt these clusters in a space- and time-controlled fashion. This balance contributes to finely regulate multiple biological functions, such as Ca^{2+} dynamics in dendritic spine microdomains, whose disruption may concur to dysfunctions of synaptic plasticity and aberrant behavioral manifestations [138].

	Description of findings	Reference
PSD95	Knock-out mice exhibit impaired spatial learning and enhanced long-term potentiation. No alterations in NMDA localization and functions.	[84]
	Knock-out animals for heparin-binding epidermal growth factor (a neurotrophic factor implicated in schizophrenia) exhibit decreases in dopamine and serotonin levels, reduction in NR1 subunit of NMDAR, and decreases in PSD95	[192]
	NR1 subunit of NMDAR is down-regulated in dopaminergic neurons of the substantia nigra in postmortem brains of schizophrenic patients, while there are no alterations in AMPA subunits. PSD95 is overexpressed.	[232]
	PSD95 expression is reduced in striatal regions of postmortem brains of bipolar patients	[195]
	Hippocampal dentate gyrus and orbitofrontal cortex of schizophrenic and bipolar disorder postmortem brains show lower levels of PSD95 expression, yet there are no alterations in NMDARs subunits	[196]
	NR1 subunit of NMDARs is increased in cingulate cortex of elderly schizophrenics postmortem brains. Increased transcription but decreased protein levels of PSD95 are found in the same brain region.	[233]
	Increased expression of NR2B subunit of NMDARs and decreased PSD95 expression in postmortem thalamus of schizophrenic and bipolar patients.	[194]
	Decreased phosphorylation of PSD95 and NR2B subunit of NMDARs in cingulate cortex and increased phosphorylation of PSD95 and NR2B in dorsolateral prefrontal cortex of postmortem schizophrenic brains	[234]
Homer1	Homer1 knock-out mice exhibit deficits in spatial learning tests, impaired prepulse inhibition and other behavioral abnormalities predictive of schizophrenia	[54]
	In Homer1 knock-out mice, the overexpression in prefrontal cortex of either the short isoform Homer1a or the long isoform Homer1c reverses behavioral abnormalities, sensitivity to cocaine and glutamate cortical content.	[235]
	In a fragile X syndrome mouse model, Homer scaffolding functions are disrupted and provide abnormal mGlu5 receptors distribution. Genetic deletion of Homer1a restores mGlu5-Homer scaffolds and corrects some phenotypes	[176]
	A SNP mutation in Homer1 gene is associated to neuropsychiatric phenotypes, such as schizophrenia	[199]
	SNP analysis in a multi-stage association study reveals a significant association of Homer2 gene with schizophrenia	[201]
	Two Homer1 polymorphisms are associated with subscales response to Positive And Negative Symptoms Scale (PANSS) by schizophrenic patients at baseline et after 4 weeks of antipsychotic treatment	[200]
Shank	The T allele of Shank1 promoter is associated with impaired auditory working memory and digit span in schizophrenic patients	[211]
	Two de novo copy number variations of Shank2 are associated with mental retardation and autism, and are responsible for impaired dendrite spine morphogenesis	[204, 205]
	Shank3 mutant mice have altered expression of Homer1b/c protein, abnormal dendritic spine morphogenesis, and dysfunctional long-term potentiation, as well as locomotor impairment	[236]
	Shank1 null mutant mice exhibit aberrant ultrasonic vocalization and scent marks, with communication deficits	[237]

Table 1. Preclinical and clinical studies implicating PSD scaffolding proteins in the pathophysiology of psychotic disorders

III.3. Homer modulation by antipsychotic drugs

Among *Homer* genes, the inducible immediate-early gene isoform *Homer1a* is known to respond to dopaminergic manipulations [139]. A number of preclinical studies have shown that *Homer1a* expression may be induced by acute antipsychotic administration in brain regions relevant to schizophrenia pathophysiology, and may be differently modulated by typical and atypical antipsychotics, potentially according to their dopaminergic receptor profile. The high D_2R-blocking antipsychotic haloperidol has been shown to induce *Homer1a* in all striatal subregions, with prominent impact on the dorsal and lateral regions, and in both the core and the shell of the nucleus accumbens [85,17,140]. Another antipsychotic with high D_2R affinity, (-)-sulpiride, may induce *Homer1a* in the ventrolateral subregion of the caudate-putamen and in the core of the accumbens [20]. Differently from typical antipsychotics, atypical antipsychotics have been demonstrated to induce a *Homer1a* region-specific expression depending also on their affinity to receptors other than the dopaminergic ones, such as the serotonergic receptors, as well as on the dose administered. Risperidone, which has elevated D_2R affinity but lower maximal binding effect compared to haloperidol [141], may induce *Homer1a* expression in the lateral regions of the caudate-putamen only [20]. Olanzapine-induced expression of *Homer1a* gene has been reported in the core of the nucleus accumbens only [85], although high doses of the compound may also elicit *Homer1a* expression in the lateral regions of the caudate-putamen [20]. Ziprasidone, a high D_2R affinity atypical antipsychotic, differentially impacts *Homer1a* expression, according to dosage. At low doses, ziprasidone may produce a striatum-specific *Homer1a* induction, while a wider gene induction, spreading also to the cortex and the nucleus accumbens, has been found at high doses, probably depending on higher involvement of serotonergic receptors [15]. Moreover, the expression of *Homer1a* in the striatum by ziprasidone is significantly higher at high doses, which are correlated to

the liability to extrapyramidal side effects in animal models [142]. Also the dopamine partial agonist aripiprazole has been demonstrated to differentially modulate *Homer1a* expression depending on the dose. A strong induction of *Homer1a* expression has been observed in all caudate-putamen subregions by acute administration of low aripiprazole doses [17]. High aripiprazole doses have no significant effects in the striatum but may induce *Homer1a* expression in the cingulate cortex and in the inner and outer layers of the frontal cortex [17]. These dose-dependent effects may be likely due to aripiprazole mixed agonist/antagonist activity at pre- and postsynaptic D_2Rs. Basically, low aripiprazole doses are supposed to exert a prevalent antagonist activity at postsynaptic D_2Rs, thus directly inducing *Homer1a* striatal expression [143], whereas high doses may exert a prevalent agonist activity at presynaptic D_2 autoreceptors, thereby having scarce effects on *Homer1a* expression [17].

Atypical antipsychotics with low D_2R affinity, such as clozapine, or with unique D_2R dissociation kinetics, such as quetiapine and sertindole, have been observed to modulate *Homer1a* expression with specific patterns in striatum. Indeed, clozapine has been shown to acutely induce *Homer1a* expression in the nucleus accumbens only [17,15]. Acute clozapine may also induce *Homer1a* expression in the cortex (in the anterior cingulate, medial agranular, somatosensory and insular cortices), probably due to its impact on serotonergic receptors [17,15]. Quetiapine, a fast dissociating D_2R antagonist, has been found to slightly induce *Homer1a* striatal expression [140]. However, quetiapine may induce a robust *Homer1a* expression in the cortex when acutely administered, whereas significantly decreasing it in chronic paradigms [19]. This feature may strengthen the hypothesis of a combined dopaminergic-serotonergic control of *Homer1a* expression in the cortex. Indeed, acute administration of the serotonergic-selective antipsychotic sertindole has been found to reduce *Homer1a* expression in the somatosensory and insular cortices [20].

Taken together, these lines of evidence support the view that *Homer1a* could represent a molecular sensor of glutamatergic postsynaptic involvement in the mechanism of action of antipsychotics. Moreover, since the above-mentioned findings suggest that *Homer1a* induction by antipsychotics may be related to their propensity to perturb dopamine transmission, the pattern of *Homer1a* expression may be considered as a predictor of the liability of each antipsychotic to induce extrapyramidal side effects [140].

Homer1a has been demonstrated to preserve its expression profile in the striatum after chronic antipsychotic administration, and it seems to be unaffected by the tolerance or desensitization phenomena observed for other immediate-early genes, such as *c-fos* [144,145]. Indeed, haloperidol has been demonstrated to modulate *Homer1a* expression with similar patterns in both acute and chronic paradigms [17,21]. Nonetheless, some adaptive changes should not be ruled out after chronic antipsychotic administration. Chronic clozapine treatment, as opposed to acute treatment, has been reported to produce no significant *Homer1a* changes in the caudate-putamen, whereas it may decrease *Homer1a* expression in the cingulate cortex and in the inner layers of both frontal and parietal cortices.

In opposition to what observed after acute treatment, chronic ziprasidone may induce *Homer1a* expression only in the lateral regions of the caudate-putamen and in the core of the nucleus accumbens [15]. Lastly, chronic aripiprazole, differently from acute administration, has been demonstrated to induce *Homer1a* in the lateral regions of the caudate-putamen while reducing it in the cingulate and in the inner layers of the frontal cortex [17]. These effects might be part of an adaptive response of the glutamatergic system to chronic antipsychotic treatment [17]. Overall, despite *Homer1a* modulation by antipsychotics appears to be not susceptible of tolerance, acute or chronic treatment may result in different patterns of gene expression, probably accounting for neuroplastic adaptations triggered by prolonged treatments.

Besides the inducible isoform *Homer1a*, dopaminergic drugs have also been demonstrated to modulate the expression of the constitutive isoforms of *Homer1* gene, thus putatively inducing direct rearrangements in synaptic architecture. The acute administration of selective antagonists at D_2Rs and D_4Rs, as well as of a D_2R partial agonist (i.e. terguride), has been demonstrated to reduce *Homer1b/c* expression in the striatum and in cortical subregions [143]. Nevertheless, the D_1R selective antagonist SCH-23390 has been described to increase *Homer1b/c* expression in the core of the nucleus accumbens, while reducing it in the motor cortex [143]. However, the evaluation of *Homer1b/c* modulation after acute or chronic antipsychotic administration has provided contrasting results. Acute haloperidol treatment, indeed, has been observed to reduce *Homer1b/c* expression in the ventrolateral caudate-putamen, in the shell of the nucleus accumbens and in the motor, somatosensory and insular cortices [143], whereas no significant differences in expression have been found after a 16-day chronic treatment by haloperidol or quetiapine [146]. However, treatment duration may be a critical factor to cause changes in *Homer1b/c* expression, which has been found to increase in both striatum and cortex following a 21-day haloperidol or sertindole treatment [21].

Taken together, these data suggest that *Homer1* genes might be crucial in the pathogenesis and in the severity of psychotic symptoms, as well as in determining the efficacy of antipsychotic drugs.

IV. Intracellular pathways of antipsychotic combined therapies: dissecting the molecular correlates of real world psychopharmacotherapy

As discussed before, dysfunctions in the interplay among multiple neurotransmitter systems have been implicated in the pathophysiology of major psychiatric disorders,

such as schizophrenia, bipolar disorder or major depression, which display a wide range of behavioral, emotional and cognitive alterations [147]. Particularly, schizophrenia is a highly complex and multidimensional disorder, which shows a large number of unmet needs in terms of positive, negative and cognitive symptoms control in patients by current available pharmacotherapy. Indeed, an extimated 30% of patients do not satisfactorily respond to present treatments [148], and only a small percentage of responding patients is able to restart a normal working life.

Thus, the complex clusters of symptoms showed by schizophrenic patients often need more than one psychiatric drug from the same or a different pharmacological class, particularly under the following conditions: 1) when monotherapy provides insufficient improvement of the core symptoms; 2) when there are concurrent additional symptoms requiring more than one class of medications; 3) to improve tolerability, by using two compounds under dose thresholds to limit side effects [149].

Currently, the choice of antipsychotic combinations is based on empirical paradigms guided by clinical responses [147]. Some empirically-supported antipsychotic combination therapies include the following: 1) the combination of atypical antipsychotics with other atypical or typical antipsychotics in clozapine-refractory schizophrenia [150]; 2) the addition of antipsychotics to mood stabilizers for acute mania [151] or for maintenance in bipolar disorder [152]; 3) the addition of antipsychotics to antidepressants in treatment-resistant major depression or in psychotic depression [153], as well as the addition of antidepressants to antipsychotics to control prominent negative symptoms in chronic schizophrenia [154].

IV.1. Indications and clinical efficacy of common antipsychotic combination strategies

IV.1.a. Antipsychotics and antidepressants

First and second generation antipsychotics (FGAs, SGAs, respectively) are the mainstay treatment of schizophrenia, but increasing evidence suggests that their efficacy in the control of negative symptoms (such as apathy, anhedonia, avolition, affective flattening and social withdrawal) is limited [155]. The co-administration of SSRIs with typical or atypical antipsychotics has been considered a potential useful option for chronic schizophrenic patients with persistent negative symptoms. Two meta-analyses [156,157] showed increased efficacy of fluoxetine when combined with typical antipsychotics. Moreover, also ritanserin and trazodone have been considered useful as add-on therapies for treating negative symptoms in schizophrenia [157]. Clinical benefits, mostly on negative symptoms, were found in small trials combining ritanserin with risperidone [158] and in trials assessing the combination of mirtazapine with either FGAs [159,160] or risperidone [161] or clozapine [162]. Besides its use is accepted as add-on antidepressant therapy to olanzapine in schizophrenia [163], fluvoxamine has recently gained interest also due to its ability to enhance efficacy and reduce side effects in clozapine-treated schizophrenic patients, probably by the inhibition of clozapine oxidative metabolism by CYP1A2 with the subsequent decrease in plasma levels of the clozapine metabolite norclozapine, which is considered responsible for most adverse effects related to clozapine treatment [164].

Antipsychotic-antidepressant combinations have been also studied in depressive diseases. Although SSRI antidepressants are first-line treatment for major depression, they are reported to significantly reduce depressive symptoms in only 40-60% of patients when administered in monotherapy [165]. Second generation antipsychotics

have been proposed as potentially helpful augmenting agents in treatment-resistant depression or in psychotic depression [166] [153], and have become the second most used add-on strategy despite the lower number of studies as compared to other treatment options, such as lithium [167]. However, the most recent meta-analyses warn clinicians to be cautious in choosing antipsychotic medications as adjunctive strategies in depressive disorders, mainly because of the actual moderate efficacy on symptoms, the lack of benefits with regard to quality of life, as well as the increase in treatment-related adverse events [168]. Three atypical antipsychotics (i.e. aripiprazole, quetiapine, and olanzapine) in the USA and one (i.e. quetiapine, extended release formulation) in Europe have received regulatory approval for combined use with antidepressants for treatment-resistant major depression in adults [169]. However, early studies on antipsychotics-antidepressants combination in major depression reported that the combination of fluoxetine and olanzapine might be more rapid and effective in treatment-resistant unipolar depression as compared to each agent alone [170]. Despite a negative result from a larger clinical sample [171], other large randomized clinical trials provided evidence of greater effects, in terms of both clinical efficacy and rapidity of action, for this combination treatment [172]. Therefore, in 2009 the olanzapine-fluoxetine combination has been approved by FDA for the treatment of resistant unipolar and bipolar depression, even if it was reported to induce an increased risk of weight gain and metabolic alterations [173].

The efficacy of olanzapine-fluoxetine combination has also been tested in the treatment of major depression with psychotic features. Indeed, olanzapine plus fluoxetine combination shows greater efficacy as compared to fluoxetine alone in patients with psychotic depression [174]. Recently, the potential efficacy and safety of aripiprazole augmentation in treatment-resistant psychotic major depressive disorder has been

reported [175] at both high and low dosages, either when combined with escitalopram [176] or with sertraline [177].

IV.1.b. Antipsychotics and mood stabilizers

As suggested by international guidelines [178], monotherapy with mood stabilizers or antipsychotics represents the first choice in the treatment of manic phase of bipolar disorder (mild and moderate mania). Combined therapies (lithium or valproate plus short-term atypical antipsychotics) are indicated for severe mania (in order to gain a more rapid control of euphoric, dysphoric, mixed or psychotic symptomatology) or as a second line in mild and moderate mania after switching medication.

With respect to acute mania treatment, some studies reported a shorter time to remission and a higher remission rates in bipolar patients when treated with olanzapine in combination with either valproate or lithium, as compared with valproate or lithium alone [179]. Greater efficacy as compared to monotherapies have been described in manic or mixed episodes also for the combined treatments with risperidone or quetiapine plus lithium or valproate [180-182].

Recent evidence suggests that antipsychotic medications, in addition to their action on acute manic symptoms, may also have a role in treating other phases of bipolar disorder [183]. Clinical trials in depressed bipolar patients demonstrated the efficacy and safety of monotherapy with SGAs (such as aripiprazole, olanzapine, and quetiapine) in the management of bipolar depression [184-186]. FDA and EMEA have registered quetiapine and olanzapine also for this indication, either in monotherapy or in combination with mood stabilizers. FDA also approved risperidone, quetiapine, olanzapine and ziprasidone (quetiapine, aripiprazole, and olanzapine in Europe), alone or in combination with mood stabilizers, for the maintenance treatment in bipolar

disorder [187,188]. These antipsychotics are believed to be able in treating euphoric or depressive phases with a low risk of inducing mood transitions, therefore acting as long-term mood stabilizers [189].

In addition to their well-established use for the treatment of bipolar disorder, in the last 30 years the mood stabilizers lithium and valproate have been empirically used as an augmentation strategy in schizophrenia, in order to improve the outcome of treatment-resistant schizophrenia or schizophrenia with persistent symptoms of hostility and anxiety [190].

Earlier studies on acute exacerbation of chronic schizophrenia demonstrated that the addition of valproate to haloperidol may result in greater improvements from baseline at the Clinical Global Impression Scale for Schizophrenia (CGI-S) and at the Brief Psychiatric Rating Scale (BPRS) than those observed with haloperidol monotherapy [191]. However, results from clinical studies on combined antipsychotic-mood stabilizing treatment in acute episodes of schizophrenia are often non conclusive. Valproate added to risperidone or olanzapine has been demonstrated to induce earlier improvement in the Positive and Negative Syndrome Scale (PANSS) total score and PANSS positive symptoms scale scores as compared to antipsychotic treatment alone [192]. However, in a subsequent study, a prolonged treatment with combined risperidone or olanzapine plus valproate treatment in acute schizophrenic exacerbations failed to demonstrate an advantage over antipsychotic monotherapy, and no differences were displayed also in the onset of side effects [193]. Thus, at present there are no clinical data that effectively support, but also contest, the use of valproate as add-on therapy in schizophrenia [194]. However, some evidence supports the view that valproate may be used to treat specific and rare effects that may onset during antipsychotic therapy, such as functional hallucinations [195] or to impact

schizophrenia-like symptoms derived from brain damage, such as in cerebellar hemorrhage, which may be resistant to antipsychotic treatment [196].

In schizophrenic inpatients with persistent aggressive behavior, the addition of valproate or topiramate to standard antipsychotic medication has been showed to significantly reduce average scores on the Overt Aggression Scale (OAS), with valproate add-on being more effective than topiramate add-on in decreasing the intensity of agitation episodes and the number of psychotic disorganization episodes [197].

Although lithium has been used in the past as an augmentation strategy in schizophrenia treatment, at present there is no trial-based evidence that lithium add-on strategies may be more effective than antipsychotic monotherapies in schizophrenic patients. Indeed, a recent systematic review evaluated 11 studies assessing the efficacy and safety of lithium in addition to typical or atypical antipsychotics versus antipsychotics alone in schizophrenia, schizophrenia-like psychoses and schizoaffective psychoses. Although the participants who received lithium augmentation had a clinically significant higher response, when participants with schizoaffective disorders were excluded from the analysis the advantage of lithium augmentation in schizophrenic patients became not significant [190]. Furthermore, a significant number of participants receiving lithium augmentation left the studies before completion, suggesting a lower compliance to lithium augmentation compared to those receiving antipsychotics alone [190].

Even if lithium add-on strategy to antipsychotics lacks compelling evidence, emerging interest is focusing on the use of lithium in particular subsets of schizophrenic patients. For instance, provided the beneficial effects of lithium treatment in keeping stable white blood cells levels in patients, the add-on treatment with lithium has been regarded as useful in order to enable clozapine administration in schizophrenic patients with pre-existent neutropenia [198,199], or in children-onset treatment resistant schizophrenic

patients, in which clozapine treatment has been demonstrated to induce high rates of neutropenia [200]. However, high caution should be taken into account when considering these therapeutic strategies, evaluating the potential hematological risks of lithium add-on to clozapine.

IV.1.c. Antipsychotics and bendodiazepines

In clinical practice in psychiatry, benzodiazepines are traditionally used to treat anxiety and sleep disorders [201]. However, benzodiazepines are usually prescribed in addition to antipsychotics early in a psychotic episode for a rapid relief of agitation and disruptive behaviors [202], and may be administered subchronically to control anxiety or motor disturbances in psychotic patients [203]. In this view, several studies have pointed out that aggressive behaviors and schizophrenia are tightly related [204]. However, matter of debate is whether aggression and anxiety might be originated by the onset of psychotic symptoms (above all "positive" ones, such as paranoid delusions or hallucinations), which may act as stressors by increasing anxiety levels and making patients "violence-prone" [205], or if aggression may derive from the underlying personality dysfunctions of psychotic patients, thereby being not a "symptom" of schizophrenia, but a premeditated behavior depending on pre-existent aggressive temperament [206].

A recent Cochrane review evaluating the global evidence from 13 placebo-controlled randomized clinical trials stated that, in terms of efficacy and safety, adding a benzodiazepine to antipsychotics may be as acceptable as antipsychotic monotherapy for schizophrenic patients, at least in clinical trials [207]. In particular, in the very short term, the addition of benzodiazepines to antipsychotics has been described to improve the global state of people with schizophrenia in several studies. This finding, likely

associated to the anxiolytic properties of denzodiazepines, is statistically significant at 30 minutes after administration, but the difference diminishes over time, with only a trend at 60 minutes and no difference occurring at 12 hours or 3 weeks. Therefore, the therapeutic advantage of benzodiazepines add-on may be helpful in the early acute phases of a psychotic episode, taking cautiously into account the dosages, in order to avoid too pronounced sedation.

IV.1.d. Antipsychotics plus antipsychotics

In agreement with schizophrenia evidence-based guidelines, combination of two or more antipsychotic drugs is currently recommended only as a "last-resort" therapeutic option for schizophrenia unresponsive to an optimized clozapine monotherapy [208]. However, combined antipsychotic treatment for schizophrenia patients is relatively frequent in routine clinical practice, with an increasing prevalence in recent years [209,210,149].

A second antipsychotic may be added to the first one based on the following clinical rationales: 1) to manage particular symptoms refractory to antipsychotic monotherapy [150]; 2) to avoid high-dose prescribing of an individual antipsychotic that would expose the patient to a higher risk of adverse effects [150]; 3) to counteract a particular adverse effect caused by the first antipsychotic—i.e. the addition of aripiprazole has been evaluated to reduce hyperprolactinemia in patients initially treated by high D_2 receptor blocking drugs, such as haloperidol or risperidone [211-213]—; 4) multiple antipsychotic treatments may result from an incomplete switch from one antipsychotic to another, if clinical improvement was found during the period of cross-tapering [214]. The most frequent case of antipsychotic-antipsychotic add-on strategy is the augmentation of clozapine with a second antipsychotic in treatment-refractory

schizophrenia not fully responding to clozapine [215]. The theoretical basis for augmentation of clozapine rely on the attempt to enforce its pleiotropic receptor effects with agents provided of relatively more selective D_2 receptor antagonism [216-218]. However, the augmentation of clozapine with a second antipsychotic is modestly superior to placebo, although equally well tolerated [215]. Converging evidence indicate sulpiride, amisulpiride and aripiprazole as favorable options for clozapine augmentation [219,218] ì, with the latter showing the best impact on metabolic parameters when combined with clozapine [209,220-222].

Overall, clinical evidence for the efficacy of antipsychotic polytherapy in refractory schizophrenia or in other clinical conditions remains limited. Only a few open label studies and case-series reports have focused on the attempt to combine different antipsychotics by virtue of their different receptor profiles. Combinations of olanzapine with risperidone [223] or sulpiride [224] and quetiapine with risperidone [225] or amisulpride [226] have been described to provide some clinical benefits. In an open-label 8-week trial, the combined olanzapine-risperidone treatment in schizophrenia patients unresponsive to sequential trials of monotherapy with olanzapine, quetiapine and risperidone showed a therapeutic response (post-treatment BPRS total score <70% of the pre-treatment value), but also higher rates of hyperprolactinemia, and increase in total cholesterol and weight gain [227].

The addition of aripiprazole to either quetiapine or risperidone in schizophrenic and schizoaffective patients unresponsive to monotherapy, although not associated with improvement of overall psychopathology, has been reported to be generally safe, well tolerated and potentially useful in particular patients subpopulation, for example in cases of hyperprolactinemia [212]. Moreover, aripiprazole add-on has been demonstrated to improve obsessive-compulsive symptoms in clozapine-treated and olanzapine-treated schizophrenic patients [228,229].

However, the real efficacy on symptoms, as well as the risks associated to such SGA combination-strategies remain to be further evaluated in larger and longer-term controlled clinical trials.

IV.1.d. Multitargeting antipsychotics

Combination therapies are a highly valid tool to counteract the complex cortege of symptoms belonging to major psychiatric diseases. However, combining drugs often means combining side effects, and sometimes generating new side effects due to pharmacokinetic or pharmacodynamics interactions amongst the drugs we are combining. Thus, recent research on novel antipsychotics has tried to move the attention on the development of drugs acting on multiple selected targets. In theory, these agents should provide a more effective approach in the treatment the complex symptoms of schizophrenia, as well as bipolar disorder [230,231]. These studies are based on the increased efficacy of atypical antipsychotics as compared to typical ones in treating negative symptoms, likely due to the ability of these drugs to act on serotonergic, noradrenergic and glutamatergic targets [232]. However, despite the diversity in pharmacological profiles of current antipsychotics, the differences in pharmacodynamics seem to be primarily translated in reduced liability to induce side effects and in ameliored tolerability, rather than in increased treatment efficacy [233,234]. Moreover, the reduced risk of hyperprolactinemia or motor side effects by new antipsychotics is often counterbalanced by increased cardiovascular risk by weight gain or metabolic dysfunctions [235]. Thus, new drugs should be virtually devoided of metabolic and motor side effects, while having increased efficacy in treating negative and cognitive symptoms and maintaining relief of positive symptoms.

The prototypical antipsychotic which responds to these newly developed "multitargeting" strategies is asenapine. Asenapine shows a broad multi-receptorial binding affinity for all serotonergic and dopaminergic receptors, with equal affinity for D2 and D1 dopamine receptors, as well as for alpha adrenergic receptors, and no affinity for muscarinic receptors [236]. It has been demonstrated to promote dopamine, serotonin and noradrenaline release in cortex and dopamine release in nucleus accumbens at doses that have antipsychotic activity in animal behavioral studies [237]. Moreover, thanks to its unique multi-receptor profile, asenapine may differentially impact glutamatergic and dopaminergic systems in cortical and subcortical regions: it, in fact, enhances glutamate NMDA-mediated currents in pyramidal cortical neurons, while it decreases NMDA receptor activity in caudate-putamen and nucleus accumbens; moreover, the chronic treatment with potentiates AMPA receptor activity in hippocampus [238]. On the other hand, asenapine may specifically enhance the dopamine bursts from VTA to the medial prefrontal cortex and the nucleus accumbens, and of noradrenaline from locus coeruleus to the cortex [237]. Recent studies have demonstrated that asenapine may exert brain region-specific differential effects on dopamine, serotonin and glutamate receptors depending on the dose administered [239-241].

Recent studies demonstrated a good efficacy and safety of asenapine in treating both schizophrenia and bipolar disorder [242,243], although literature metanalyses suggested that asenapine and the other new multitargeting antipsychotics on the market (i.e. lurasidone) display no significant differences in treatment efficacy as compared to "older" antipsychotics [244]. However, significant impact on cognitive and negative symptoms have been reported by patient's outcome interviews, as compared to other antipsychotics [245].

V. Aims of the research

Although still dearth at present, data from preclinical studies suggest that combined therapies may induce molecular changes that are sharply different, and often synergistic, as compared to those induced by individually administered drugs.

For instance, several studies describe a specific impact of antipsychotic-SSRI combination treatment on the expression of immediate-early genes and neurotrophic factors, different from that obtained by the administration of each drug alone [246,247].

Moreover, preclinical studies have also demonstrated that both mood stabilizers and antipsychotics may impact common intracellular target molecules that are involved in the transductional pathways of dopamine signaling (i.e. AKT/GSK-3 pathway**,** MAP kinases pathway, postsynaptic density proteins) [138]. Finally, new multitargeting drugs, such as asenapine, have been demonstrated to concurrently impact different neurotransmission systems [248], which may crosslink at crucial steps along neural transductional pathways, thereby synergistically reinforce downstream signaling in selected brain areas deputed to control cognitive and behavioral functions.

These observations support the hypothesis that convergence at crucial steps of intracellular dopaminergic pathways could be responsible for synergistic effects obtained by the co-administration of apparently heterogeneous compounds [249].

Understanding the biological mechanisms by which combined and multitargeting treatments act could enable a targeted selection of drugs, as well as provide further insights into the pathophysiology of neuropsychiatric symptoms [147].

Here we provide a set of preclinical studies whose aim was to investigate the postsynaptic molecular responses to either combined treatment strategies or novel multitargeting agents currently used in psychiatric clinical practice.

First aim was to evaluate whether combined treatments may impact differentially postsynaptic genes/proteins as compared to treatments individually administered. With

regards to multitargeting agents, we compared them to “older” antipsychotics in order to evaluate the different impact on postsynaptic molecules. Second goal was to determine whether combined strategies or multitargeting agents may activate postsynaptic transcripts in brain areas that are different from that elicited by standard therapies, and that may suggest better clinical efficacy on some cluster symptoms, or possibly some new adverse effects. Through topographic analysis, we aimed at providing imagines of this differential region-specific brain gene expression by the distinct compounds evaluated.

Finally, we aimed at investigating if the different gene/protein modulation by agents administered was elicited in functionally correlated brain areas and whether animal behavior responses may relate to such a selective cortical-subcortical integrated postsynaptic molecules modulation.

VI. Study n.1: acute and chronic effects of combined antipsychotic-mood stabilizing treatment on the expression of cortical and striatal postsynaptic density genes

The frequent use of antipsychotics/mood stabilizer combination prompted us to investigate the effect of such co-administration on the expression of brain genes that have been putatively implicated in synaptic remodeling. Moreover, in order to resemble more closely the treatment conditions of bipolar disorder in clinical practice, we also compared the effects on gene expression of an antidepressant agent widely used in bipolar depression (citalopram) with a low dose of quetiapine, which has been suggested to display antidepressant actions [250]. Indeed, as recently reviewed [251], the use of antidepressants in bipolar depression is common in clinical practice, but is rarely countenanced, preferring the initial prescription of a mood stabilizer or an antipsychotic, such as quetiapine, which yields a well-established effect on dopamine and serotonin systems, both strongly implicated in the pathogenesis of bipolar disorder [252]. The detection of changes in brain gene expression after the administration of mood stabilizers, alone or in combination with antipsychotics, and of antidepressants in animal models of drug treatment, may represent a valuable strategy to explore their key molecular targets in a pharmacological paradigm that closely resemble the real world of the pharmacotherapy of bipolar disorder.

Thus we investigated, in both acute and chronic paradigms, the expression of specific postsynaptic density genes (*Homer1a, Homer1b/c, PSD95, GSK3b, and ERK*) after the administration of haloperidol, quetiapine (both at high and low dosages), valproate, a combination of haloperidol plus valproate or quetiapine plus valproate, and citalopram. However, the genes selected for the study are a small subset of genes whose function has been correlated to the mechanisms of action of antipsychotics, antidepressants, and

mood stabilizers and that, due to their specific intracellular interactions, may represent a putative crossroad between the molecular pathways activated by the drugs investigated. *Homer* genes encode for a family of scaffolding proteins located at the postsynaptic density (PSD) of glutamatergic synapses that act as multimodal adaptors along different transduction pathways, above all the dopaminergic and the glutamatergic [36,253]. Changes in gene expression of PSD molecules, as Homers, are predicted to underlie changes in the composition and function of this ultra-structure.

Homers are subdivided in constitutive (Homer1b/c, Homer2, Homer3) and inducible isoforms (Homer1a, and its splice variant ania-3). Constitutive Homers interact with multiple PSD targets and are able to multimerize [93,83], while inducible isoforms act as "dominant negative", disrupting long-Homers clusters. Long Homers have been described to physically bridge metabotropic glutamate receptors type I (mGluRsI) to inositol 1,4,5-trisphosphate receptors (IP3Rs) (Tu et al., 1998). Moreover, the multimeric Homer clusters may link the N-methyl-D-aspartate glutamate receptors (NMDARs) with mGluRsI through a Shank-GKAP-PSD95 complex [92]. The induction of *Homer1a* has been shown to transiently and directly modify several biological functions involved in transduction of synaptic signal [254,255]. We have demonstrated that *Homer1a* is selectively induced by antagonists at dopamine D2 receptors in striatal regions [143]. Consistently with this finding, our early studies have shown that *Homer1a* is differentially induced in striatum by typical and atypical antipsychotics [85,99,140,17]. *Homer* has been involved in several neuropsychiatric disorders [136,128,79] and has been implicated in cognition as well as in motor dysfunction [256]. Thus, *Homers* may be candidate genes for behavioral diseases and for their pharmacotherapy.

GSK3b is an ubiquitous kinase which has been found in both neurons and glia, where it is constitutively active and component of diverse signaling pathways [257], with

multiple targets [258]. The best studied pathways in which GSK3b has been involved are: the insulin/insulin like growth factor signaling, the neurotrophic factor signaling, and the Wnt signaling. Among these, the PI3 kinase-Akt pathway, which could modulate GSK3b functions, has been well established in mediating neurotrophic and neuroprotective effects. Recent evidence reported a direct regulation of GSK3b function by mood stabilizing agents, such as lithium and valproate (see [259] for a review), and a possible implication of *GSK3b* gene in the pathogenesis of bipolar disorder and in the response to antimanic agents [260-262]. Furthermore, GSK3b may be modulated by several antipsychotics, such as clozapine, haloperidol and risperidone [263-265], and by antidepressants [266,267]. Finally, more recent studies have implicated the Akt-GSK3b signaling in behavioral changes induced by drugs which may impact both dopaminergic and serotonergic systems, with strong implications in clinical practice [249].

Erk (Extracellular signal-regulated kinase) 1 and 2 are involved in the regulation of multiple cellular activities, including inducible gene expression [268]. Several stimuli, including glutamate stimulation, have been demonstrated to modulate Erk1/2 phosphorylation/dephosphorylation status [269]. It is believed that Erk has unique implications in the regulation of neuronal signal transduction, being considered a crucial integrator of multiple signaling pathways converging on the modulation of important transcription factors (i.e. Elk1, CREB), that regulate the expression of essential cellular genes, such as *c-fos* [269,270].

Recent studies have demonstrated a significant increase in Erk activity by the synergistic activation of ionotropic and metabotropic glutamate receptors, depending on the crosstalk between the NMDAR-associated protein PSD95 and the mGluR5-linked adaptor Homer 1b/c [105]. Furthermore, the mood stabilizers lithium and valproate have been shown to stimulate the Erk pathway in rat hippocampus and frontal cortex, so inducing neuronal growth and neurogenesis [271,272]. Antidepressant drugs seem to

differently modulate Erk activation status, being this regulation probably associated with their therapeutic effects on the treatment of depression [273]. Also, it has been proposed a crucial role of the Erk pathway in the mechanism of action of both typical and atypical antipsychotic drugs [105,274]. Finally, altered levels of Erk signaling proteins have been reported in postmortem brains of patients affected by mood disorders and schizophrenia [275].

Through exploring changes in the expression of these postsynaptic density genes, we aimed at dissecting the involvement of dopaminergic and glutamatergic systems in the action of drugs used in bipolar disorder and to describe the topographical patterns of this action. Therefore, we evaluated expression of the genes in specific regions of the rat forebrain that have been considered dysfunctional in several psychiatric disorders [276-278] and that could likely represent the site of action of psychoactive compounds [279-281]. Moreover, the assessment of PSD genes modulation by compounds with different receptor profile may provide information on the interplay between the glutamatergic and other neurotransmitter systems, above all the dopaminergic and the serotonergic.

Experimental procedures

Rats housing and handling

Male Sprague-Dawley rats (mean weight 250g) were obtained from Charles-River Labs. (Lecco, Italy). The animals were housed and let to adapt to human handling in a temperature and humidity controlled colony room with 12/12 h light–dark cycle (lights on from 6:00 a.m. to 6:00 p.m.) with *ad libitum* access to laboratory chow and water. All procedures were conducted in accordance with the NIH Guide for Care and Use of Laboratory Animals (NIH Publication No. 85-23, revised 1996) and were approved by

local Animal Care and Use Committee. All efforts were made to minimize animal number and suffering.

Drugs preparation and injection

Quetiapine fumarate powder (Astra-Zeneca, Italy), Valproate sodium salt powder (Sigma-Aldrich, Italy), Citalopram hydrobromide powder (Sequoia Research Products, UK), and Haloperidol injectable solution (Lusofarmaco, Italy) were dissolved in a vehicle composed by saline solution (NaCl 0.9%) and a few drops of Acetic Acid 1%. All solutions were adjusted to physiological pH value and injected i.p. at a final volume of 1 ml/kg.

Rats were randomly assigned to one of the following treatment groups (n=7 animals for each treatment group): Vehicle (SAL); Citalopram 14 mg/kg (CIT); Quetiapine 15 mg/kg (QUE15); Quetiapine 30 mg/kg (QUE30); Haloperidol 0.8 mg/kg (HAL); Valproate 500 mg/kg (VAL); Haloperidol 0.8 mg/kg + Valproate 500 mg/kg (HAL+VAL); Quetiapine 30mg/kg + Valproate 500 mg/kg (QUE30+VAL).

Valproate, in association with haloperidol or quetiapine was not merged in a single injection, because of the high risk of precipitation and toxic reaction. Thus, animals were treated by two subsequent injections. In order to avoid biases, rats assigned to the other groups, with one drug treatment, were also exposed to an adjunctive injection by vehicle.

All drugs were given in a dose-range known to elicit changes in gene expression [247,17,140,282]. Since some controversy may arise over the appropriateness of drug dosages in animal studies [283], above all regarding the major differences in pharmacodynamics and pharmacokinetics between human and rodents, we chose specific dosages which have been previously evaluated in gene expression and behavior studies, trying to achieve a patient-equivalent effect in the brain of experimental

animals. Haloperidol and quetiapine were administered at doses known to elicit rat behaviors related to antagonism on D2 receptors and to provide substantial striatal D2 receptor occupancy [284-287]. The dose of haloperidol we used (0.8 mg/kg) is 20% lower than that (1 mg/kg) most commonly used in gene expression studies and lied in the range of 0.25-1 mg/kg used in more recent studies [288-290]. Quetiapine was administered at two dosages that have been demonstrated to reach a dopamine D2 receptors occupancy which could elicit behavioral responses in rats that are highly related to clinical efficacy in humans [291]. Finally, doses of valproate and citalopram were chosen based on previous studies in which these drugs evoked a well-established pharmacologic effect (i.e. dopamine release in cortical and subcortical structures) that may predict clinical effects in humans [292-294].

In the acute paradigm animals were injected intraperitoneally (i.p.), and killed 90 minutes after administration. In the chronic paradigm animals received daily treatments for 16 days and then sacrificed 90 minutes after the last administration. In both paradigms rats were mildly anaesthetized by chloral hydrate just before killing.

Tissue preparation and sectioning

After killing, the brains were rapidly removed, quickly frozen on powdered dry ice and stored at -70°C prior to sectioning. Serial coronal sections of 12 μm were cut on a cryostat at -18°C through the forebrain at the level of the middle-rostral striatum (approx. from Bregma 1.20mm to 1.00mm), using the rat brain atlas by Paxinos and Watson [295] as an anatomical reference. Care was taken to select identical anatomical levels of treated and control sections. Sections were thaw-mounted onto gelatin-coated slides, and stored at -70ºC for subsequent analysis.

Probes

Details of all the probes are listed in Table 2.

Probes for *In Situ* Hybridization Histochemistry

Probe	cDNA length (bp)	cDNA position	mRNA	GenBank #
Homer1a	48	2527-2574	*Homer1a*	U92079
Homer1b/c	48	1306-1353	*Homer1b/c*	AF093268
PSD-95	45	225-269	*PSD-95*	M96853
GSK3b	48	1057-1104	*GSK3b*	NM_032080.1
ERK	48	222-269	*ERK (MAPK1)*	NM_053842.1

Homer 1a, PSD-95 and *Homer1b/c* probes were oligodeoxyribonucleotides derived from identical probes used in previous hybridization studies [85,17]. All the other probes were designed from GenBank sequences and checked with BLAST in order to avoid cross-hybridization. All the oligodeoxyribonucleotides were purchased from MWG Biotech (Firenze, Italy).

Probe radiolabeling and purification

For each probe a 50µl labeling reaction mix was prepared on ice using DEPC treated water, 1X tailing buffer, 7.5pmol/µl of oligo, 125 Units of TdT and 100mCi ^{35}S-dATP. The mix was incubated 20 min at 37°C. The unincorporated nucleotides were separated from radiolabeled DNA using ProbeQuant G-50 Micro Columns (Amersham-GE Healthcare Biosciences; Milano, Italy). As an assessment of the probe specificity, the autoradiographic signal distribution was compared and found to be consistent with previous *in situ* hybridization studies [81,99]. The specificity of each probe was also tested by pilot control experiment using the corresponding sense oligodeoxyribonucleotide.

In situ hybridization

Sections were processed for radioactive *in situ* hybridization according to previously published protocols [296]. All solutions were prepared with sterile double-distilled water. The sections were fixed in 4% formaldehyde in 0.12 M phosphate buffered saline (PBS, pH 7.4), quickly rinsed three times with 1X PBS, and placed in 0.25% acetic anhydride in 0.1 M triethanolamine/0.9% NaCl, pH 8.0, for 10 minutes. Next, the sections were dehydrated in 70%, 80%, 95% and 100% ethanol, delipidated in chloroform for 5 minutes, rinsed again in 100% and 95% ethanol and air dried. Sections were hybridized with 0.4-0.6x106 cpm of radiolabeled oligonucleotide in buffer containing 50% formamide, 600mM NaCl, 80mM Tris-HCl (pH 7.5), 4mM EDTA, 0.1% pyrophosphate, 0.2mg/ml heparin sulfate, and 10% dextran sulfate. Slides were covered with coverslips and incubated at 37oC in a humid chamber for 22-24 hours. After hybridization the coverslips were removed in 1X SSC (saline sodium citrate solution) and the sections were washed 4x15 minutes in 2X SSC/50% formamide at 43-44oC, followed by two 30 min washes with 1X SSC at room temperature. The slides were rapidly rinsed in distilled water and then in 70% ethanol.

Autoradiography

The sections were dried and exposed to Kodak-Biomax MR Autoradiographic film (Sigma-Aldrich, Milano, Italy). A slide containing a scale of 16 known amounts of ^{14}C standards (ARC-146C, American Radiolabeled Chemical, Inc., St. Louis, MO, USA) was co-exposed with the samples. The autoradiographic films were exposed in a time range of 14-30 days. The optimal time of exposure was chosen to maximize signal-to-noise ratio but to prevent optical density from approaching the limits of saturation. Film development protocol included a 1.5 min dip in the developer solution and 3 min in the fixer.

Image analysis

The quantitation of the autoradiographic signal was performed using a computerized image analysis system including: a transparency film scanner (Microtek Europe B. V., Rotterdam, The Netherlands), an Apple iMac, and ImageJ software (v. 1.47, Rasband, W.S., http://rsb.info.nih.gov/ij/). Sections on film were captured individually. The original characteristics of the scanned images (i.e. contrast, brightness, resolution) were preserved. Each experimental group contained 4-6 slides. Each slide contained 3 adjacent sections of a single animal. All hybridized sections were exposed on the same sheet of X-ray film. Signal intensity analysis was carried out on digitized autoradiograms measuring mean optical density within outlined Regions of Interest (ROIs) in correspondence of the cortex, caudate-putamen and nucleus accumbens (Figure 6). These cortical and striatal subregions are structurally and functionally interconnected through projections from the cortex, which targets specific striatal sectors. ROIs in the cortex were selected based on recent data describing functional and anatomical correlation between cortical and striatal subregions [297] ROIs in the striatum have been chosen according to classical subdivision of this region [298].
An oval template, proportional to the dimensions of the anatomical subregion, was used for computerized quantitations in each one of the ROIs depicted.
Sections were quantitated blind to the treatment conditions. In order to test for inter-observer reliability, an independent quantitation was performed by a second investigator. Results obtained by the first investigator were considered reliable, and then reported, only when they were quantitatively comparable, in terms of consistency of the statistically significant effects found, to that obtained by the second investigator.

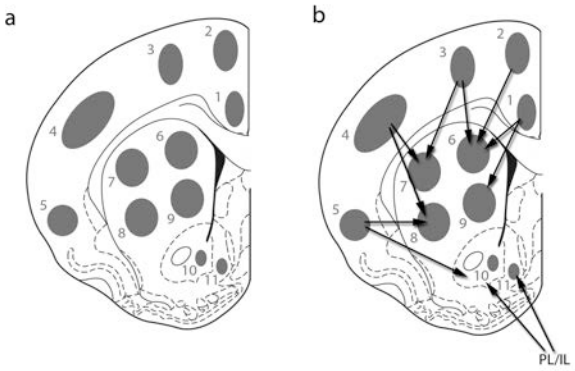

Figure 6. *Panel a.* Diagram of regions of interest (ROIs) quantitated on autoradiographic film images in rat forebrain (section coordinates are approximately from Bregma 1.20 mm to 1.00 mm). 1 = anterior cingulate cortex (AC); 2 = medial agranular/premotor cortex (M2); 3 = motor cortex (M1); 4 = somatosensory cortex (SS); 5 = insular cortex (I); 6 = dorsomedial caudate-putamen (CPDM); 7 = dorsolateral caudate-putamen (CPDL); 8 = ventrolateral caudate-putamen (CPVL); 9 = ventromedial caudate-putamen (CPVM); 10 = core of accumbens (AcCo); 11 = shell of accumbens (AcSh). Modified from Paxinos and Watson (1997).
Panel b. Illustration of cortico-striatal projections among the ROIs in which gene expression induced by mood stabilizers was measured. PL/IL = prelimbic/infralimbic cortices (not shown).

Data processing

Measurements of mean optical density within ROIs were converted using a calibration curve based on the standard scale co-exposed to the sections. ^{14}C standard values from 4 through 12 were previously cross-calibrated to ^{35}S brain paste standards, in order to assign a dpm/mg tissue wet weight value to each optical density measurement through a calibration curve. For this purpose a "best fit" 3rd degree polynomial was used. For each animal, measurements from the 3 adjacent sections were averaged and the final data were reported in relative dpm as mean ± S.E.M. A One-Way Analysis of Variance (ANOVA) was used to analyze treatment effects. To minimize standard error within groups, outlier values were not taken in account when analyzing treatment effect. The Student-Neumann-Keuls (SNK) *post hoc* test was used to determine the locus of effects in any significant ANOVA.

Results

Acute paradigm

The acute impact on glutamatergic and dopaminergic systems of the various drugs administered was assessed through exploring the changes in gene expression of *Homer1a, ERK, PSD95, GSK3b* and *Homer1b/c* in specific cortical and striatal subregions which have been considered the site of action of psychoactive compounds and which may be directly related to the pathophysiology of major psychiatric diseases (Figure 6).

Homer1a

(results, with respective ANOVA values, are detailed in Table 3; autoradiographic images are shown in Figure 7)

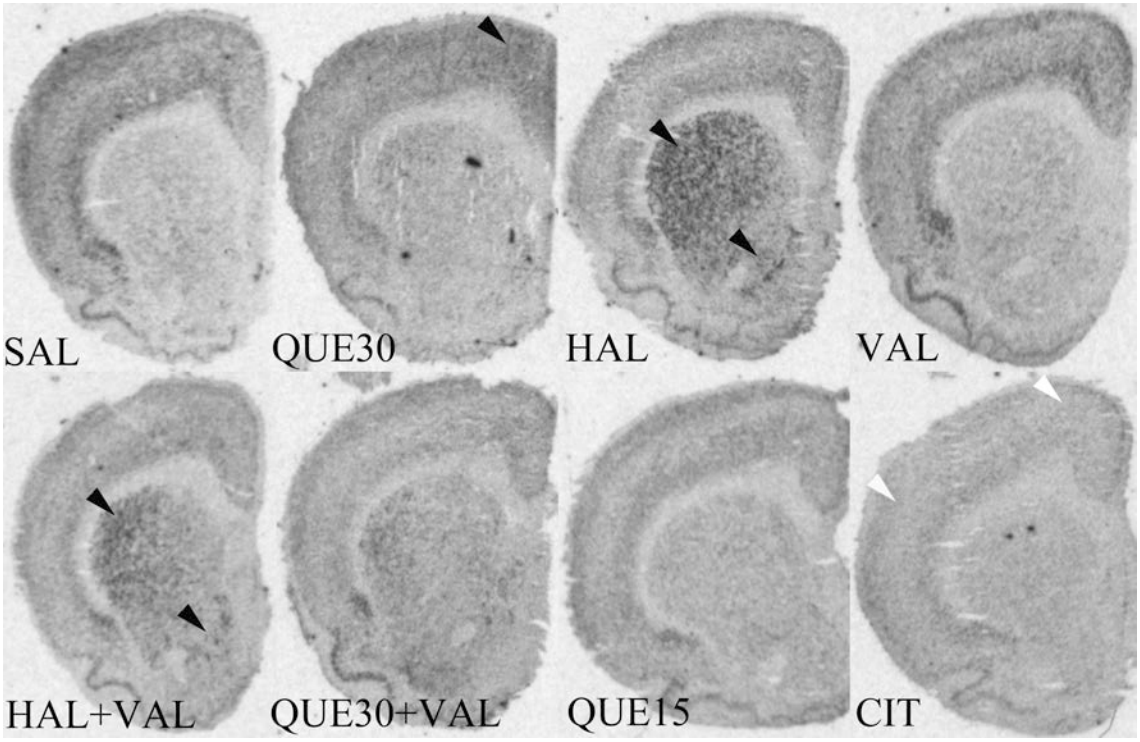

Figure 7. Representative autoradiographic film images of *Homer 1a* mRNA detected by means of *in situ* hybridization histochemistry (ISHH) in coronal brain sections after acute treatment with vehicle (SAL), quetiapine 30mg/kg (QUE30), haloperidol 0.8mg/kg (HAL), valproate 500mg/kg (VAL),

haloperidol+valproate (HAL+VAL), quetiapine 30mg/kg + valproate (QUE30+VAL), quetiapine 15mg/kg (QUE15), citalopram 14mg/kg (CIT). Brain areas in which significant changes in gene expression occurred with respect to vehicle are pointed out with black arrows for increases and white arrows for decreases.

Percentage of *Homer1a* expression by treatments as compared to vehicle in acute and chronic paradigms

Homer1a Acute	**QUE30**	**HAL**	**VAL**	**HAL+VAL**	**QUE30+VAL**	**QUE15**	**CIT**	**p-Value**	**$F_{(df)}$-Value**
Cortex									
AC	140.42±4							0.0002	$F_{(7,26)}$=7.7918
M2	126.68±2							0.0002	$F_{(7,26)}$=7.9059
M1	116.92±5						71.24±1	<0.0001	$F_{(7,26)}$=10.0459
SS							69.46±0.8	0.0018	$F_{(7,26)}$=5.2770
I							64.53±5	<0.0001	$F_{(7,27)}$=8.7503
Caudate-putamen									
DM		162.72±7		129.07±9				<0.0001	$F_{(7,26)}$=15.4234
DL		193.01±7		161.66±4				<0.0001	$F_{(7,26)}$=40.5786
VL		179.86±11		141.69±8				<0.0001	$F_{(7,26)}$=21.0805
VM		146.77±1		125.44±9				<0.0001	$F_{(7,26)}$=10.1481
Nucleus Accumbens									
Core		156.99±5		154.91±8				<0.0001	$F_{(7,28)}$=19.6507
Shell		131±3						0.0004	$F_{(7,28)}$=6.4996
Homer1a Chronic									
Cortex									
AC									
M2	71.51±9	77.6±4				76.32±4		0.0075	$F_{(7,30)}$=3.7434
M1	69.61±8	78.42±8				75.12±5		0.0065	$F_{(7,30)}$=3.8519
SS	72.47±8					73.42±4		0.0085	$F_{(7,30)}$=3.6566
I									
Caudate-putamen									
DM		124.90±3						0.0037	$F_{(7,30)}$=4.2776
DL		127.26±4						0.0211	$F_{(7,30)}$=3.0164
VL		131.01±4						0.0015	$F_{(7,30)}$=5.0167
VM		119.77±2						0.0089	$F_{(7,30)}$=3.6240
Nucleus Accumbens									
Core		121.5±5						0.0473	$F_{(6,26)}$=2.6411
Shell									

Table 3. The table summarizes significant changes *vs*. controls of *Homer1a* expression in cortex and striatum after acute (upper side) and chronic (lower side) treatment by quetiapine 30mg/kg (QUE30), haloperidol 0.8mg/kg (HAL), valproate 500mg/kg (VAL), haloperidol+valproate (HAL+VAL), quetiapine 30mg/kg + valproate (QUE30+VAL), quetiapine 15mg/kg (QUE15), citalopram 14mg/kg (CIT). Data are expressed as a percentage of vehicle (SAL) relative dpm. mean value ± S.E.M. and listed by brain region analyzed, along with the relative ANOVA *p* and *F*(*df*) values. Increases in gene expression are shaded in dark grey and decreases in light grey.

A significant induction of *Homer1a* gene expression was observed in anterior cingulate cortex (AC, p=0.0002; $F_{(7,26)}$=7.7918), premotor cortex (M2, p=0.0002; $F_{(7,26)}$=7.9059) and motor cortex (M1, p<0.0001; $F_{(7,26)}$=10.0459) following the treatment with quetiapine 30 mg/kg, as compared to the vehicle (Figure 8, panel a). Notably, the signal induction by the high dosage of quetiapine was significantly more pronounced than that by the low dosage in all subregions.

As opposed, the treatment with citalopram 14 mg/kg significantly decreased *Homer1a* expression as compared to all the other treatments in M1 ($p<0.0001$; $F_{(7,26)}=10.0459$), somatosensory cortex (SS, $p=0.0018$; $F_{(7,26)}=5.2770$), and insular cortex (I, $p<0.0001$; $F_{(7,27)}=8.7503$) (Figure 3, panel a).

In the caudate-putamen, *Homer1a* was significantly induced in all subregions (dorsomedial, CPDM, $p<0.0001$; $F_{(7,26)}=15.4234$; dorsolateral, CPDL, $p<0.0001$; $F_{(7,26)}=40.5786$; ventromedial, CPVM, $p<0.0001$; $F_{(7,26)}=21.0805$; ventrolateral, CPVL, $p<0.0001$; $F_{(7,26)}=10.1481$) following the treatment with haloperidol 0.8 mg/kg and haloperidol+valproate, as compared to all the other treatments (Figure 8, panel b). Notably, the administration of haloperidol alone induced *Homer1a* gene expression at a significantly higher extent than the co-administration of haloperidol+valproate in all subregions, with the exclusion of CPVM.

Both haloperidol and haloperidol+valproate treatments induced a significant *Homer1a* signal elevation in the nucleus accumbens core (AcCo, $p<0.0001$; $F_{(7,28)}=19.6507$) as compared to all the other treatments (Figure 8, panel b).

In the shell (AcSh, $p=0.0004$; $F_{(7,28)}=6.4996$), the gene was significantly induced by haloperidol as compared to all the other treatments excepted for the combinations of haloperidol+valproate and quetiapine 30mg/kg+valproate (Figure 8, panel b).

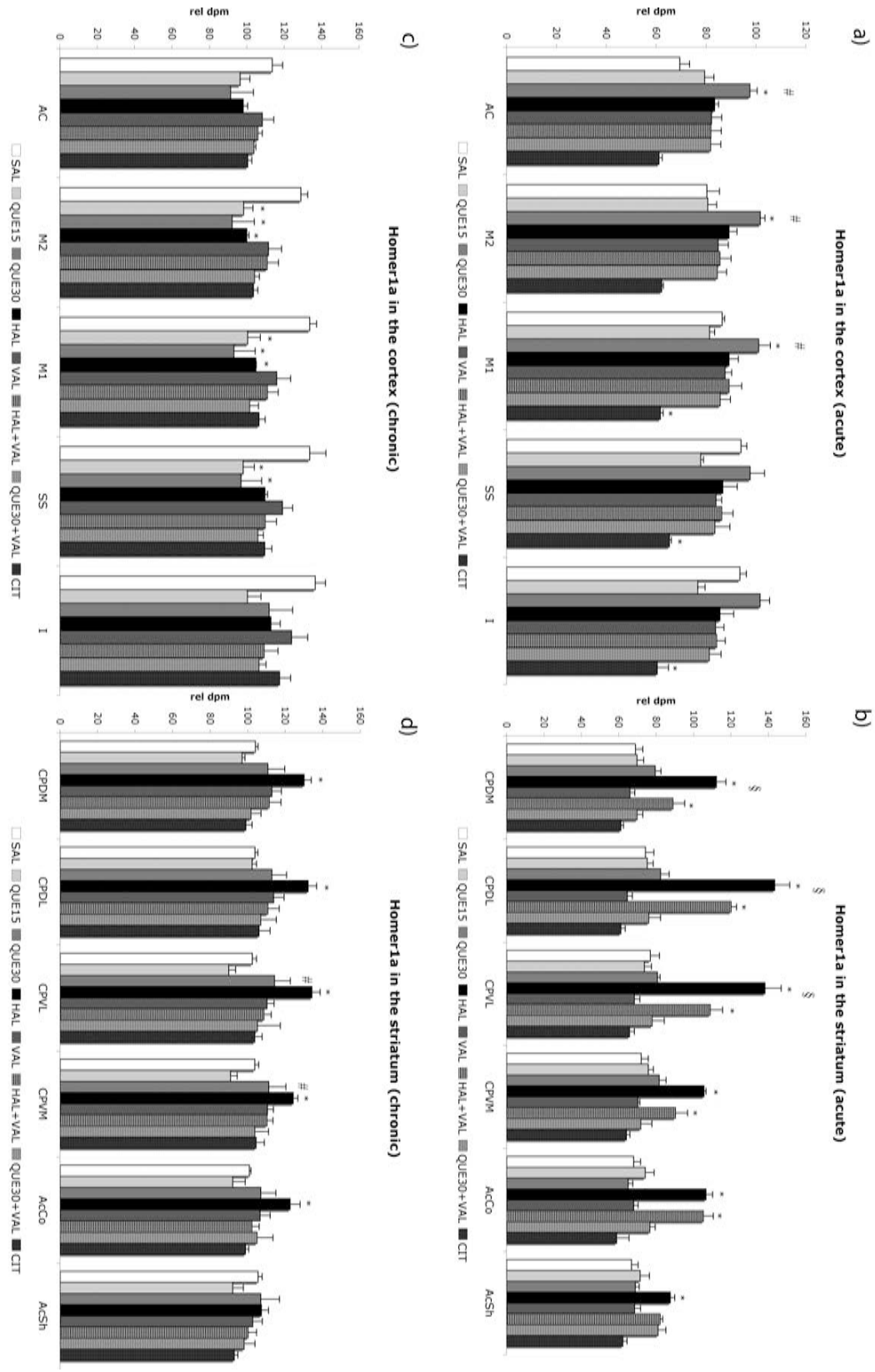

Figure 8. Homer 1a mRNA levels after acute (panels a and b) and chronic (panels c and d) treatment in cortex, caudate-putamen and nucleus accumbens. Data are reported in relative dpm as mean ± S.E.M. SAL=vehicle; QUE15=quetiapine 15mg/kg; QUE30=quetiapine 30mg/kg; HAL=haloperidol 0.8mg/kg; VAL=valproate 500mg/kg; HAL+VAL=haloperidol + valproate; QUE+VAL=quetiapine 30mg/kg + valproate; CIT=citalopram 14mg/kg.
SNK post hoc test: * = vs. SAL ($p<0.05$); # = QUE30 vs. QUE15 ($p<0.05$); § = HAL vs. HAL+VAL ($p<0.05$)

ERK

(results, with respective ANOVA values, are detailed in Table 4; autoradiographic images are shown in Figure 9)

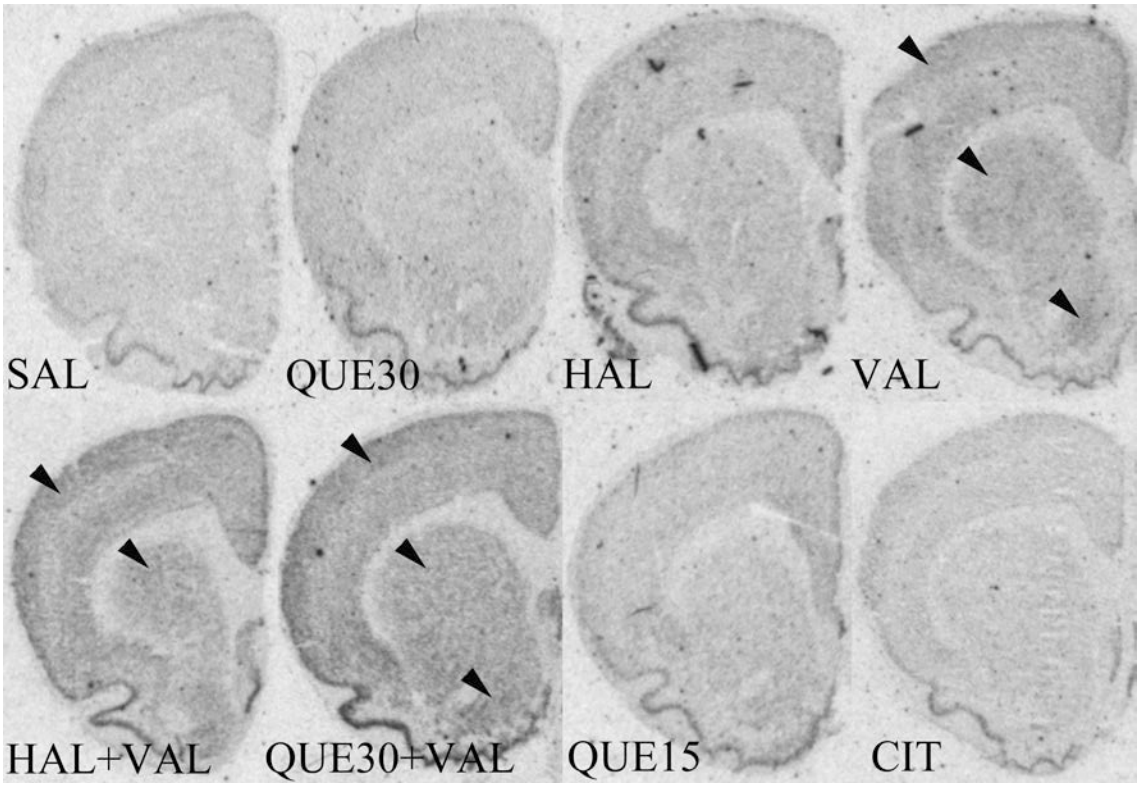

Figure 9. Representative autoradiographic film images of *ERK* mRNA detected by means of *in situ* hybridization histochemistry (ISHH) in coronal brain sections after acute treatment with vehicle (SAL), quetiapine 30mg/kg (QUE30), haloperidol 0.8mg/kg (HAL), valproate 500mg/kg (VAL), haloperidol+valproate (HAL+VAL), quetiapine 30mg/kg + valproate (QUE30+VAL), quetiapine 15mg/kg (QUE15), citalopram 14mg/kg (CIT). Brain areas in which significant changes in gene expression occurred with respect to vehicle are pointed out with black arrows for increases and white arrows for decreases.

Percentage of *PSD95* (upper side) and *ERK* (lower side) expression by treatments as compared to vehicle in acute paradigm

PSD95 Acute	QUE30	HAL	VAL	HAL+VAL	QUE30+VAL	QUE15	CIT	p-Value	$F_{(df)}$-Value
Cortex									
AC				125.64±9			133.98±12	0.0001	$F_{(7,39)}$=6.1728
M2		81.01±2				79.51±4	128.95±11	0.0001	$F_{(7,39)}$=6.1259
M1		72.23±2				72.73±3		0.0006	$F_{(7,39)}$=5.0817
SS				135.12±12			143.01±8	0.0004	$F_{(7,39)}$=5.3201
I							137.1±6	0.0004	$F_{(7,39)}$=5.4647
Caudate-putamen									
DM				122.74±12			135.57±12	0.0002	$F_{(7,38)}$=5.8089
DL							130.39±9	0.0007	$F_{(7,39)}$=5.0029
VL							127.33±4	0.0006	$F_{(7,38)}$=5.0935
VM							128.75±7	0.0002	$F_{(7,38)}$=5.8798
Nucleus Accumbens									
Core		80±3					123.6±5	0.0001	$F_{(7,39)}$=6.3589
Shell							120.77±11	0.0314	$F_{(7,39)}$=2.5812
ERK Acute									
Cortex									
AC			118.17±2	123.76±4	126.36±3			0.0005	$F_{(7,29)}$=6.0215
M2			120.26±4	124.96±6	125.52±4			0.0003	$F_{(7,29)}$=6.702
M1			120.58±7	122.47±7	126.27±2			0.0009	$F_{(7,29)}$=5.5293
SS			115±4	119.89±6	117.6±5			0.0105	$F_{(7,29)}$=3.551
I				115.53±4				0.036	$F_{(7,29)}$=2.6836
Caudate-putamen									
DM			121.28±5	126.72±8	122±6			0.0068	$F_{(7,29)}$=3.8757
DL			119.26±3	123.67±5	122.13±3			0.0016	$F_{(7,29)}$=5.0539
VL			114.77±2	116.8±5				0.0149	$F_{(7,29)}$=3.2995
VM			115.8±5	117.15±5	114.89±6			0.0061	$F_{(7,29)}$=3.9541
Nucleus Accumbens									
Core			120.03±3		124.15±4			0.0177	$F_{(7,29)}$=3.1738
Shell									

Table 4. The table summarizes significant changes *vs*. controls of *PSD95* and *ERK* expression in cortex and striatum after acute treatment by quetiapine 30mg/kg (QUE30), haloperidol 0.8mg/kg (HAL), valproate 500mg/kg (VAL), haloperidol+valproate (HAL+VAL), quetiapine 30mg/kg + valproate (QUE30+VAL), quetiapine 15mg/kg (QUE15), citalopram 14mg/kg (CIT). Data are expressed as a percentage of vehicle (SAL) relative dpm. mean value ± S.E.M. and listed by brain region analyzed, along with the relative ANOVA *p* and *F*(*df*) values. Increases in gene expression are shaded in dark grey and decreases in light grey

The treatment with valproate 500mg/kg, alone (VAL) or in association with either quetiapine 30mg/kg (QUE30+VAL) or haloperidol 0.8 mg/kg (HAL+VAL), elicited a significant upregulation of *ERK* gene expression in all cortical subregions analysed with respect to all the other treatments administered (Figure 10, panel a; AC, p=0.0005 $F_{(7,29)}$=6.0215; M2, p=0.0003 $F_{(7,29)}$=6.702; M1, p=0.0009 $F_{(7,29)}$=5.5293; SS, p=0.0105 $F_{(7,29)}$=3.551; I, p=0.036 $F_{(7,29)}$=2.6836)

Moreover, VAL, HAL+VAL and QUE30+VAL induced the overexpression of *ERK* in CPDM (p=0.0068; $F_{(7,29)}$=3.8757), CPDL (p=0.0016; $F_{(7,29)}$=5.0539) and CPVM (p=0.0061; $F_{(7,29)}$=3.9541) as compared to all the other treatments (Figure 10, panel b). In CPVL, valproate and haloperidol+valproate treatments significantly upregulated the gene as compared to SAL, HAL, QUE30 and QUE15 (p=0.0149; $F_{(7,29)}$=3.2995).

Finally, in the AcCo valproate, both alone or in association with quetiapine 30mg/kg, significantly increased *ERK* gene expression as compared to all the other treatments (Figure 10, panel b; $p=0.0177$; $F_{(7,29)}=3.1738$)

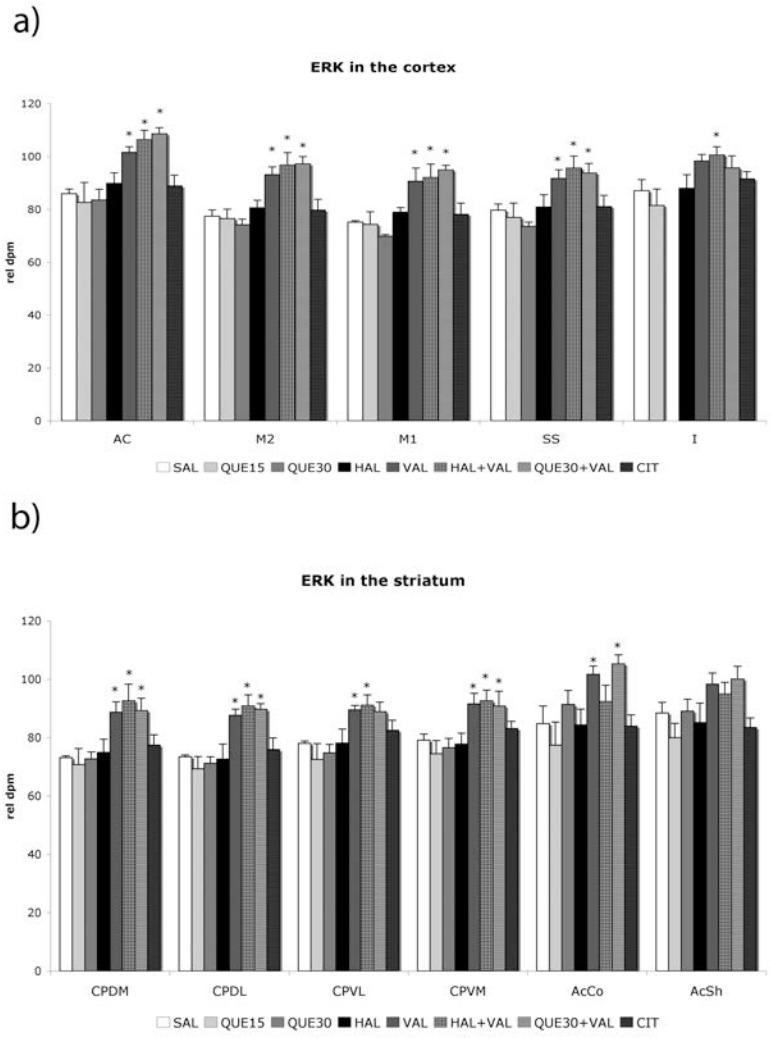

Figure 10. *ERK* mRNA levels after acute treatment in cortex, caudate-putamen and nucleus accumbens. Data are reported in relative dpm as mean ± S.E.M.
SAL=vehicle; QUE15=quetiapine 15mg/kg; QUE30=quetiapine 30mg/kg; HAL=haloperidol 0.8mg/kg; VAL=valproate 500mg/kg; HAL+VAL=haloperidol + valproate; QUE+VAL=quetiapine 30mg/kg + valproate; CIT=citalopram 14mg/kg.SNK *post hoc* test: * = *vs.* SAL ($p<0.05$)

PSD95

(results, with respective ANOVA values, are detailed in Table 4; autoradiographic images are shown in Figure 11)

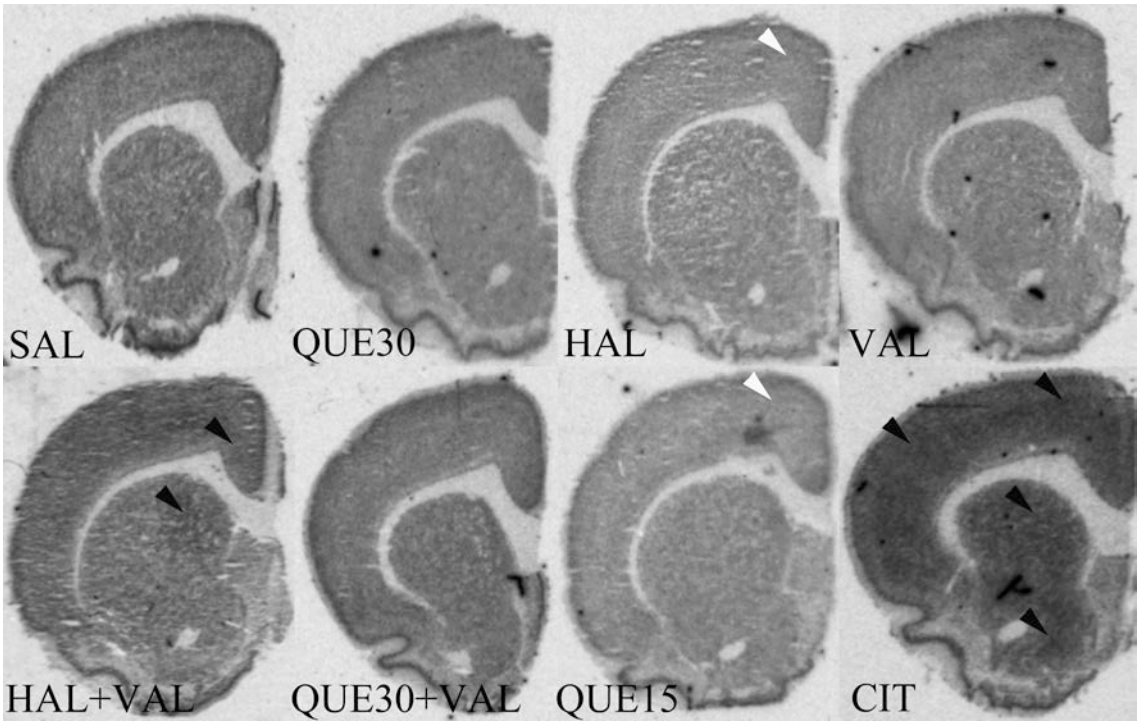

Figure 11. Representative autoradiographic film images of *PSD95* mRNA detected by means of *in situ* hybridization histochemistry (ISHH) in coronal brain sections after acute treatment with vehicle (SAL), quetiapine 30mg/kg (QUE30), haloperidol 0.8mg/kg (HAL), valproate 500mg/kg (VAL), haloperidol+valproate (HAL+VAL), quetiapine 30mg/kg + valproate (QUE30+VAL), quetiapine 15mg/kg (QUE15), citalopram 14mg/kg (CIT). Brain areas in which significant changes in gene expression occurred with respect to vehicle are pointed out with black arrows for increases and white arrows for decreases.

The acute administration of citalopram 14mg/kg significantly upregulated *PSD95* gene expression in AC ($p=0.0001$; $F_{(7,39)}=6.1728$), M2 ($p=0.0001$; $F_{(7,39)}=6.1259$), SS ($p=0.0004$; $F_{(7,39)}=5.3201$) and I ($p=0.0004$; $F_{(7,39)}=5.4647$) subregions of the cortex, with respect to all the other treatments (Figure 12, panel a).

Also the co-administration of haloperidol and valproate increased *PSD95* signal in AC ($p=0.0001$; $F_{(7,39)}=6.1728$) and SS ($p=0.0004$; $F_{(7,39)}=5.3201$) as compared to vehicle.

Oppositely, in both M2 ($p=0.0001$; $F_{(7,39)}=6.1259$) and M1 ($p=0.0006$; $F_{(7,39)}=5.0817$) the expression of *PSD95* was found decreased with respect to the vehicle, following the administration of haloperidol alone or quetiapine 15mg/kg.

PSD95 gene expression was significantly upregulated in all striatal subregions by CIT as compared to all the other treatments (Figure 5, panel a; CPDM, $p=0.0002$ $F_{(7,38)}=5.8089$; CPDL, $p=0.0007$ $F_{(7,39)}=5.0029$; CPVL, $p=0.0006$ $F_{(7,38)}=5.0935$; CPVM, $p=0.0002$ $F_{(7,38)}=5.8798$; AcCo, $p=0.0001$ $F_{(7,39)}=6.3589$; AcSh, $p=0.0314$ $F_{(7,39)}=2.5812$).

Interestingly, the association of haloperidol+valproate induced the acute overexpression of *PSD95* in the dorsomedial caudate-putamen ($p=0.0002$ $F_{(7,38)}=5.8089$), whereas the treatment with haloperidol alone significantly reduced *PSD95* expression in the AcCo with respect to all the other treatments ($p=0.0001$ $F_{(7,39)}=6.3589$)

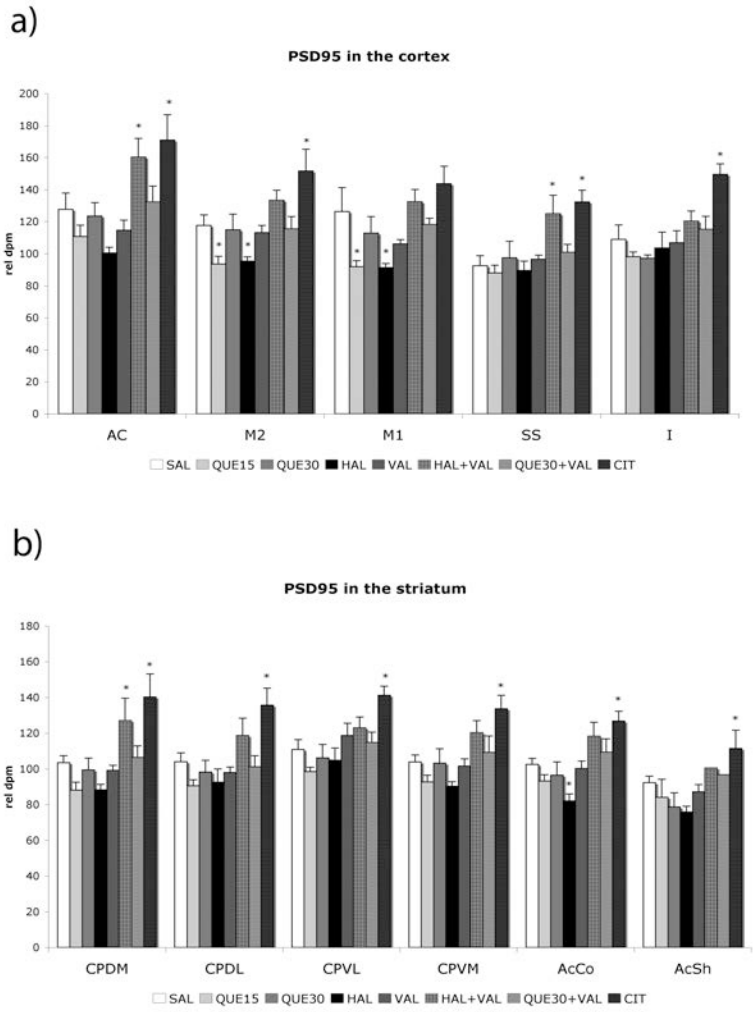

Figure 12. *PSD95* mRNA levels after acute treatment in cortex, caudate-putamen and nucleus accumbens. Data are reported in relative dpm as mean ± S.E.M.
SAL=vehicle; QUE15=quetiapine 15mg/kg; QUE30=quetiapine 30mg/kg; HAL=haloperidol 0.8mg/kg; VAL=valproate 500mg/kg; HAL+VAL=haloperidol + valproate; QUE+VAL=quetiapine 30mg/kg + valproate; CIT=citalopram 14mg/kg.SNK *post hoc* test: * = *vs.* SAL ($p<0.05$)

GSK3b, Homer1b/c

ANOVA did not reveal any significant difference among groups in both cortical and subcortical regions ($p<0.05$).

Chronic paradigm

We evaluated the impact on the postsynaptic density of the prolonged administration of quetiapine (15 mg/kg and 30 mg/kg), haloperidol, valproate, citalopram and the association of valproate with quetiapine 30mg/kg or haloperidol, by assessing the expression of *Homer1a, ERK, PSD95, GSK3b* and *Homer1b/c* after daily administration of the drugs over a period of 16 days.

Homer1a

(results, with respective ANOVA values, are detailed in Table 4, autoradiographic images are shown in Figure 13)

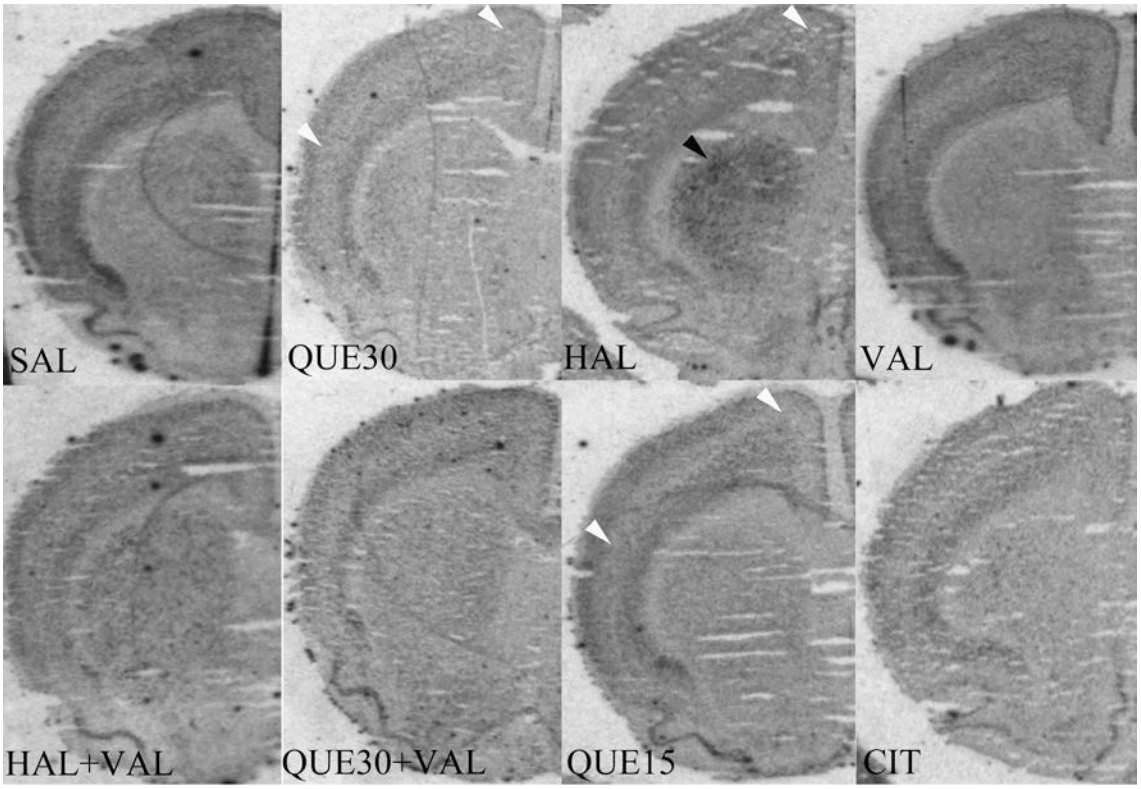

Figure 13. Representative autoradiographic film images of *Homer1a* mRNA detected by means of *in situ* hybridization histochemistry (ISHH) in coronal brain sections after chronic treatment with vehicle (SAL), quetiapine 30mg/kg (QUE30), haloperidol 0.8mg/kg (HAL), valproate 500mg/kg (VAL), haloperidol+valproate (HAL+VAL), quetiapine 30mg/kg + valproate (QUE30+VAL), quetiapine 15mg/kg (QUE15), citalopram 14mg/kg (CIT). Brain areas in which significant changes in gene expression occurred with respect to vehicle are pointed out with black arrows for increases and white arrows for decreases.

The chronic treatment with haloperidol 0.8mg/kg, quetiapine 15 mg/kg and quetiapine 30mg/kg significantly decreased the *Homer1a* signal in premotor cortex (M2, p=0.0075; $F_{(7,30)}$=3.7434) and motor cortex (M1, p= 0.0065; $F_{(7,30)}$=3.8519) with respect to vehicle. Also, both the low and the high dosage of quetiapine reduced *Homer1a* expression in SS (p=0.0085; $F_{(7,30)}$=3.6566) as compared to SAL (Figure 8, panel c).

As described in previous works [85,99], the expression of *Homer1a* was significantly induced by chronic haloperidol treatment in all caudate-putamen subregions and in the nucleus accumbens core as compared to all the other treatments (Figure 3, panel d; CPDM, p=0.0037 $F_{(7,30)}$=4.2776; CPDL, p=0.0211 $F_{(7,30)}$=3.0164; CPVL, p=0.0015 $F_{(7,30)}$=5.0167; CPVM, p=0.0089 $F_{(7,30)}$=3.6240; AcCo, p=0.0473 $F_{(6,26)}$=2.6411). No statistically significant differences were noticed in AcSh subregion (p>0.05).

Notably, in ventral striatal regions (CPVM, CPVL), the increase in *Homer1a* signal by QUE30 was significantly higher than QUE15 (Figure 8, panel d).

ERK, PSD95, GSK3b, Homer1b/c

ANOVA did not reveal any statistically significant change for these genes either in cortical or subcortical subregions analysed (p>0.05).

Discussion

Results showed that, in the acute paradigm, the combined treatment with haloperidol plus valproate induced striatal *Homer1a* expression at a lesser extent as compared to that induced by haloperidol alone. In fact, as already described in our previous studies

[99,85,140,17,247], in caudate-putamen *Homer1a* expression was strongly induced by haloperidol compared to all the other treatments. Indeed, haloperidol plus valproate association also robustly induced the gene, but demonstrated a significant reduction in the extent of the increase of *Homer1a* signal as compared to haloperidol alone. Since several clinical and preclinical studies demonstrated that haloperidol and valproate do not interfere with each other with regard to their plasma concentrations [299] and that haloperidol does not potentiate valproate action on DNA methylation and histone deacetylase activity [300,301], we could hypothesize that the reduced extent in *Homer1a* induction may depend upon a direct interaction between the intracellular pathways activated by the two different drugs. This view might be supported by the recent evidence that valproate may modulate the Akt-GSK3b and ERK signaling [272,259], which could be also regulated by antipsychotics (Beaulieu et al., 2009; [302]. Acute haloperidol administration is known to increase dopamine release in the striatum [303], and to induce immediate-early genes expression [304]; Polese et al., 2002) through a mechanism involving NMDAR activation [305]. Little is known about the intracellular pathway implicated in this action. It is possible that haloperidol increases the release of dopamine by blocking the negative feedback mechanism of nigrostriatal dopamine system and the released dopamine stimulates D1 receptors, which in turn may directly impact NMDA currents in striatum [306]. Recent observations stated that NMDA-D1 interaction may lead to a synergistic enhancement of ERK1/2 pathway activation [307], which has been demonstrated to promote Homer1a transduction [308]. Alternatively, haloperidol might stimulate *Homer1a* expression through promoting directly ERK activation via a D2-mediated mechanism in specific striatal neurons [302]. Moreover, recent studies found that GSK3b seems to be specifically required in NMDA-D2 receptors subcellular interaction [309]. Thus, we could hypothesize that the reduction in the extent of *Homer1a* striatal expression when valproate is associated to

haloperidol may be due to a direct modulation by valproate of the Akt-GSK3b/ERK transductional pathway stimulated by haloperidol, which controls *Homer1a* transcription.

Nevertheless, no significant differences among treatments were detected with regard to *GSK3b* expression, in both acute and chronic paradigm of our study. This finding may apparently diverge from results of recent literature that implicates GSK3b in the mechanisms of action of mood stabilizers [310]. On the other hand, recent observations demonstrated that valproate may impact GSK3b phosphorylation, thus reducing functions of this protein, but it is not able to modify *GSK3b* mRNA levels [311]. Therefore, it is possible that valproate (and some other mood stabilizers), might be able to regulate GSK3b activity without impact its gene expression.

In the chronic paradigm, haloperidol induced *Homer1a* expression in all the subregions of the caudate-putamen and in the nucleus accumbens core. These results closely resemble those of our previous works, confirming the correlation between *Homer* expression and the degree of dopamine D2 receptors blockade in specific regions of the striatum and remarking that *Homer1a* may respond to prolonged dopaminergic stimuli without displaying tolerance phenomena. Moreover, it is notable that the combined treatment with haloperidol plus valproate did not elicit any significant change in *Homer1a* expression in the chronic protocol. This may strengthen the hypothesis that valproate could perturb the transductional pathways eventually stimulated by haloperidol, thus impacting the downstream leading to *Homer1a* expression. Obviously, more studies are warranted on this hypothesis. Recently, several animal models have been proposed [312] that mimic the behavioral phenotype of bipolar disorder, although this is yet a challenging field of study. Nevertheless, the fact that some of these models originate from genetic manipulations just in the genes which have been the subjects of

our work (i.e. *GSK3b*), might help to clarify the impact of mood stabilizers and antipsychotics, as well as of their combination, on these transductional pathways. The present data also demonstrated that quetiapine and haloperidol have divergent effects in corticostriatal regions with regard to *Homer1a* induction. In previous works [143] we hypothesized that *Homer1a* expression may be region-specific and directly correlated to the dopaminergic neurotransmission in both cortical and subcortical regions. Moreover, this gene may respond to drugs impacting serotonergic neurotransmission in cortical subregions [17,247]. Results showed, in fact, that *Homer1a* gene expression was decreased in motor, somatosensory and insular cortices by citalopram acute administration. Indeed, recent studies identified both secondary motor and somatosensory cortices as primary targets of citalopram anxiolytic effects [313]. Furthermore, the high dose of quetiapine strongly induced *Homer1a* expression in anterior cingulate, premotor and motor subregions of the cortex, resulting in a statistically significant increase as compared to the lower dose. This would strengthen the hypothesis that the serotonergic neurotransmission might exert an essential role in controlling the transductional pathways in which *Homer* is involved in the cortex. Nevertheless, the substantial opposite direction of *Homer1a* expression by citalopram and quetiapine in the cortex may be explained by the different mechanisms of action of the two drugs. Quetiapine has multiple binding profiles, with stronger affinities to 5HT1a and 5HT2a serotonin receptors than to dopamine D2 receptors [314], exerting partial agonism at 5HT1a, antagonism at 5HT2a and antagonism at D2 receptors. Several studies described that high doses, but not low doses, of quetiapine may induce dopamine release in the cortex, without affecting serotonin [315,316,286]. Moreover, neither the sole D2 antagonism, nor the 5HT2a antagonism, may affect dopamine or serotonin cortical release [317,318], while combined 5HT2a-D2 antagonism may strongly increase dopamine release in prefrontal cortex [319]. Citalopram alone has

been demonstrated not to affect dopamine release in the cortex, whereas it stimulates a strong serotonin release and potentiates dopamine release induced by antipsychotic agents [293]. The hypothesis of a combined serotonergic-dopaminergic control of *Homer* expression in the cortex may explain the lack of effect by acute haloperidol alone in this region and is consistent with findings of our previous work [247]. Furthermore, the fact that the citalopram-induced *Homer1a* down-regulation was found only in acute administration, whereas we found that haloperidol and quetiapine decreased the gene in the chronic paradigm, may confirm the prominent dopaminergic control of *Homer* expression after long-term stimulation [140,17].

Taken together, our data seem consistent with recent evidence of the downregulation of *Homer1* gene in animal models of depression [320] and a modulation of this gene by quetiapine administration [321], further reinforcing the hypothesis of a potential antidepressant-like action of this antipsychotic drug.

ERK gene was upregulated in both cortical and striatal regions by acute administration of valproate and valproate plus haloperidol or quetiapine, while neither haloperidol nor quetiapine alone significantly impacted the expression of the gene. These results are in agreement with recent evidence that valproate may promote Erk-dependent pathways (Hao et al., 2004). As discussed above, it is possible that both haloperidol and quetiapine, when administered in combination with valproate, might lead to a synergistic activation of intracellular pathways that could in turn enforce specific downstream cascades. Since no significant changes were noticed in the chronic paradigm, we could hypothesize that molecular modifications induced by valproate might occur with a peculiar time-course, as observed for *Homer1a*.

PSD95 showed a significant upregulation by acute citalopram and by haloperidol plus valproate in the cortical subregions analysed, as well as in the nucleus accumbens. Haloperidol and quetiapine 30mg/kg, oppositely, significantly reduced the expression of

the gene. Furthermore, in the caudate-putamen, citalopram induced increase in *PSD95* expression, in the acute paradigm.

PSD95 is a postsynaptic scaffold protein, which could interact with Homer long isoforms in order to form clusters that physically connect mGluRs with NMDAR downstream pathways (NMDAR-PSD95-GKAP-Shank-Homer cluster) [322]. Actually, there is a substantial dearth of data on *PSD95* modulation by psychotropic drugs, therefore our findings stimulate further investigations about this issue. However, our results show that changes in *PSD95* expression were found only after acute administration. It is likely to hypothesize that some PSD elements may display tolerance phenomena during prolonged administration, because of synaptic rearrangements. This view seems to be consistent with recent findings that PSD95 modifications in psychostimulants self-administration protocols are shown only during the first phases of cocaine extinction, and they are not more noticeable after some days [323,324].

It could be hypothesized that changes in gene expression described in this study may correlate with possible toxic effects of the drugs administered, triggered by high doses. However, drugs were used here in doses known to elicit biological and behavioral effects related to the interaction with their primary target rather than with secondary non-specific targets [285-287,284]. Nonetheless, the possibility remains that high drug doses may cause toxic effects for excessive interaction with their primary target. According to this consideration, a strong suggestion has been previously made by us [325] that increased *Homer1a* expression may be related to motor side effects of antipsychotic drugs, which become more evident with increasing doses of these compounds. Indeed, overexpression of striatal *Homer1a* has been associated to the impairment of locomotor activity [256]. A future dose-response study will help clarifying this intriguing issue.

With regard to the differential regional impact of the distinct drugs administered in this study, it is noteworthy that they affected the expression of the diverse PSD genes in brain regions that have specifically been implicated in the pathophysiology of bipolar disorder (for a review, see [277]). Indeed, several studies have demonstrated that functionally distinct cortical subregions project to specific striatal areas, and that analyzing gene expression changes induced by psychotropic drugs may elucidate the functional domains affected by these drugs [298,297]. For instance, both quetiapine and valproate (alone or in association) modified the expression of *Homer1a* in cortical regions that are functionally involved in motor control (medial agranular and motor cortices) and in monitoring cognitive and behavioral aspects of emotion (cingulate and insular cortices). The cortical premotor and motor areas project specifically to the dorsolateral regions of the striatum, which specifically control somatomotor inputs; cingulate and insular cortices project to the ventral striatum, mostly implicated in behavioral control. Both motor and behavioral aspects have been specifically considered as primary characteristics of the symptomatology of bipolar disorder. Thus, albeit preliminary, our data about the different response pattern of PSD genes to the different drugs commonly used in clinical practice to treat bipolar disorder may provide an additional avenue of investigation in clarifying their action in specific brain areas involved in mood modulation.

VII. Study n.2: Chronic treatment with lithium or valproate modulates the expression of *Homer1b/c* and its related genes *Shank* and *Inositol 1,4,5–trisphosphate receptor*

As previously discussed, the combined administration of antipsychotics and valproate (VPA) may induce differential modulation of PSD genes—particularly *Homer*-related genes—compared to the effects observed when these drugs were administered individually [146]. However, to the best of our knowledge, no study to date has investigated the manner in which the mood stabilizers lithium and VPA regulate *Homer* genes. This is unexpected, given that clinical [326] and preclinical [327] evidence have implicated glutamate in the pathophysiology of bipolar disorder, and that dopamine neurotransmission is believed to play a role in the mechanism of action of mood stabilizers [249]. In addition, recent studies have directly implicated *Homer1* in the etiology of mood disorders [328]. This dearth of information is even more surprising considering that Homer proteins modulate the phosphoinositide (PI) signaling pathway [329], one of the most extensively studied targets of lithium, and which has also recently been studied as a putative target of VPA [330,331]. Furthermore, Homer has been implicated in the modulation of the phosphatidylinositol-3-kinase – Akt (PI3K-Akt) pathway [332], which, in turn, was shown to directly regulate the function of glycogen synthase kinase 3β (GSK-3β), a well-recognized molecular target of mood stabilizers [259].

An intriguing connection also appears to exist between the Homer proteins, the mGluRs, intracellular calcium concentrations, and the enzyme protein kinase C (PKC) [88], whose protein levels are also affected by chronic *in vivo* administration of lithium and VPA [333]. In addition, recent observations suggest that Homers play a major role in modulating the complex signaling machinery that routes signals from postsynaptic

receptors (mGluRs and N-methyl-D-aspartate receptors (NMDARs)) to the Mitogen activated protein kinase – Extracellular signal-regulate kinase1/2 (MAPK-ERK1/2) pathway [334], which has been putatively implicated in mood modulation and in the mechanism of action of mood stabilizers [271,335].

The present study investigated the manner in which chronic administration of lithium and VPA, at therapeutic doses, modulates the inducible and constitutive transcripts of *Homer1.* We evaluated the expression of *Homer* genes by means of *in situ* hybridization histochemistry, focusing on the cortex, caudate-putamen, and nucleus accumbens; all of these areas are believed to be involved in the pathophysiology of bipolar disorder [277] and in the mechanism of action of mood stabilizers [336].

We chose to explore both inducible and constitutive Homer isoforms (i.e. *Homer1a* and *Homer 1b/c* respectively) based on previous studies (Tomasetti et al., 2007; Iasevoli et al., 2010) showing that chronic administration of antipsychotics may affect both transcripts. A recent study from our laboratory (Tomasetti et al., 2011) analyzed *Homer1a* following the administration of VPA—alone or in association with antipsychotic drugs—in both acute and chronic paradigm of injected administration; building on that work, the present study compared the effects of both lithium and VPA on *Homer1* transcripts in a chronic paradigm of oral administration. This model was chosen in order to more closely approximate the conditions necessary to obtain pharmacological effects with mood stabilizers in clinical practice, and to assess the impact of prolonged oral drug administration on *Homer* expression.

We also evaluated the possible involvement of *Shank* and *Inositol 1,4,5 trisphosphate receptor* (*IP3R)*, two genes tightly related to *Homer* function, and which share a prominent role in synaptic plasticity.

Experimental Procedures

Animals, drug treatments, and tissue preparation

Adult male Wistar-Kyoto (WKY) rats (weight 175–200g) were housed in a temperature- and humidity-controlled colony room with access to water and food *ad libitum*, maintained under a 12-hour light/dark cycle, and allowed a one-week accommodation period before initiation of experiments. All experimental procedures were carried out in accordance with the guidelines published in the National Research Council (NRC) *Guide for the Care and Use of Laboratory Animals* (NIH Publication N.85-23, revised 1996), and were approved by the National Institute of Mental Health (NIMH) Animal Care and Use Committee. All efforts were made to minimize the number of animals used and their suffering.

Rats (n=5 for each experimental group) were randomly assigned to a treatment group and fed either: 1) regular rodent chow (control), 2) lithium carbonate-containing chow (2.4 g/kg), or 3) VPA-containing chow (20 g/kg) (custom produced by Bio-Serv, Frenchtown, NJ, USA) for four weeks. In addition to tap water, a bottle of saline was available to rats in order to minimize any electrochemical imbalance that might occur during the treatment. At the end of treatment, rats were killed by decapitation between 9:00 A.M. and 12:00 P.M., trunk blood samples were collected in order to monitor drug concentrations, and the whole brain was rapidly removed, quickly frozen on powdered dry ice, and stored at -80°C. Serum drug concentrations were confirmed to be within the therapeutic range (lithium 0.5~1.0mEq/l, VPA 50~100μg/ml).

Serial coronal sections of 12μm were cut on a cryostat at -18°C at the level of the striatum (approx. from Bregma -1.20mm to -1.00mm), using the rat brain atlas of

Paxinos and Watson [295] as an anatomical reference. Sections were stored at -80°C for subsequent analysis.

Radiolabeling

Details for all the probes are listed in Table 5.

Probes for *In Situ* Hybridization Histochemistry

Probe	cDNA length (bp)	cDNA position	mRNA	GenBank #
Homer1a	48	2527-2574	*Homer1a*	U92079
Ania-3	48	1847-1894	*ania-3*	AF030088
Homer1b/c	48	1306-1353	*Homer1b/c*	AF093268
Shank	48	2757-2804	*Shank1*	AF131951
IP3R	48	7938-7985	*IP3R*	J05510

Homer 1a, ania-3, and *Homer1b/c* probes were oligodeoxyribonucleotides derived from identical probes used in previous hybridization studies [99,17]. All other probes were designed from GenBank sequences and checked with BLAST to avoid cross-hybridization. All oligodeoxyribonucleotides were purchased from MWG Biotech (Firenze, Italy).

For each probe, a 50µl labeling reaction mix was prepared on ice using DEPC-treated water, 1X tailing buffer, 7.5pmol/µl of oligodeoxyribonucleotide, 125 Units of Terminal deoxynucleotidyl Transferase (TdT) and 100mCi ^{35}S-dATP. The mix was incubated for 20 minutes at 37°C. The unincorporated nucleotides were separated from radiolabeled DNA using ProbeQuant G-50 Micro Columns (Amersham-GE Healthcare Biosciences, Milano, Italy). To assess probe specificity, the autoradiographic signal distribution was compared and found to be consistent with previous *in situ* hybridization studies [81,99].

In Situ Hybridization Histochemistry

Sections were processed for radioactive *in situ* hybridization [296]. All solutions were prepared with sterile double-distilled water. The sections were fixed in 4% formaldehyde in 0.12 M phosphate buffered saline (PBS, pH 7.4), quickly rinsed three times with 1X PBS, and placed in 0.25% acetic anhydride in 0.1 M triethanolamine/0.9% NaCl, pH 8.0 for 10 minutes. Next, the sections were dehydrated in 70%, 80%, 95%, and 100% ethanol, delipidated in chloroform for five minutes, rinsed again in 100% and 95% ethanol, and air-dried.

Sections were hybridized with 0.4-0.6x10^6 cpm of radiolabeled oligonucleotide in buffer containing 50% formamide, 600mM NaCl, 80mM Tris-HCl (pH 7.5), 4mM EDTA, 0.1% pyrophosphate, 0.2mg/ml heparin sulfate, and 10% dextran sulfate. Slides were covered with coverslips and incubated at 37°C in a humid chamber for 22-24 hours. After hybridization, the coverslips were removed in 1X saline sodium citrate solution (SSC) and the sections were washed 4x15 minutes in 2X SSC/50% formamide at 43-44°C, followed by two 30-minute washes with 1X SSC at room temperature. The slides were rapidly rinsed in distilled water and then in 70% ethanol.

Autoradiography and Image Analysis

The sections were dried and exposed to Kodak-Biomax MR Autoradiographic film (Sigma-Aldrich, Milano, Italy). A slide containing a scale of 16 known amounts of ^{14}C standards (American Radiolabeled Chemicals, St. Louis, US) was co-exposed with the samples. The autoradiographic films were exposed over 14-30 days. The optimal time of exposure was chosen to maximize signal-to-noise ratio but to prevent optical density from approaching saturation limits. Film development protocol included a 1.5-minute dip in the developer solution and three minutes in the fixer. The quantitation of the autoradiographic signal was performed using a computerized image analysis system,

including: a transparency film scanner (Microtek Europe B. V., Rotterdam, The Netherlands), an Apple iMac, and ImageJ software (v. 1.40, Rasband, W.S., http://rsb.info.nih.gov/ij/). Brain sections on film were captured individually. Scanned images were showed in inverted look-up table (LUT) color, although all the other original characteristics (i.e. contrast, brightness, resolution) were preserved. Each experimental group contained five animals. Each slide contained three adjacent sections of a single animal. All hybridized sections were exposed on the same sheet of X-ray film. Signal intensity analysis was carried out on digitized autoradiograms measuring mean optical density within outlined Regions of Interest (ROIs) corresponding to subregions of the cortex, caudate-putamen, and nucleus accumbens (Figure 14). These cortical and striatal subregions are structurally and functionally interconnected through projections from the cortex, which targets specific striatal sectors. Thus, ROIs were chosen based on functional mapping studies of gene expression [297] and other studies analyzing *Homer* expression in response to drugs [146]. Sections were quantitated blind to the treatment conditions. To test for inter-observer reliability an independent quantitation was performed by a second investigator. Results were considered reliable only when the statistical significance of effects obtained by the second investigator was quantitatively consistent with the results obtained by the first investigator.

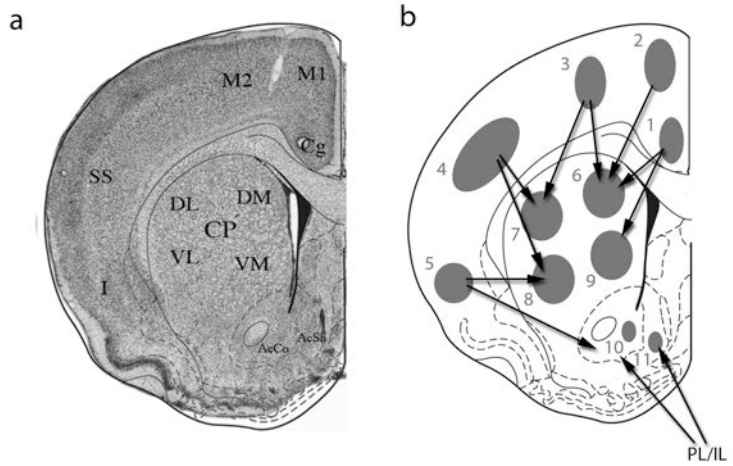

Figure 14. *Panel a.* Diagram of regions of interest (ROIs) quantitated on autoradiographic film images in rat forebrain (section coordinates are approximate from Bregma 1.20 mm to 1.00 mm). 1 = cingulate cortex (Cg); 2 = medial agranular cortex (M2); 3 = motor cortex (M1); 4 = somatosensory cortex (SS); 5 = insular cortex (I); 6 = dorsomedial caudate-putamen (CPDM); 7 = dorsolateral caudate-putamen (CPDL); 8 = ventrolateral caudate-putamen (CPVL); 9 = ventromedial caudate-putamen (CPVM); 10 = core of nucleus accumbens (AcCo); 11 = shell of nucleus accumbens (AcSh). Modified from Paxinos and Watson (1997).
Panel b. Illustration of cortico-striatal projections among the ROIs in which gene expression induced by mood stabilizers was measured. PL/IL = prelimbic/infralimbic cortices (not shown).

Data processing

Measurements of mean optical density within ROIs were converted using a calibration curve based on the standard scale co-exposed to the sections. ^{14}C standard values were previously cross-calibrated to ^{35}S brain paste standards, in order to assign a dpm/mg tissue wet weight value to each optical density measurement through a calibration curve. For this purpose, a "best fit" 3rd degree polynomial was used. For each animal, measurements from the three adjacent sections were averaged and the final data were reported in relative disintegrations per minute (rel d.p.m.) as mean ± the standard error of the mean (S.E.M.). A one-way ANOVA was used to analyze treatment effects. Statistical significance was established at $p<0.05$. The Tukey's *post hoc* test was used to determine the locus of effects for significant ANOVA results.

Results

The effects of chronic administration of lithium or VPA on *Homer1b/c*, *Shank*, *IP3R* *Homer1a,* and *ania-3* gene expression in each forebrain subregion analyzed are presented in Table 6.

mRNA levels of *Homer1b/c*, *Shank*, *IP3*, *Homer1a* and *ania-3* after chronic administration of lithium or valproate

	Homer1b/c			
	Lithium	Valproate	P-Value	$F_{(df)}$-Value
Cg	93.96±2.9	87.52±2.1*	0.0137	$5.491_{(2,18)}$
M2	90.96±3.2	87.41±2.1*	0.016	$5.249_{(2,18)}$
M1	90.54±3.4	88.57±2.2*	0.0337	$4.115_{(2,18)}$
SS	92.57±3.7	89.4±3.0	0.117	$2.414_{(2,18)}$
I	85.59±2.5*	86.68±2.8*	0.0158	$5.265_{(2,18)}$
CPDM	92.6±2.3	83.9±2.5*	0.004	$7.398_{(2,18)}$
CPDL	88.3±2.1*	80.7±1.7*	0.0001	$15.552_{(2,18)}$
CPVL	91.8±2.8	83.3±1.9*	0.002	$8.536_{(2,18)}$
CPVM	92.2±3	89.6±2.8*	0.009	$6.108_{(2,18)}$
AcCo	90.4±3.6	85.7±2*	0.015	$5.432_{(2,17)}$
AcSh	96.8±3.2	89.5±3	0.154	$2.091_{(2,17)}$

	Shank				IP3R			
	Lithium	Valproate	P-Value	$F_{(df)}$-Value	Lithium	Valproate	P-Value	$F_{(df)}$-Value
Cg	103.48±2.1	96.35±0.6	0.0047	$7.466_{(2,17)}$	90.25±1.5*	93.64±2.2	0.0456	$4.038_{(2,12)}$
M2	101.26±2.1	94.6±0.7*	0.0107	$5.993_{(2,17)}$	86.79±1.2	92.55±3	0.0823	$3.097_{(2,12)}$
M1	99.53±1.8	94.85±1*	0.034	$4.153_{(2,17)}$	83.35±1.4*	86.73±2	0.048	$3.952_{(2,12)}$
SS	101.06±1.5	96.53±0.9	0.0157	$5.359_{(2,17)}$	86.06±0.9*	86.85±1.8	0.0181	$5.712_{(2,12)}$
I	102.61±2.6	94.74±1.6	0.0178	$5.155_{(2,17)}$	89.82±1.2*	90.17±1.4	0.0346	$4.510_{(2,12)}$
CPDM	100.9±3.2	94.9±2.5	0.29	$1.326_{(2,18)}$	89.63±1.9	89.12±2.4	0.096	$2.821_{2,13)}$
CPDL	101.3±3.5	97.9±2.9	0.679	$0.395_{(2,18)}$	83.65±1.6	81.3±2.8*	0.0265	$4.863_{(2,13)}$
CPVL	102.6±3.3	96.7±2.3	0.333	$1.167_{(2,18)}$	87.53±2.2	83.51±2.4	0.138	$2.311_{(2,13)}$
CPVM	104.6±3.4	99.2±2.2	0.3	$1.288_{(2,18)}$	86.87±1.6	85.66±1.9	0.0788	$3.128_{(2,13)}$
AcCo	101.5±2.2	96.9±1.3	0.352	$1.107_{(2,18)}$	95.17±2.1	92.22±0.9	0.296	$1.336_{(2,13)}$
AcSh	102.4±2.2	97.2±1.4	0.248	$1.505_{(2,18)}$	89.39±2	90.13±2.9	0.0423	$4.074_{(2,13)}$

	Homer1a				Ania-3			
	Lithium	Valproate	P-Value	$F_{(df)}$-Value	Lithium	Valproate	P-Value	$F_{(df)}$-Value
Cg	85.63±7.4	88.4±11.2	0.671	$0.410_{(2,13)}$	90.13±5.1	89.67±6	0.448	$0,843_{(2,16)}$
M2	87.03±5.6	90.31±10.3	0.556	$0.614_{(2,13)}$	90.91±3.9	89.93±5.9	0.332	$1.180_{(2,16)}$
M1	88.85±3.8	103.32±9.9	0.369	$1.075_{(2,13)}$	93.2±2.9	93.43±4.7	0.398	$0.974_{(2,16)}$
SS	90.19±8	100.15±8	0.553	$0.620_{(2,13)}$	93.54±3.7	101.19±3.7	0.264	$1.448_{(2,16)}$
I	80.74±5.1	83.74±7	0.0594	$2.822_{(2,13)}$	88.67±3.8	95.55±3.8	0.107	$2.569_{(2,16)}$
CPDM	98.3±11.3	87.2±8.6	0.258	$1.483_{(2,15)}$	93.8±4.4	97.3±3.3	0.466	$0.805_{(2,14)}$
CPDL	95.7±4.5	88.4±5.4	0.364	$1.082_{(2,15)}$	99.2±4.8	98.2±2.8	0.921	$0.082_{(2,14)}$
CPVL	97.6±6	91.7±4.4	0.486	$0.756_{(2,15)}$	95.9±2.9	100±2.4	0.481	$0.770_{(2,14)}$
CPVM	93.8±4.6	85.1±6.3	0.191	$1.849_{(2,15)}$	92.4±2.2	96.9±3.9	0.29	$1.351_{(2,14)}$
AcCo	94.9±5.4	88.6±5.7	0.463	$0.810_{(2,15)}$	94.7±2.9	96±4.4	0.544	$0.635_{(2,14)}$
AcSh	104.2±6.7	92.6±7	0.593	$0.541_{(2,15)}$	97.5±2.7	95.7±5.3	0.788	$0.242_{(2,14)}$

Table 6. mRNA levels of Homer1b/c, Shank, IP3, Homer1a and ania-3 after chronic administration of lithium or valproate. Data are expressed as a percentage of control (CTR) relative dpm mean value ± S.E.M and listed by brain region analyzed along with the relative ANOVA values ($p<0.05$). Cg= cingulate cortex; M2= medial agranular cortex; M1= motor cortex; SS= somatosensory cortex; I= insular cortex; CPDM= dorsomedial caudate-putamen; CPDL= dorsolateral caudate-putamen; CPVL= ventrolateral caudate-putamen; CPVM= ventromedial caudate-putamen; AcCo = nucleus accumbens core; AcSh = nucleus accumbens shell.
* = significant differences from CTR at the Tukey's post hoc test

Homer1b/c (Figure 15)

We analyzed the autoradiographic signal of *Homer1b*/c mRNA in the cortex, caudate-putamen, nucleus accumbens core, and nucleus accumbens shell. In the cortex, the *Homer1b/c* signal was significantly reduced in cingulate (Cg; $p=0.0137$; $F_{(dl)}=5.491_{(2,18)}$), medial agranular (M2; $p=0.016$; $F_{(dl)}=5.249_{(2,18)}$), motor (M1; $p=0.0337$; $F_{(dl)}=4.115_{(2,18)}$), and insular (I; $p=0.0158$; $F_{(dl)}=5.265_{(2,18)}$) areas by VPA treatment compared to control. The lithium-treated group displayed a similar pattern of *Homer1b/c* signal reduction in cortical subregions as the VPA-treated group, but these results did not reach statistical significance.

In the striatum, the ANOVA analysis revealed that both lithium and VPA significantly decreased the *Homer1b/c* signal compared to control in the dorsolateral caudate-putamen (CPDL; $p=0.0001$; $F_{(dl)}=15.552_{(2,18)}$). In all the other subregions of the caudate-putamen, *Homer1b/c* expression was significantly reduced only by VPA compared to control (dorsomedial (CPDM; $p=0.004$; $F_{(dl)}=7.398_{(2,18)}$), ventrolateral (CPVL; $p=0.002$; $F_{(dl)}=8.536_{(2,18)}$), and ventromedial (CPVM; $p=0.009$; $F_{(dl)}=6.108_{(2,18)}$).

In the core of the nucleus accumbens, the densitometric analysis of autoradiographic images showed a statistically significant decrease in *Homer1b*/*c* expression after chronic treatment with VPA compared to control ($p=0.015$; $F_{(dl)}=5.432_{(2,18)}$). No significant results were found in the nucleus accumbens shell.

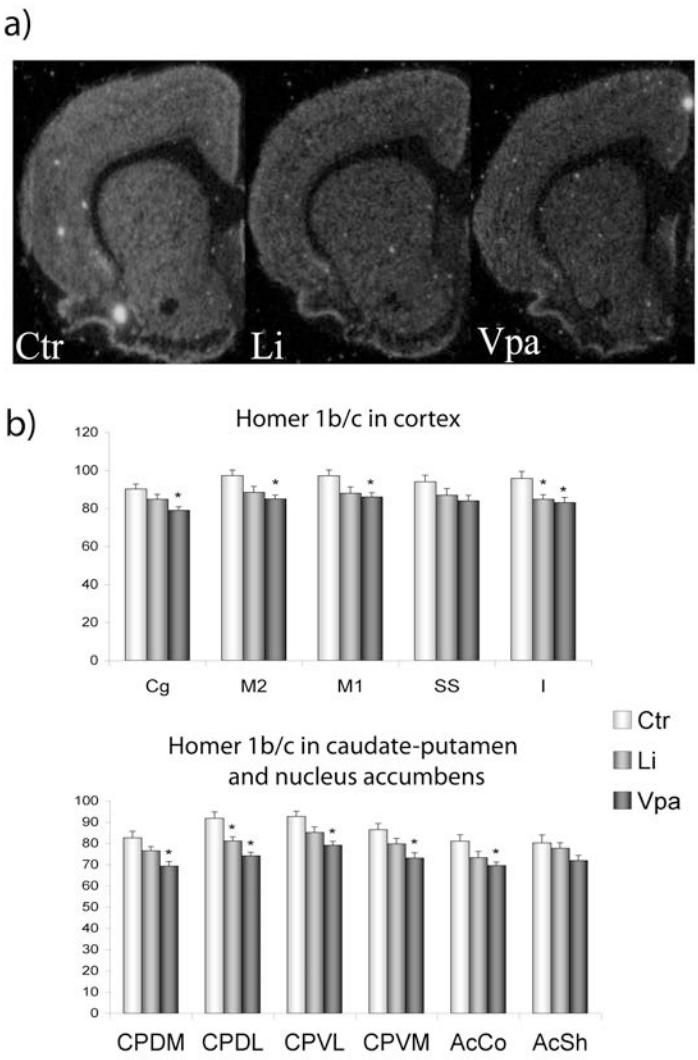

Figure 15. *Panel a*: autoradiographic film images of *Homer 1b/c* mRNA detected by means of *in situ* hybridization histochemistry in coronal brain sections after chronic treatment with control (CTR), lithium (Li), or valproate (VPA).
Panel b: *Homer 1b/c* mRNA levels in subregions of the cortex, caudate-putamen, and nucleus accumbens. Data are reported in relative d.p.m. as mean ± S.E.M. Tukey's *post hoc* test: * = *vs.* CTR ($p<0.05$)

Shank (Figure 16, panels a and c)

Shank mRNA was detected in the frontal and parietal cortices, and a lower signal was detected in the caudate-putamen and nucleus accumbens. The densitometric analysis of autoradiographic images showed a significant decrease of *Shank* signal in M2 with VPA treatment compared to control and lithium ($p=0.0107$; $F_{(dl)}=5.993_{(2,17)}$), and in M1 compared to control ($p=0.034$; $F_{(dl)}=4.153_{(2,17)}$). In Cg ($p=0.0047$; $F_{(dl)}=7.466_{(2,18)}$), SS (somatosensory cortex; $p=0.0157$; $F_{(dl)}=5.359_{(2,17)}$) and I ($p=0.0178$; $F_{(dl)}=5.155_{(2,17)}$),

VPA significantly reduced *Shank* expression compared to lithium. No significant differences were noted in striatal subregions.

IP3R (Figure 16, panel b and d)

The *IP3R* mRNA autoradiographic signal was distributed in both cortical and striatal regions. Significant differences between groups were detected in all subregions of both frontal and parietal cortices. Post-hoc tests showed that lithium significantly reduced the *IP3R* signal in Cg ($p=0.0456$; $F_{(dl)}=4.038_{(2,12)}$), M1 ($p=0.048$; $F_{(dl)}=3.952_{(2,12)}$), SS ($p=0.0181$; $F_{(dl)}=5.712_{(2,12)}$), and I ($p=0.0346$; $F_{(dl)}=4.510_{(2,12)}$) compared to control. In the striatum, chronic treatment with VPA significantly decreased the *IP3R* signal in CPDL compared to control ($p=0.0265$; $F_{(dl)}=4.863_{(2,13)}$).

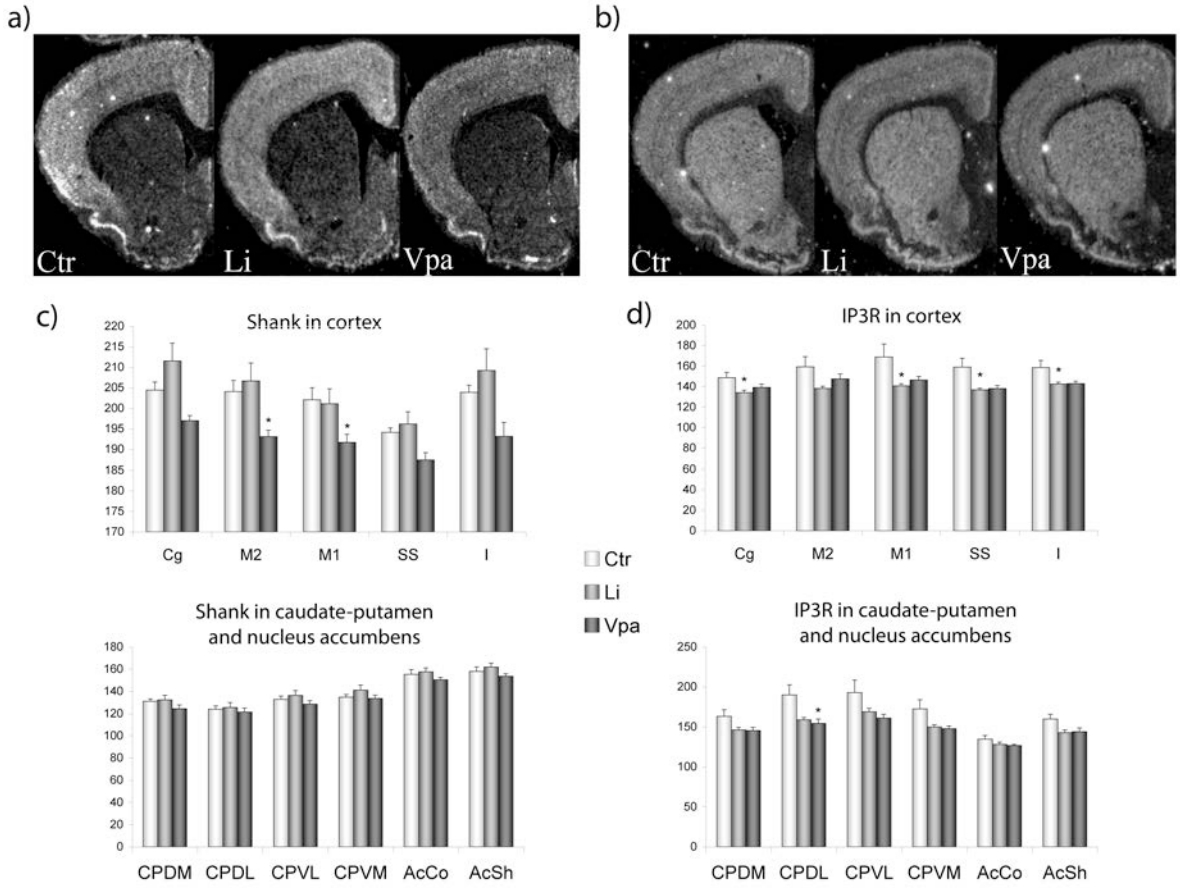

Figure 16. *Panels a and b*: Autoradiographic film images of *IP3* and *Shank* mRNA detected by means of *in situ* hybridization histochemistry in coronal brain sections after acute treatment with control (CTR), lithium (Li), or valproate (VPA).

Panels b and c: *IP3* and *Shank* mRNA levels after chronic treatment in the subregions of the cortex, caudate-putamen, and nucleus accumbens. Data are reported in relative d.p.m. as mean ± S.E.M. Tukey's *post hoc* test: * = *vs.* CTR ($p<0.05$).

Homer1a and ania-3

Homer1a and *ania-3* gene expression was detected in several cortical and subcortical brain regions of the control group, with a signal distribution similar to that obtained in previous studies [99,17]; however, no significant differences between treatment groups were noted for either gene in all analyzed areas.

Discussion

Lithium and VPA affect Homer1b/c expression in brain areas involved in mood modulation

Several lines of evidence suggest that Homer proteins may be involved in multiple signal transduction pathways—including PI3K-Akt, IP3R, and MAPK-ERK1/2—all of which have also been implicated in the putative mechanism of action of mood stabilizers and in the pathophysiology of mood disorders. This study is the first to demonstrate that chronic *in vivo* treatment with therapeutically relevant doses of lithium or VPA decreases the transcription of *Homer1b/c*, the constitutive isoform of the *Homer1* gene; notably, this gene has been implicated in the pathophysiology of psychiatric disorders [36,128]. We found that *Homer1b/c* expression was significantly reduced in the cingulate, medial agranular, motor, and insular subregions of the cortex by chronic treatment with VPA. In the striatum, both lithium and VPA downregulated *Homer1b/c* in the dorsolateral caudate-putamen, but only VPA administration reduced expression of the gene in other striatal subregions (dorsomedial, ventrolateral, and ventromedial) and in the nucleus accumbens core.

Although distinct differences exist between VPA and lithium, the direction of the effects of both these mood stabilizers on *Homer* expression in cortical and subcortical regions is consistent with these compounds having a potential common transductional pathway; this feature, in turn, has been considered pivotal in elucidating the mechanism of action of these drugs, which both act as mood stabilizers despite their structural differences. Nevertheless, it is noteworthy that both of these mood stabilizers affected *Homer1b/c* expression in brain regions that have specifically been implicated in the pathophysiology of bipolar disorder (for a review, see [277]). Indeed, several studies have demonstrated that functionally distinct cortical subregions project to specific striatal areas, and that analyzing gene expression changes induced by psychotropic drugs may elucidate the functional domains affected by these drugs [297]. In the present study, VPA modified the expression of *Homer1b/c* in cortical regions critical to motor control (medial agranular and motor cortices) and to cognitive and behavioral aspects of emotion (cingulate and insular cortices). The cortical premotor and motor areas project specifically to the dorsolateral regions of the striatum, which specifically control somatomotor inputs; cingulate and insular cortices project to the ventral striatum, which is mostly implicated in behavioral control. Albeit preliminary, these data describing the different response pattern of constitutive *Homer* genes to different mood stabilizers may provide an additional avenue of investigation for clarifying their mechanism of action in specific brain areas involved in mood modulation.

Functional implications of Homer1 modulation by mood stabilizers

Given the multifunctional role of Homers as scaffolding and adaptor proteins, the effects of lithium and VPA on *Homer1b/c* expression suggest a direct impact on postsynaptic remodeling. The reduced transcription of *Homer1b/c* in cortical and

subcortical regions might involve the putative modulation of signal transduction pathways starting at mGluR1/5. For instance, decreased Homer1b/c function may impair the coupling of mGluRs1/5 to IP3Rs mediated by Homer clusters [88], thereby lowering calcium-dependent signal transduction. This might thus constitute an additional mechanism of action for lithium and VPA; both agents have already been shown to reduce IP3 and diacylglycerol signaling, which comprises a crucial pathway for synaptic plasticity [331,330].

Moreover, Homer proteins are known to organize the distribution of mGluRs1/5 in specific neuronal sectors. In particular, *Homer1b/c* expression appears to be essential for arranging mGluRs1/5 in membrane clusters on dendritic spines in order to facilitate excitatory neuronal responses [337]. Therefore, it is possible that *Homer1b/c* downregulation, induced by both lithium and VPA, might lead to lowered sensitivity of the postsynaptic neuron to excitatory stimuli via the rearranging of mGluR1/5 localization.

Finally, Homer1b/c has been reported to play a major role in linking mGluRs1/5 with the postsynaptic effectors MAPK-ERK1/2 in a calcium-independent manner, generating a signaling pathway that acts in parallel to and coordinates with the conventional IP3R-calcium pathway [338]. Thus, a decrease in Homer1b/c function by chronic treatment with lithium or VPA might affect ERK1/2 activation and, consequently, its impact on gene transcription.

Furthermore, these effects of lithium and VPA on Homer1b/c-mediated mGluR signaling may contribute to the overall ability of these two mood stabilizers to treat the elevated glutamatergic activity found in specific brain areas of patients with bipolar disorder [339]. This is consistent with the evidence that both lithium and VPA may also reduce brain NMDA-mediated calcium signaling in distinct regions of the forebrain [340,341].

Is Homer1 a possible link between dopamine and mood stabilizers?

Several studies implicated *Homer* genes in transductional pathways specifically correlated to dopaminergic function, and downstream of dopaminergic receptors [143]. Our previous work [17,99] described a peculiar pattern of *Homer* gene induction in the rat forebrain following the acute or chronic administration of typical and atypical antipsychotics. In particular, the expression of the inducible isoforms of *Homer1* seems to be correlated with the degree of dopamine D2 receptor blockade induced by various antipsychotics. Recent evidence suggests that both lithium and VPA may affect dopaminergic function in multiple ways; for instance, both mood stabilizers can reverse the abnormal behaviors induced by indirect agonists (e.g., apomorphine or amphetamine) [342,343]. Other studies noted that VPA may potentiate dopamine efflux by antipsychotics in cortical regions [344]. Recent work from our laboratory demonstrated that VPA, when co-administered with a typical or atypical antipsychotic, may modify the impact on *Homer*-related postsynaptic gene expression exerted by individual administration of these drugs [146]; interestingly, this evidence is highly consistent with recent observations that both mood stabilizers might directly act on dopaminergic transductional pathways, such as the Akt-GSK3b cascade [249]. Given the putative role of Homer proteins in the signaling cascade of dopamine receptors in cortical and striatal regions, our finding that lithium and VPA modulate *Homer1b/c* may provide additional information regarding the possible impact of these two agents on dopaminergic signaling.

Lithium and VPA modulate Shank and IP3R expression: possible differential regional impact on calcium-dependent synaptic plasticity

Shank and *IP3R*—the two *Homer*-related genes analyzed—were both found to be affected in cortical regions after chronic administration of either lithium or VPA, although some differences in their modulation exist. Indeed, *Shank* expression was mildly impacted by chronic lithium in the cortex, while VPA significantly downregulated gene expression in motor and insular cortices. It is important to note that although both mood stabilizers promoted *IP3R* cortical downregulation, only lithium treatment significantly decreased *IP3R* expression in almost all cortical subregions. In contrast, in the dorsolateral caudate-putamen, *IP3R* was downregulated by VPA, while lithium slightly—and non-significantly—decreased gene expression.

Shank proteins are known to dually interact with NMDARs through a PSD95-GKAP (postsynaptic density 95/guanylate kinase-associated protein) complex, and with mGluRs1/5 by linking Homer1b/c, which interacts with IP3Rs to connect this machinery to the intracellular calcium stores [345]. Notably, recent studies demonstrated that Shank and Homer1b/c play a major role in regulating calcium intracellular oscillations by interacting directly with each other and with IP3Rs localized on calcium cisterns [88]. Therefore, the impact on *Shank* and *IP3R* transcripts following chronic administration of either lithium or VPA in both cortex and striatum may reflect the overall regulation of calcium-dependent glutamatergic activity exerted by these two mood stabilizers in cortical and subcortical regions. However, the differences in the expression patterns of *Shank* and *IP3R* by the two distinct mood stabilizers may suggest a differential regulation of calcium intracellular networks with a possible neuroanatomical specificity. Indeed, although lithium and VPA share common mechanisms of action with respect to the intracellular pathways activated (e.g. Akt/GSK3b signaling; phosphoinositide pathway) [259,346], several reports have

demonstrated that the effects of the two mood stabilizers may diverge depending upon neural cell type [347]. Moreover, lithium and VPA have also been reported to impact gene expression with differential regional specificity [281]. The present findings contribute additional data regarding this issue, thereby stimulating further investigation to elucidate the mechanisms by which lithium and VPA may differentially trigger calcium-dependent pathways in a region-specific manner.

In addition, the fact that both *Shank* and *IP3R*—like *Homer1b/c*— were modulated in brain regions specifically involved in cognitive-behavioral and motor aspects of emotion may further confirm the essential role that these PSD proteins play in the transductional pathways implicated in the mechanism of action of mood stabilizers.

Lithium and VPA did not impact Homer1 inducible transcripts: new ways to synaptic rearrangements by mood stabilizers?

In contrast to the constitutive isoform of the *Homer1* gene, neither the inducible form *Homer1a* nor its splice variant *ania-3* were affected by chronic administration of lithium or VPA. These results are consistent with other reports showing a negligible induction of IEGs (i.e. *c-fos*) following the chronic administration of lithium or VPA [281]. Moreover, the present findings support our previous work in this area[146], which found that neither acute nor chronic VPA administration modulated *Homer1a* expression, even though the co-administration of VPA with an antipsychotic induced changes in gene expression that differed from those elicited by the individually-administered compounds. These findings suggest that chronic treatment with mood stabilizers—although they impact *Homer*-dependent signalling—may not affect the *Homer* constitutive/inducible forms ratio, as seen in our previous study of

antipsychotics [21]. Thus, it is more likely that they have a direct impact on structural constituents of the postsynaptic network, such as *Homer* long forms, *Shank,* and *IP3Rs*. Taken together, these results provide the first evidence that chronic administration of the mood stabilizers lithium and VPA modulate *Homer1b/c* and its related postsynaptic genes *Shank* and *IP3R.* Notably, all of these genes encode multifunctional proteins that interact with well-known targets of mood stabilizers, and all have been implicated in long-term synaptic changes. Therefore, *Homer* genes may represent a new molecular substrate for the mechanism of action of mood stabilizers, a finding that clearly warrants further investigation.

VIII. Study n.3: Progressive recruitment of cortical and subcortical brain regions by inducible and constitutive postsynaptic density transcripts after increasing doses of antipsychotics with different receptor profiles.

Our previous studies suggest that PSD genes expression can be modulated by psychotropic drugs that mainly, albeit not exclusively, impact dopaminergic, serotonergic and glutamatergic neurotransmission [85,99,140,17]. In particular, *Homer* transcripts show a specific pattern of expression in cortical and subcortical regions depending on both the degree of dopamine D2 receptors blockade and the ratio of serotonergic/dopaminergic activity by the antipsychotic drugs administered [85,99,140,17], as well as *Homer* shows peculiar responses in cortical regions by drugs impacting selectively the serotonergic neurotransmission, such as antidepressants, alone or in combination with antipsychotics [247]. Last, PSD genes, in particular inducible *Homer1a*, have been demonstrated to display differential patterns of expression in selected rat brain regions by combined administration of antipsychotics and mood stabilizers (an add-on strategy tightly resembling the real world of clinical pharmacotherapy of psychosis), as compared to each drug class when individually administered [146].

A large amount of studies have tried to map the brain regions affected by antipsychotics administration, both by functional MRI in humans and by gene expression patterning in animal models, in order to better define the mechanisms of action by which these drugs exert their clinical effects. To this purpose, measurement of immediate-early genes (IEG) expression in response to drug exposure has proven useful in defining brain regions recruited by antipsychotic action. [348]. Indeed, drug-related IEG patterns of expression may provide both spatial and temporal profile of antipsychotic brain responses. For instance, haloperidol has been demonstrated to increase brain activity in

striatal regions at functional MRI, as well as to concurrently reduce prefrontal cortex glucose utilization [349]. Moreover, a recent study reported that haloperidol may reduce connectivity between basal ganglia and prefrontal cortex, and impair coupling between substantia nigra and cortical motor areas, putatively reflecting the liability of haloperidol to induce motor side effects in psychotic patients [350]. These findings tightly resemble preclinical data reporting a preferential pattern of striatal genes expression by haloperidol acute and chronic administration in rat forebrain [17,146]. By contrast, atypical antipsychotics preferentially activate prefrontal cortical brain areas and ventral striatum in humans [349] corresponding to a selective pattern of gene expression in medial agranular and somatosensory cortices, as well as in ventral striatum and nucleus accumbens, in the rat forebrain [20,21].

However, despite being a potential translational issue, a few studies have been performed on the differential activation of brain areas following increasing doses of antipsychotics, which is the most widely used therapeutic titration protocol in clinical practice to start (or even to switch) antipsychotic medications in patients. Indeed, understanding which brain region or sub-region is progressively activated by increasing doses of antipsychotic and how antipsychotics with different receptor profile may impact on such activation is potentially relevant to better correlate the mechanism of action of antipsychotics bot with their efficacy and side effects.

Thus, in the present study we addressed the following questions:

1. How different cortical and striatal subregions are progressively "recruited" by increasing doses of antipsychotic resembling clinical titration protocols
2. Whether different receptor profile may influence the recruitment of new brain regions beyond dopamine receptor blockade
3. Whether cortical and subcortical regions activated by the same doses of antipsychotic are functionally correlated.

To this purpose, we analyzed the differential expression of postsynaptic density transcripts induced by different doses of two antipsychotics: haloperidol, the prototypical first generation antipsychotic with prevalent dopamine D2 receptor blocking action, and asenapine, a novel antipsychotics characterized also by multiple receptor occupancy and with an equal ratio of D1 and D2 receptors blockade. We also compared the pattern of gene expression by increasing haloperidol and asenapine with that of a fixed dose of the atypical antipsychotic olanzapine, as a further touchstone.
The new atypical antipsychotic asenapine shows a broad multi-receptorial binding affinity and has been demonstrated to promote dopamine, serotonin and noradrenaline release in cortex and dopamine release in nucleus accumbens at doses that have antipsychotic activity in animal behavioral studies [237]. Moreover, thanks to its unique multi-receptor profile, asenapine may differentially impact glutamatergic and dopaminergic systems in cortical and subcortical regions: it, in fact, enhances glutamate NMDA-mediated currents in pyramidal cortical neurons, while it decreases NMDA receptor activity in caudate-putamen and nucleus accumbens; moreover, the chronic treatment with potentiates AMPA receptor activity in hippocampus [238]. On the other hand, asenapine may specifically enhance the dopamine bursts from VTA to the medial prefrontal cortex and the nucleus accumbens, and of noradrenaline from locus coeruleus to the cortex [237]. Recent studies have demonstrated that asenapine may exert brain region-specific differential effects on dopamine, serotonin and glutamate receptors depending on the dose administered [239-241].
In order to explore the topography of transcript distribution after different doses of antipsychotic we chose to investigate the expression of postsynaptic density genes that have been demonstrated to be responsive to typical and atypical antipsychotics treatment and to be involved in synaptic plasticity process believed to be relevant for schizophrenia and other psychosis pathophysiology. Specifically we studied the cortical

and subcortical topography of Homer-related IEG transcripts, *Homer1a*, *c-fos*, *Arc* and *Zif268*, together with the related interacting constitutive genes *Homer1b/c* and *PSD95* under incremental doses of antipsychotics. Moreover, we paralleled *Homer1a* patterns of gene expression to the corresponding Homer1a protein expression in striatal regions. Lastly, we performed a behavioral locomotor analysis of experimental animals to test different responses to increasing doses.

Materials and Methods.

Animals.

Male Sprague-Dawley rats (mean weight 250g) were obtained from Charles-River Labs (Lecco, Italy). The animals were housed and let to adapt to human handling in a temperature and humidity controlled colony room with 12/12 h light–dark cycle (lights on from 6:00 a.m. to 6:00 p.m.) with ad libitum access to laboratory chow and water. All procedures were conducted in accordance with the NIH Guide for Care and Use of Laboratory Animals (NIH Publication No. 85-23, revised 1996) and were approved by local Animal Care and Use Committee. All efforts were made to minimize animal number and suffering.

Drug treatment.

Asenapine powder (gently supplied by H. Lundbeck A/S, Copenaghen, Denmark), ketamine hydrochloride powder powder (Sigma-Aldrich, St. Louis, MO, USA), and haloperidol injectable solution (Lusofarmaco, Italy) were all dissolved in saline solution (NaCl 0.9%). All solutions were adjusted to physiological pH value and injected i.p. at a final volume of 1 ml/kg.

Rats were randomly assigned to one of the following treatment groups (n=7 for each treatment group): Saline solution (NaCl 0.9%, SAL); haloperidol 0.25 mg/kg (HAL0.25); haloperidol 0.5 mg/kg (HAL0.5); haloperidol 0.8 mg/kg (HAL0.8); asenapine 0.05 mg/kg (ASE0.05); asenapine 0.1 mg/kg (ASE0.1); asenapine 0.3 mg/kg (ASE0.3); olanzapine 2.5mg/kg (OLA).

All drugs were given at behaviorally active doses, based on previous works. Animals were killed by decapitation 90 minutes after administration, the brains were rapidly removed, quickly frozen on powdered dry ice and stored at -70°C prior to sectioning. Serial coronal sections of 12 μm were cut on a cryostat at -18°C through the forebrain at the level of the middle-rostral striatum (approx. from Bregma 1.20mm to 1.00mm), using the rat brain atlas by Paxinos and Watson [295] as an anatomical reference. Care was taken to select identical anatomical levels of treated and control sections using thionin-stained brain sections. Sections were thaw-mounted onto gelatin-coated slides, and stored at -70ºC for subsequent analysis.

In Situ Hybridization Histochemistry

Probes

Probes used for radioactive in situ hybridization were oligodeoxyribonucleotides complementary to bases sequence of target genes mRNAs. The *Homer1a* probe is complementary to bases 2527-2574 (GenBank #U92079; MWG Biotech, Firenze). The *Arc* probe is complementary to bases 789-833 (GenBank #NM019361; MWG Biotech, Firenze). The *c-fos* probe is complementary to bases 111-158 (GenBank #AY780203; MWG Biotech, Firenze). The *Zif-268* probe is complementary to bases

352–399 (GenBank#M18416; MWG Biotech, Firenze). The *Homer1b/c* probe is complementary to bases 1306-1354 (GenBank#AF093267; MWG Biotech, Firenze). The *PSD95* probe is complementary to bases 225–269 (GenBank#M96853; MWG Biotech, Firenze). All probes were designed from GenBank sequences and checked with BLAST in order to avoid cross-hybridization.

Probe radiolabeling

For each probe a 50µl labeling reaction mix was prepared on ice using DEPC treated water, 1X tailing buffer, 7.5pmol/µl of oligo, 125 Units of TdT and 100mCi 35S-dATP. The mix was incubated 20 min at 37°C. The unincorporated nucleotides were separated from radiolabeled DNA using ProbeQuant G-50 Micro Columns (Amersham-GE Healthcare Biosciences; Milano, Italy). As an assessment of the probe specificity, the autoradiographic signal distribution was compared and found to be consistent with previous in situ hybridization studies [17]. The specificity of each probe was also tested by pilot control experiment using the corresponding oligodeoxyribonucleotide.

In situ hybridization

Sections were processed for radioactive *in situ* hybridization according to previously published protocols [296]. All solutions were prepared with sterile double-distilled water. The sections were fixed in 4% formaldehyde in 0.12 M PBS (pH 7.4), quickly rinsed three times with 1X PBS, and placed in 0.25% acetic anhydride in 0.1 M triethanolamine/0.9% NaCl, pH 8.0, for 10 minutes. Next, the sections were dehydrated in 70%, 80%, 95% and 100% ethanol, delipidated in chloroform for 5 minutes, rinsed again in 100% and 95% ethanol and air-dried.

Sections were hybridized with 0.4-0.6x10^6 cpm of radiolabeled oligonucleotide in buffer containing 50% formamide, 600mM NaCl, 80mM Tris-HCl (pH 7.5), 4mM

EDTA, 0.1% pyrophosphate, 0.2mg/ml heparin sulfate, and 10% dextran sulfate. Slides were covered with coverslips and incubated at 37oC in a humid chamber for 22-24 hours. After hybridization the coverslips were removed in 1X SSC and the sections were washed 4x15 minutes in 2X SSC/50% formamide at 43°-44°C, followed by two 30 min washes with 1X SSC at room temperature. The slides were rapidly rinsed in distilled water and then in 70% ethanol.

The sections were dried and exposed to Kodak-Biomax MR Autoradiographic film (Sigma-Aldrich, Milano, Italy). A slide containing a scale of 16 known amounts of ^{14}C standards (ARC-146C, American Radiolabeled Chemical, Inc., St. Louis, MO, USA) was co-exposed with the samples. The autoradiographic films were exposed in a time range of 14-30 days. The optimal time of exposure was chosen to maximize signal-to-noise ratio but to prevent optical density from approaching the limits of saturation. Film development protocol included a 1.5 min dip in the developer solution and 3 min in the fixer.

Image analysis

The quantitation of the autoradiographic signal was performed using a computerized image analysis system including: a transparency film scanner (Microtek Europe B. V., Rotterdam, The Netherlands), an iMac computer, and ImageJ software (v. 1.47, Rasband, W.S., http://rsb.info.nih.gov/ij/). The original characteristics of the scanned images (i.e. contrast, brightness, resolution) were preserved. Each slide contained 3 adjacent sections of a single animal. All hybridized sections used for comparative statistical analysis were exposed on the same sheet of X-ray film. Signal intensity analysis was carried out on digitized autoradiograms measuring mean optical density within outlined ROIs in correspondence of the cortex, caudate putamen and nucleus

accumbens (Figure 17). These cortical and striatal subregions are structurally and functionally interconnected through projections from the cortex, which targets specific striatal sectors. Thus, ROIs were chosen based on functional mapping studies of gene expression [297] and other studies analyzing Homer expression in response to drugs [17,146]. A template, proportional to the dimensions of the anatomical subregion, was used for computerized quantitations in each one of the ROIs depicted.
Sections were quantitated blind to the treatment conditions. In order to test for inter-observer reliability an independent quantitation was performed by a second investigator. Results obtained by the first investigator were considered reliable, and then reported, only when they were quantitatively comparable, in terms of consistency of the statistically significant effects found, to that obtained by the second investigator.

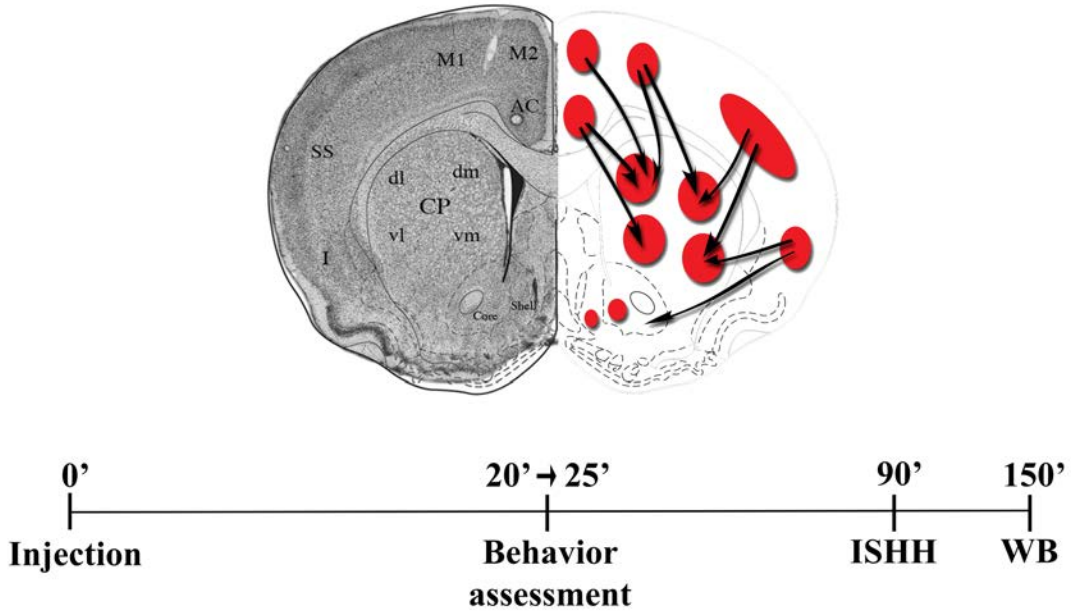

Figure 17. *Upper panel*. Diagram of regions of interest (ROIs) quantitated on autoradiographic film images in rat forebrain (section coordinates are approximate from Bregma 1.20 mm to 1.00 mm) and illustration of cortico-striatal projections among the ROIs in which gene expression induced by mood stabilizers was measured. AC = anterior cingulate cortex; M2 = medial agranular cortex; M1 = motor cortex; SS = somatosensory cortex; I = insular cortex; dmCP = dorsomedial caudate-putamen; dlCP = dorsolateral caudate-putamen; vlCP = ventrolateral caudate-putamen; vmCP = ventromedial caudate-putamen; core = core of nucleus accumbens; shell = shell of nucleus accumbens. Modified from Paxinos and Watson (1997). *Lower panel*. Schematic diagram of experimental timeline. ISHH = In Situ Hybridization Histochemistry. WB = Western Blot.

Data processing

Measurements of mean optical density within ROIs were converted using a calibration curve based on the standard scale co-exposed to the sections. ^{14}C standard values from 4 through 12 were previously cross-calibrated to ^{35}S brain paste standards, in order to assign a dpm/mg tissue wet weight value to each optical density measurement through a calibration curve. For this purpose a "best fit" 3rd degree polynomial was used. For each animal, measurements from the 3 adjacent sections were averaged and the final data were reported in relative dpm as mean ± S.E.M. ANOVA was used to analyze treatment

effects. The Tukey's post hoc test was used to determine the locus of effects in any significant ANOVA.

Signal distribution and brain areas correlations were assessed considering the measurements from each treatment group as the dependent variable, and the ROIs in which expression was measured as the independent variable (i.e.: measurements were analyzed per region effect). Kruskal-Wallis test was used to investigate the null hypothesis that no significant differences can be found in mRNA expression throughout cortical or striatal subregions. Significant differences among groups were analyzed by the Wilcoxon test for multiple comparisons.

Western Blot Analysis

After fresh-frozen collection, rat brains were dissected to isolate the prefrontal cortical area, the caudate-putamen, the nucleus accumbens and the hippocampus. Dissected region specimens were placed on ice in 1.5ml tubes and treated with Thermoscientific SynPER Synaptic Protein Reagent ™ (10ml per gram of tissue), with protease inhibitors added immediately before use, and then homogenated with Dounce. Homogenates were rapidly transferred to appropriate centrifuge tubes and centrifuged at 1200g for 10 minutes at 4°C. The pellet was discarded and supernatant was transferred to new tubes and centrifuged at 15000g for 20 minutes at 4°C. Thus, we obtained two fractions in which supernatant formed cytosolic component and the pellet formed the synaptic component. Protein amount was measured by Bradford sampling and then 2ml SynPER Reagent per gram of tissue was added for storage at -80°C in 5% (v/v) DMSO for subsequent analyses.

4µg/µl protein was run in wells per each experimental group using Bio-Rad Mini-PROTEAN® system, mixed to equal amount v/v of Laemmli ™ buffer for visualization

and separated on SDS-PAGE 10% polyacrylamide gel. Proteins were transferred to nitrocellulose membranes (Amersham Hybond-ECL, GE Healthcare) and blocked in blocking buffer (5% nonfat dry milk in PBS and 0.1% Tween 20) for 1 h. The blots were incubated in primary rabbit polyclonal antibody for rat Homer1 (Merck Millipore) 1:1000 and mouse β-Actin 1:5000 (Sigma-Aldrich) at 4°C overnight. This was followed by appropriate washes in TBS and 1 h incubation in a goat horseradish peroxidase-linked anti-rabbit and rabbit anti-mouse secondary antibodies respectively (Sigma-Aldrich). Blots were developed with LiteABlot® Extended chemiluminescent substrate (EuroClone) and exposed on Fujifilm® western blot films.

Three different rats for each experimental group were analysed with WB analysis, in order to grant statistical significance.

The quantitation of the blot signal was performed using a computerized image analysis system including: a transparency film scanner (Microtek Europe B. V., Rotterdam, The Netherlands), an iMac computer, and ImageJ software (v. 1.47, Rasband, W.S., http://rsb.info.nih.gov/ij/).

Signal intensity by each band (corresponding to each experimental group) was relativized by dividing for the corresponding standard band (the β-Actin band), thus obtaining a relative signal density standardized per protein total amount (which is usually considered as the intensity of β-Actin signal by each specimen). For each animal (i.e. band), measurements from the 3 different rats blotted were averaged and the final data were reported in relative intensity as mean ± S.E.M. ANOVA was used to analyze treatment effects. The Student-Neumann-Keuls's post hoc test was used to determine the locus of effects in any significant ANOVA.

Behavioral Activity Monitoring

Rats were placed three in each cage which corresponded to a specific treatment group. Activity was evaluated in transparent (210 square inches floor) plastic enclosures using a computerized photocamera system (Apple computer ™) and it was measured by using a motion capture system, which simultaneously labeled and tracked movements by each rat in the cage (Kinovea®). Motion was calculated using centimeters walked through in continuous shot as the dependent variable for total activity. Locomotor activity monitoring following each treatment administration was for a period of 5 minutes. Distance walked though by each rat was averaged with the others belonging to the same treatment group and expressed as centimeters ± S.E.M. ANOVA was used to analyze treatment effects comparing measurements both before and after treatments administration. The Student-Neumann-Keuls's post hoc test was used to determine the locus of effects in any significant ANOVA.

Results

I. Haloperidol and asenapine dose-dependently induce IEGs, but not constitutive genes, expression in distinct cortical and subcortical brain regions

a) *Homer1a*

Homer1a gene expression was analyzed in several cortical and subcortical regions of rat forebrain. Results are summarized in Figure 18. As in previous works [17], haloperidol administration induced a robust *Homer1a* expression in striatal regions. Specifically, HAL0.25 treatment significantly induced *Homer1a* expression in dmCP

($F_{(7,36)}$=4.2876; p=0.0023), dlCP ($F_{(7,36)}$=4.9198; p=0.0009) and vlCP ($F_{(7.36)}$=4.3211; p=0.0022) as compared to controls. HAL0.5 significantly induced *Homer1a* in all caudate-putamen subregions (dmCP [$F_{(7,36)}$=4.2876; p=0.0023], dlCP [$F_{(7,36)}$=4.9198; p=0.0009], vlCP [$F_{(7,36)}$=4.3211; p=0.0022] , and vmCP [$F_{(7,36)}$=3.7519; p=0.0052]). The most robust induction of *Homer1a* gene expression was achieved by HAL0.8 treatment, which elicited significant signal induction in all caudate-putamen subregions (dmCP [$F_{(7,36)}$=4.2876; p=0.0023], dlCP [$F_{(7,36)}$=4.9198; p=0.0009], vlCP [$F_{(7,36)}$=4.3211; p=0.0022] , and vmCP [$F_{(7,36)}$=3.7519; p=0.0052]), as well as in both core ($F_{(7,36)}$=4.5485; p=0.0016) and shell ($F_{(7,36)}$=4.6606; p=0.0013) of the nucleus accumbens, as compared to control. Moreover, as in previous works (Polese et al., 2002; Iasevoli et al., 2010), olanzapine induced *Homer1a* significant gene expression in all the striatum (dmCP [$F_{(7,36)}$=4.2876; p=0.0023], dlCP [$F_{(7,36)}$=4.9198; p=0.0009], vlCP [$F_{(7,36)}$=4.3211; p=0.0022], vmCP [$F_{(7,36)}$=3.7519; p=0.0052], core [$F_{(7,36)}$=4.5485; p=0.0016], and shell [$F_{(7,36)}$=4.6606; p=0.0013]), as compared to controls, as well as in AC ($F_{(7,36)}$=3.8010; p=0.0048), M2 ($F_{(7,36)}$=3.7359; p=0.0053), M1 ($F_{(7,36)}$=3.9105; p=0.0041) and I ($F_{(7,36)}$=43.6924; p=0.0057) cortical subregions.

Differently from both haloperidol and olanzapine, a unique *Homer1a* gene modulation was induced by asenapine. Indeed, both ASE0.05 and ASE0.1 induced a robust *Homer1a* signal expression in cortical and subcortical regions. Specifically, ASE0.05 stimulated *Homer1a* significant expression as compared to controls in AC ($F_{(7,36)}$=3.8010; p=0.0048) , M2 ($F_{(7,36)}$=3.7359; p=0.0053), M1 ($F_{(7,36)}$=3.9105; p=0.0041), and SS ($F_{(7,36)}$=3.6220; p=0.0063) cortical regions, as well as in dmCP ($F_{(7,36)}$=4.2876; p=0.0023), dlCP ($F_{(7,36)}$=4.9198; p=0.0009), vlCP ($F_{(7,36)}$=4.3211; p=0.0022) and vmCP ($F_{(7,36)}$=3.7519; p=0.0052) and in the nucleus accumbens core ($F_{(7,36)}$=4.5485; p=0.0016). ASE0.1 induced a wider *Homer1a* gene expression than ASE0.05, thus stimulating the gene signal expression in all cortical and subcortical

subregions, and in all the nucleus accumbens. By contrast, the highest asenapine dose, ASE0.3, stimulated no *Homer1a* signal induction in the cortex, but induced a robust gene expression in all the caudate-putamen, as well as in both core and shell of the nucleus accumbens. Notably, the expression of *Homer1a* by ASE0.3 in lateral striatal subregions was significantly higher than that induced by haloperidol (all the dosages) and olanzapine.

b) Arc

Arc gene expression was significantly reduced as compared to controls in all cortical subregions (Figure 18) with the exception of AC (M2 [$F_{(7,38)}$=1.7428; p=0.0128], M1 [$F_{(7,38)}$=1.4556; p=0.0358], SS [$F_{(7,38)}$=1.6088; p=0.0299], and I [$F_{(7,38)}$=1.48396; p=0.0425]) , by HAL0.25 treatment, whereas the same treatment significantly induced expression of the gene in both nucleus accumbens core ($F_{(7,38)}$=2.4165; p=0.0426) and shell ($F_{(7,38)}$=2.7214; p=0.0254). By contrast, no cortical impact was noticed by HAL0.5 treatment, while it significantly induced *Arc* expression in lateral caudate-putamen subregions (dlCP [$F_{(7,38)}$=2.6917; p=0.0267] and vlCP [$F_{(7,38)}$=3.0320; p=0.0151), as well as in both core ($F_{(7,38)}$=2.4165; p=0.0426) and shell ($F_{(7,38)}$=2.7214; p=0.0254). The highest dose of haloperidol, HAL0.8, significantly stimulated *Arc* gene expression in dmCP ($F_{(7,38)}$=1.5939; p=0.0439), dlCP ($F_{(7,38)}$=2.6917; p=0.0267), vlCP ($F_{(7,38)}$=3.0320; p=0.0151) and in all the nucleus accumbens (core [$F_{(7,38)}$=2.4165; p=0.0426] and shell [$F_{(7,38)}$=2.7214; p=0.0254]), as compared to controls. Moreover, HAL0.8 also significantly reduced *Arc* expression in all cortical subregions (AC [$F_{(7,38)}$=1.3788; p=0.0329], M2 [$F_{(7,38)}$=1.7428; p=0.0128], SS [$F_{(7,38)}$=1.6088; p=0.0299], and I [$F_{(7,38)}$=1.48396; p=0.0425]), with the exception of the motor cortex (M1).

The lowest dose of asenapine, ASE0.05, as well as olanzapine, showed a *Arc* signal distribution similar to the controls, whereas ASE0.1 significantly reduced expression of

the gene in AC ($F_{(7,38)}$=1.3788; p=0.0329), M2 ($F_{(7,38)}$=1.7428; p=0.0128) and M1 ($F_{(7,38)}$=1.4556; p=0.0358) cortical regions. ASE0.3 showed no *Arc* gene modulation in the cortex, but significantly induced the gene expression in lateral caudate-putamen (dlCP [$F_{(7,38)}$=2.6917; p=0.0267] and vlCP [$F_{(7,38)}$=3.0320; p=0.0151]) and in the nucleus accumbens core ($F_{(7,38)}$=2.4165; p=0.0426).

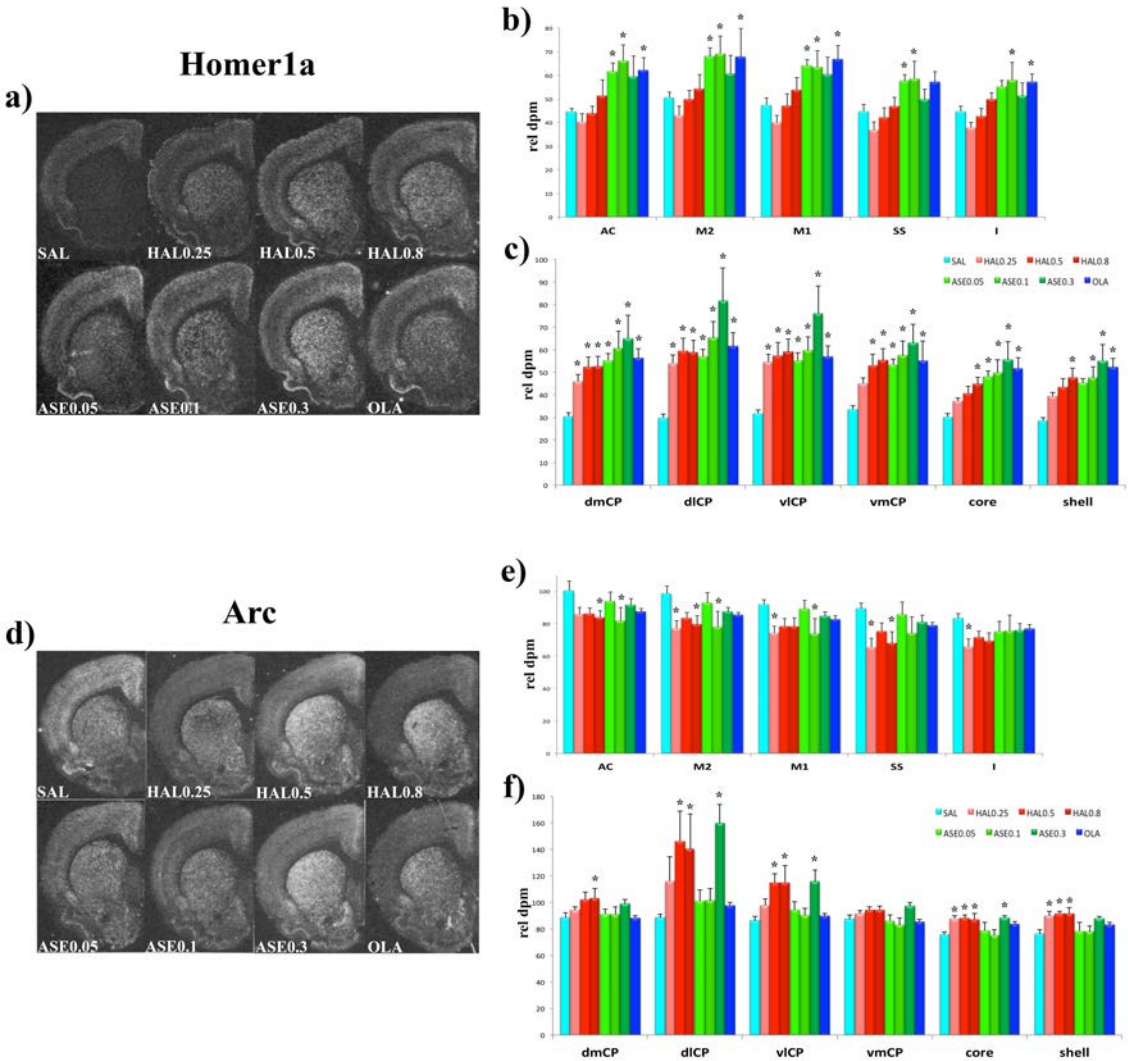

Figure 8. *Panel a and d*. Autoradiographic film images respectively of *Homer1a* and *Arc* mRNA detected by means of *in situ* hybridization histochemistry in coronal brain sections after acute treatment with vehicle (SAL), haloperidol 0.25mg/kg (HAL0.25), haloperidol 0.5mg/kg (HAL0.5), haloperidol 0.8mg/kg (HAL0.8), asenapine 0.05mg/kg (ASE0.05), asenapine 0.1mg/kg (ASE0.1), asenapine 0.3mg/kg (ASE0.3), olanzapine 2.5mg/kg (OLA). *Panel b and c*: *Homer 1a* mRNA levels in subregions of the cortex, caudate-putamen, and nucleus accumbens. Data are reported in relative d.p.m. as mean ± S.E.M. Tukey's *post hoc* test: * = *vs.* SAL ($p<0.05$). *Panel e and f*: *Arc* mRNA levels in subregions of the cortex, caudate-putamen, and nucleus accumbens. Data are reported in relative d.p.m. as mean ± S.E.M. Tukey's *post hoc* test: * = *vs.* SAL ($p<0.05$).

c) c-fos

Similarly to *Homer1a*, *c-fos* gene expression was differentially modulated by the distinct doses of haloperidol in the striatum (Figure 19). HAL0.25, indeed, significantly stimulated *c-fos* expression in dlCP ($F_{(7,36)}$=5.3869; p=0.0005) and vmCP ($F_{(7,36)}$=5.4120; p=0.0005), as well as in the shell ($F_{(7,36)}$=7.1069; p<0.0001), as compared to controls. HAL0.5 induced *c-fos* in dlCP ($F_{(7,36)}$=5.3869; p=0.0005), vlCP ($F_{(7,36)}$=7.6394; p<0.0001), vmCP ($F_{(7,36)}$=5.4120; p=0.0005) and in the shell ($F_{(7,36)}$=7.1069; p<0.0001) as compared to controls. The widest *c-fos* induction was obtained by HAL0.8 treatment, which significantly stimulated expression of the gene in all the caudate-putamen subregions, as well as in both nucleus accumbens core and shell (dmCP [$F_{(7,36)}$=2.8064; p=0.0233], dlCP [$F_{(7,36)}$=5.3869; p=0.0005], vlCP [$F_{(7,36)}$=7.6394; p<0.0001] , vmCP [$F_{(7,36)}$=5.4120; p=0.0005], core [$F_{(7,36)}$=2.9124; p=0.0196], and shell [$F_{(7,36)}$=7.1069; p<0.0001]).

No signal induction was noticed in ASE0.05 and in ASE0.1 subgroups, whereas ASE0.3 dose induced significant *c-fos* expression in all the striatum and the nucleus accumbens as compared to controls, resembling the signal distribution by HAL0.8 treatment. Olanzapine, by contrast, induced *c-fos* expression only in ventral caudate-putamen subregions (vlCP [$F_{(7,36)}$=7.6394; p<0.0001] and vmCP [$F_{(7,36)}$=5.4120; p=0.0005]).

d) Zif268

Similar *Zif268* gene signal induction was noticed for all the doses of haloperidol (Figure 9), which induced significant expression of this gene in all the striatum and the nucleus accumbens shell (dmCP [$F_{(7,37)}$=8.2153; p<0.0001], dlCP [$F_{(7,37)}$=14.0835; p<0.0001], vlCP [$F_{(7,37)}$=11.4395; p<0.0001] , vmCP [$F_{(7,37)}$=24.1296; p<0.0001], core

[$F_{(7,37)}$=5.4012; p=0.0004], and Ha [$F_{(7,37)}$=7.0829; p<0.0001]) as compared to controls, with the exception of HAL0.25, in which no core signal was observed.

All three doses of asenapine induced a similar pattern of *Zif268* gene expression, with significant signal distribution in all caudate-putamen subregions (dmCP [$F_{(7,37)}$=8.2153; p<0.0001], dlCP [$F_{(7,37)}$=14.0835; p<0.0001], vlCP [$F_{(7,37)}$=11.4395; p<0.0001] and vmCP[$F_{(7,37)}$=24.1296; p<0.0001]) and in the nucleus accumbens shell ($F_{(7,37)}$=7.0829; p<0.0001).

Olanzapine significantly stimulated *Zif268* gene expression in dlCP ($F_{(7,37)}$=14.0835; p<0.0001) and vlCP ($F_{(7,37)}$=11.4395; p<0.0001), as well as in the nucleus accumbens shell ($F_{(7,37)}$=7.0829; p<0.0001).

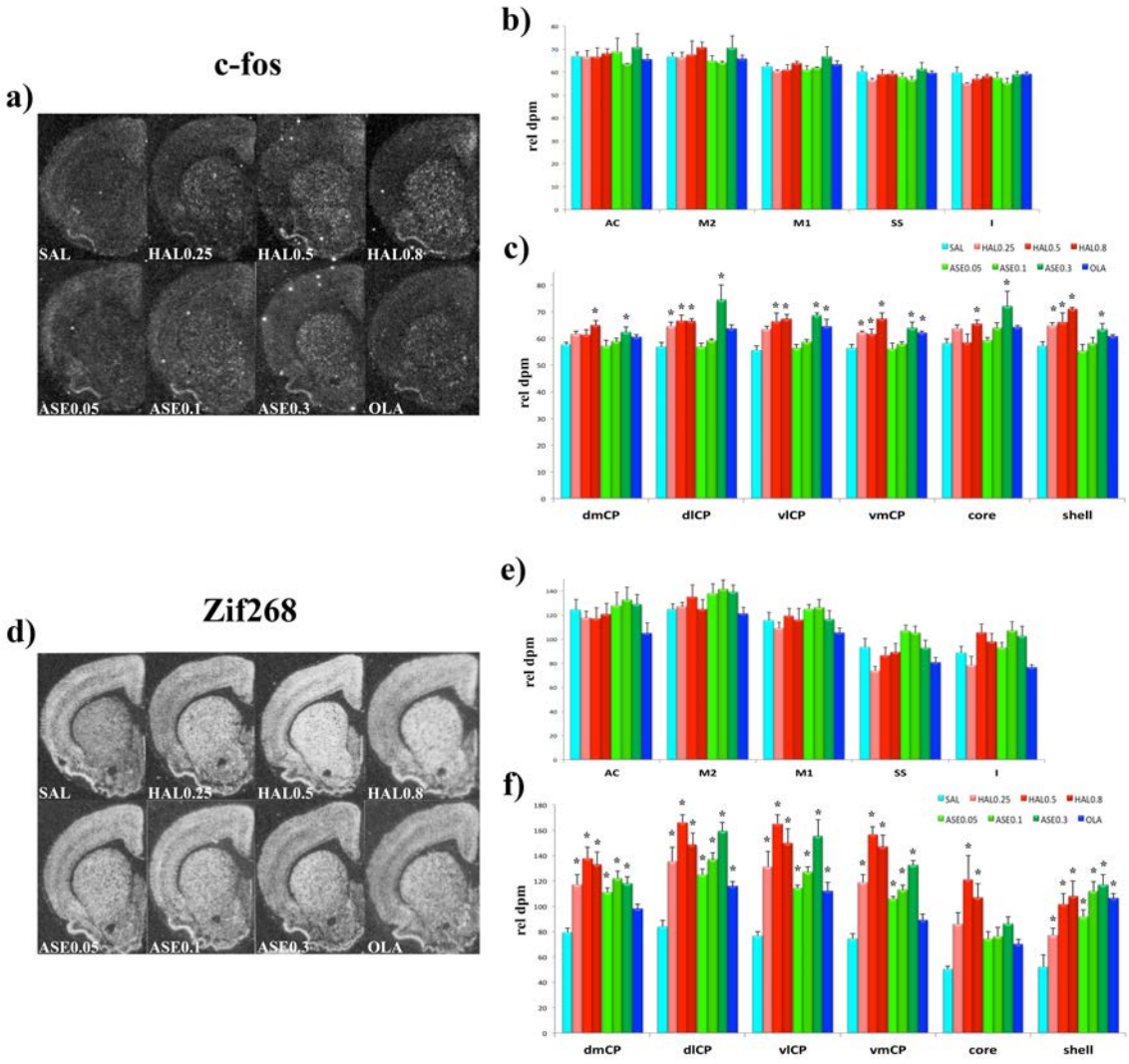

Figure 19. *Panel a and d*. Autoradiographic film images respectively of *c-fos* and *Zif268* mRNA detected by means of *in situ* hybridization histochemistry in coronal brain sections after acute treatment with vehicle (SAL), haloperidol 0.25mg/kg (HAL0.25), haloperidol 0.5mg/kg (HAL0.5), haloperidol 0.8mg/kg (HAL0.8), asenapine 0.05mg/kg (ASE0.05), asenapine 0.1mg/kg (ASE0.1), asenapine 0.3mg/kg (ASE0.3), olanzapine 2.5mg/kg (OLA). *Panel b and c*: *c-fos* mRNA levels in subregions of the cortex, caudate-putamen, and nucleus accumbens. Data are reported in relative d.p.m. as mean ± S.E.M. Tukey's *post hoc* test: * = *vs.* SAL ($p<0.05$). *Panel e and f*: *Zif268* mRNA levels in subregions of the cortex, caudate-putamen, and nucleus accumbens. Data are reported in relative d.p.m. as mean ± S.E.M. Tukey's *post hoc* test: * = *vs.* SAL ($p<0.05$).

e) Homer1b/c

The long isoform of Homer1 gene was robustly induced in AC ($F_{(7,38)}$=2.7438; p=0,0244), M2 ($F_{(7,38)}$=2.5434; p=0.0343) and M1 ($F_{(7,38)}$=3.1902; p=0.0116) cortical subregions by HAL0.8, ASE0.1, ASE0.3, and OLA treatments as compared to SAL (Figure 4). HAL0.5 only stimulated *Homer1b/c* expression in motor cortical subregion (M1, $F_{(7,38)}$=3.1902; p=0.0116). All treatments, with the exception of ASE0.05 induced nucleus accumbens core overexpression of *Homer1b/c* ($F_{(7,38)}$=2.7532; p=0.0240). No other significant signal changes in both cortical and subcortical regions were noticed by treatments.

f) PSD95

A strong increase in signal intensity was noticed in both cortex and striatum, as well as in the nucleus accumbens, by all asenapine dosages and by olanzapine treatments (AC: $F_{(7,34)}$=4.4175; p=0.0022; M2: $F_{(7,34)}$=3.6184; p=0.0071; M1: $F_{(7,34)}$=4.6418; p=0.0016; SS: $F_{(7,34)}$=4.7392; p=0.0014; I: $F_{(7,34)}$=7.4855; p<0,0001; dmCP: $F_{(7,34)}$=4.2978; p=0.0026; dlCP: $F_{(7,34)}$=4.8850; p=0.0012; vlCP $F_{(7,34)}$=4.6296; p=0.0016; vmCP: $F_{(7,34)}$=5.5809; p=0.0005; AcCo: $F_{(7,34)}$=4.3186; p=0.0025; AcSh: $F_{(7,34)}$=4.2426; p=0.0028). HAL0.5 induced *PSD95* overexpression only in AC and M1 cortex subregions, whereas HAL0.8 overexpressed the gene in AC, M2, M1 and I, as well as in dmCP, dlCP, vmCP, AcCo and AcSh (Figure 20).

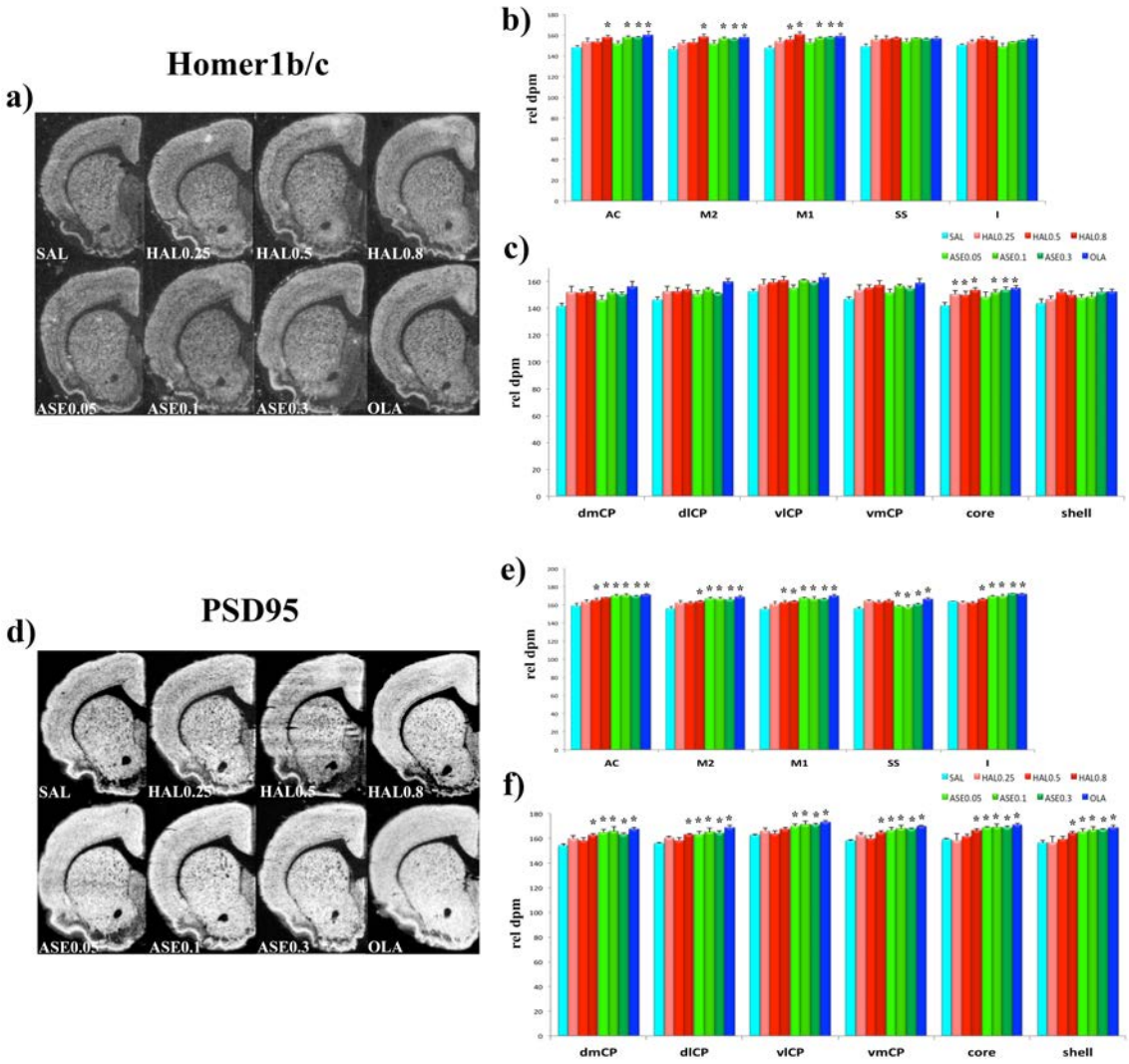

Figure 20. *Panel a and d*. Autoradiographic film images respectively of *Homer1b/c* and *PSD95* mRNA detected by means of *in situ* hybridization histochemistry in coronal brain sections after acute treatment with vehicle (SAL), haloperidol 0.25mg/kg (HAL0.25), haloperidol 0.5mg/kg (HAL0.5), haloperidol 0.8mg/kg (HAL0.8), asenapine 0.05mg/kg (ASE0.05), asenapine 0.1mg/kg (ASE0.1), asenapine 0.3mg/kg (ASE0.3), olanzapine 2.5mg/kg (OLA). *Panel b and c*: *Homer1b/c* mRNA levels in subregions of the cortex, caudate-putamen, and nucleus accumbens. Data are reported in relative d.p.m. as mean ± S.E.M. Tukey's *post hoc* test: * = *vs.* SAL ($p<0.05$). *Panel e and f*: *PSD95* mRNA levels in subregions of the cortex, caudate-putamen, and nucleus accumbens. Data are reported in relative d.p.m. as mean ± S.E.M. Tukey's *post hoc* test: * = *vs.* SAL ($p<0.05$).

II. Haloperidol and asenapine dose-dependently recruit progressive postsynaptic IEGs expression in cortical and subcortical areas

Signal distribution analysis was performed in order to address the issue whether increasing doses of antipsychotics may differentially impact IEGs and constitutive genes expression in selected rat forebrain areas that are functionally connected.

a) Homer1a

Kruskal-Wallis non-parametric test revealed that haloperidol acute administration dose-dependently induced *Homer1a* expression with a dorsal-to-ventral progressive subregions recruitment (Figure 21). Indeed, Wilcoxon post-hoc comparison showed that HAL0.25 increased *Homer1a* expression significantly in dorsomedial, dorsolateral and ventromedial caudate-putamen, as compared to other striatal subregions (χ^2=55.4510$_{(df=10)}$; p<0.0001). The higher dose HAL0.5, on the other hand, showed a significant signal increase in all the caudate-putamen, as compared to other subregions (χ^2=32.2663$_{(df=10)}$; p=0.0004). Finally, the highest dose HAL0.8 induced *Homer1a* signal in the whole striatum, with no significant differences amongst striatal areas (χ^2=17.2611$_{(df=10)}$; p=0.0688).

On the other hand, the lowest dose of asenapine, ASE0.05, significantly induced *Homer1a* signal in AC, M2, M1 and SS, as compared to I, as well as in all the caudate-putamen and in the core as compared to the shell (χ^2=50.1667$_{(df=10)}$; p<0.0001). The intermediate dose ASE0.1 induced a widely distributed *Homer1a* expression overall the cortex and the striatum, without any significant difference amongst subregions (χ^2=15.7408$_{(df=10)}$; p=0.1073). Last, the highest dose ASE0.3 induced a strong *Homer1a* expression in the caudate-putamen and in the whole nucleus accumbens as compared to

the cortex, being the dorsal regions of caudate-putamen significantly hyperactivated as compared to the other subregions (χ^2=26.5679$_{(df=10)}$; p=0.0030).

b) Arc

Arc gene expression distribution by Kruskal-Wallis analysis showed a progressive recruitment of striatal areas by increasing doses of haloperidol, which occurred concurrently to a signal decrease in cortical subregions (Figure 21). HAL0.5, indeed, induced significant *Arc* signal enhancement in both core and shell of the nucleus accumbens as compared to the all the rest of the striatum (χ^2=91.3984$_{(df=10)}$; p<0.0001). HAL0.5 showed significant *Arc* signal induction in the dorsal areas of striatum and in the whole nucleus accumbens as compared to ventral caudate-putamen, as well as there was no gene modulation in the cortex (χ^2=100.5614$_{(df=10)}$; p<0.0001). HAL0.8 promoted the widest *Arc* distribution, located in dlCP, dmCp and vlCP, as well as in the nucleus accumbens, and a significant signal reduction in AC, M2 an SS as compared to all the other brain areas (χ^2=84.3869$_{(df=10)}$; p<0.0001).

No significant differences in brain signal distribution were noticed in *Arc* gene expression by ASE0.05 treatment (χ^2=19.4017$_{(df=10)}$; p=0.0554). ASE0.1, instead, significantly reduced *Arc* signal in AC, M2 and M1 cortical subregions as compared to all the other brain areas (χ^2=21.3817$_{(df=10)}$; p=0.0186). Last, ASE0.3 significantly induced *Arc* signal in the dorsal caudate-putamen and in the nucleus accumbens core as compared to the other striatal regions (χ^2=85.3798$_{(df=10)}$; p<0.0001)

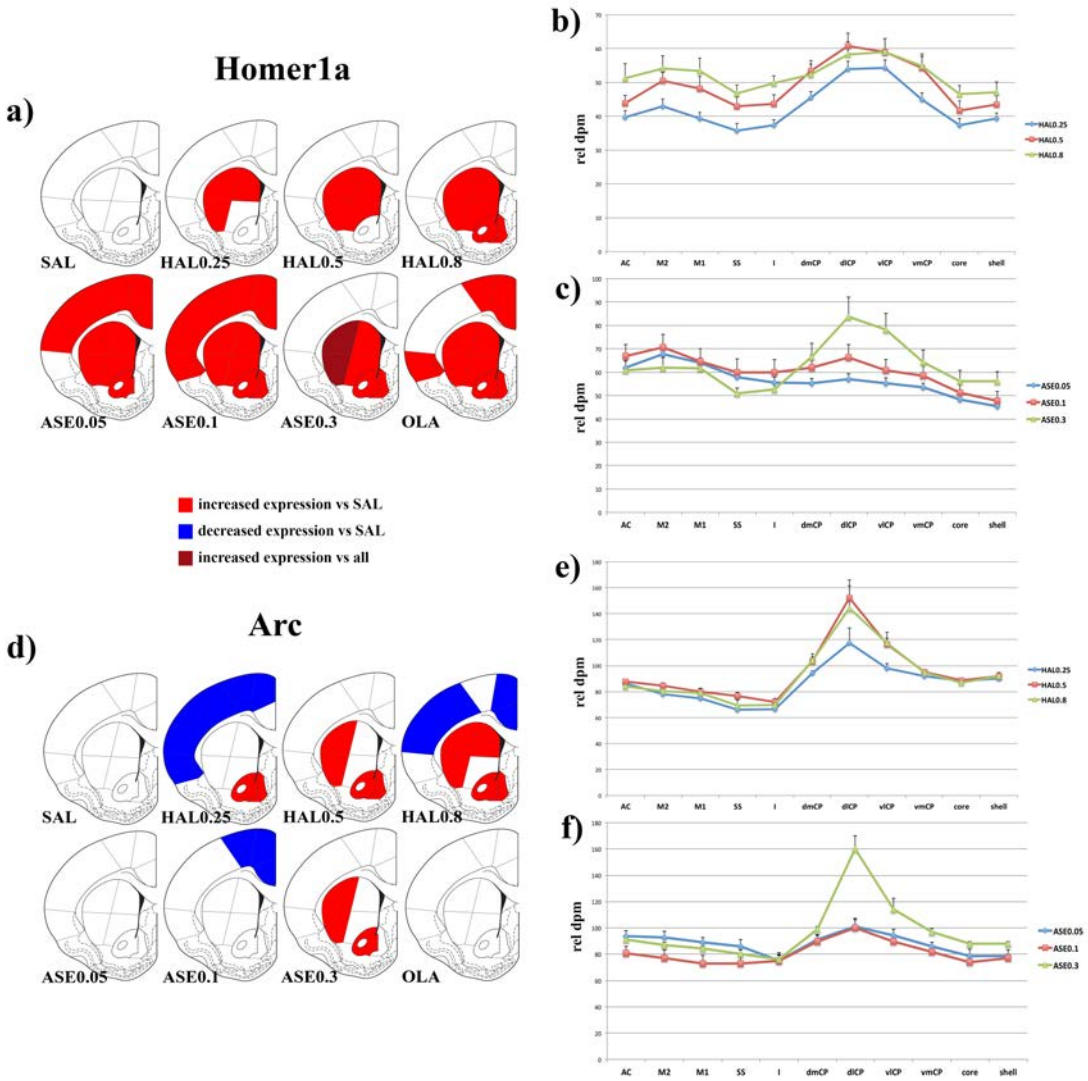

Figure 21. *Panel a and d.* Schematic depiction respectively of *Homer1a* and *Arc* gene expression recruitment in cortical and subcortical regions by the different treatments administered: vehicle (SAL), haloperidol 0.25mg/kg (HAL0.25), haloperidol 0.5mg/kg (HAL0.5), haloperidol 0.8mg/kg (HAL0.8), asenapine 0.05mg/kg (ASE0.05), asenapine 0.1mg/kg (ASE0.1), asenapine 0.3mg/kg (ASE0.3), olanzapine 2.5mg/kg (OLA). Red label: increased expression *vs.* other regions at Wilcoxon multiple comparison test ($p<0.05$). Blue label: decreased expression *vs.* other regions at Wilcoxon multiple comparison test ($p<0.05$). Dark red label: increased expression *vs.* other regions at Wilcoxon multiple comparison test ($p<0.05$). *Panel b and c*. Graphical representation of *Homer1a* gene expression distribution respectively by haloperidol or asenapine incremental dosages in the ROIs analyzed. *Panel e and f*. Graphical representation of *Arc* gene expression distribution respectively by haloperidol or asenapine incremental dosages in the ROIs analyzed. Data are expressed in relative d.p.m as mean ± S.E.M. considering the measurements from each treatment group as the dependent variable, and the ROIs in which expression was measured as the independent variable.

c) c-fos

Similarly to *Homer1a* gene expression, *c-fos* signal was progressively recruited in striatal areas by increasing haloperidol dosages (Figure 22). The low dose HAL0.25 induced *c-fos* significant signal in dlCP and vmCP, as well as in the shell, as compared to all the other striatal subregions (χ^2=43.2130$_{(df=10)}$; p<0.0001). By increasing the dose to HAL0.5, *c-fos* gene expression was induced also in vlCP, besides dlCP, dmCP and shell, as compared to all the rest of the striatum (χ^2=33.7414$_{(df=10)}$; p=0.0002). Finally, the highest dose HAL0.8 induce a strong *c-fos* expression throughout the striatum, which was significantly higher than the other brain regions (χ^2=50.1200$_{(df=10)}$; p<0.0001).

Both the low and the intermediate dosages of asenapine induced a *c-fos* brain signal distribution which was no significantly different amongst brain areas (ASE0.05 χ^2=15.3797$_{(df=10)}$; p=0.0504; ASE0.1 χ^2=17.5439$_{(df=10)}$; p=0.0521). Oppositely, ASE0.3 strongly induced *c-fos* gene expression in the whole striatum, as compared to the other brain regions (χ^2=47.0056$_{(df=10)}$; p<0.0001).

d) Zif268

Zif268 signal distribution was revealed by Kruskal-Wallis as progressively recruited by the intermediate and the high haloperidol dosages, as compared to the lowest dose (Figure 22). HAL0.25 induced significant *Zif268* signal distribution in the whole caudate-putamen and in the shell, as compared to the core (χ^2=77.7060$_{(df=10)}$; p<0.0001). Both HAL0.5 and HAL0.8 induced a wide striatal distribution of *Zif268* gene expression significantly higher as compared to the other brain regions (HAL0.5 χ^2=53.2013$_{(df=10)}$; p<0.0001; HAL0.8 χ^2=51.3852$_{(df=10)}$; p<0.0001).

All the dosages of asenapine, in the other hand, induced the same *Zif268* gene expression distribution in the whole caudate-putamen and in the shell, as compared to

the rest of the forebrain (ASE0.05 $\chi^2=52.7305_{(df=10)}$; $p<0.0001$; ASE0.1 $\chi^2=43.3033_{(df=10)}$; $p<0.0001$; ASE0.3 $\chi^2=73.2122_{(df=10)}$; $p<0.0001$)

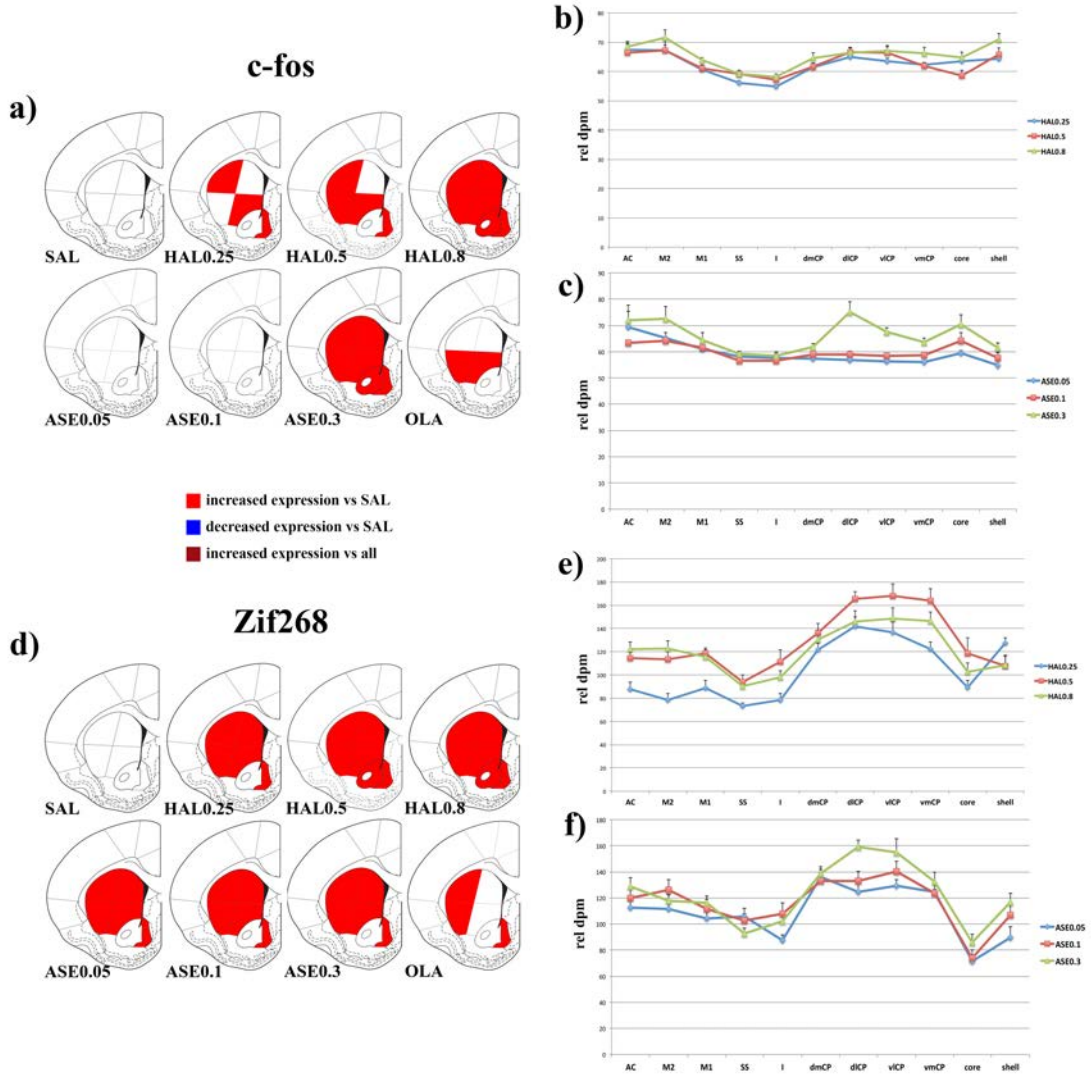

Figure 22. *Panel a and d.* Schematic depiction respectively of *c-fos* and *Zif268* gene expression recruitment in cortical and subcortical regions by the different treatments administered: vehicle (SAL), haloperidol 0.25mg/kg (HAL0.25), haloperidol 0.5mg/kg (HAL0.5), haloperidol 0.8mg/kg (HAL0.8), asenapine 0.05mg/kg (ASE0.05), asenapine 0.1mg/kg (ASE0.1), asenapine 0.3mg/kg (ASE0.3), olanzapine 2.5mg/kg (OLA). Red label: increased expression *vs.* other regions at Wilcoxon multiple comparison test ($p<0.05$). Blue label: decreased expression *vs.* other regions at Wilcoxon multiple comparison test ($p<0.05$). Dark red label: increased expression *vs.* other regions at Wilcoxon multiple comparison test ($p<0.05$). *Panel b and c*. Graphical representation of *c-fos* gene expression distribution respectively by haloperidol or asenapine incremental dosages in the ROIs analyzed. *Panel e and f.* Graphical representation of *Zif268* gene expression distribution respectively by haloperidol or asenapine incremental dosages in the ROIs analyzed. Data are expressed in relative d.p.m as mean ± S.E.M. considering the measurements from each treatment group as the dependent variable, and the ROIs in which expression was measured as the independent variable.

Western Blot Analysis

No significant differences in Homer1a protein expression were noticed amongst all treatment groups. However, a trend of reduction in protein expression was detected corresponding to both HAL or ASE increasing dosages (Figure 23).

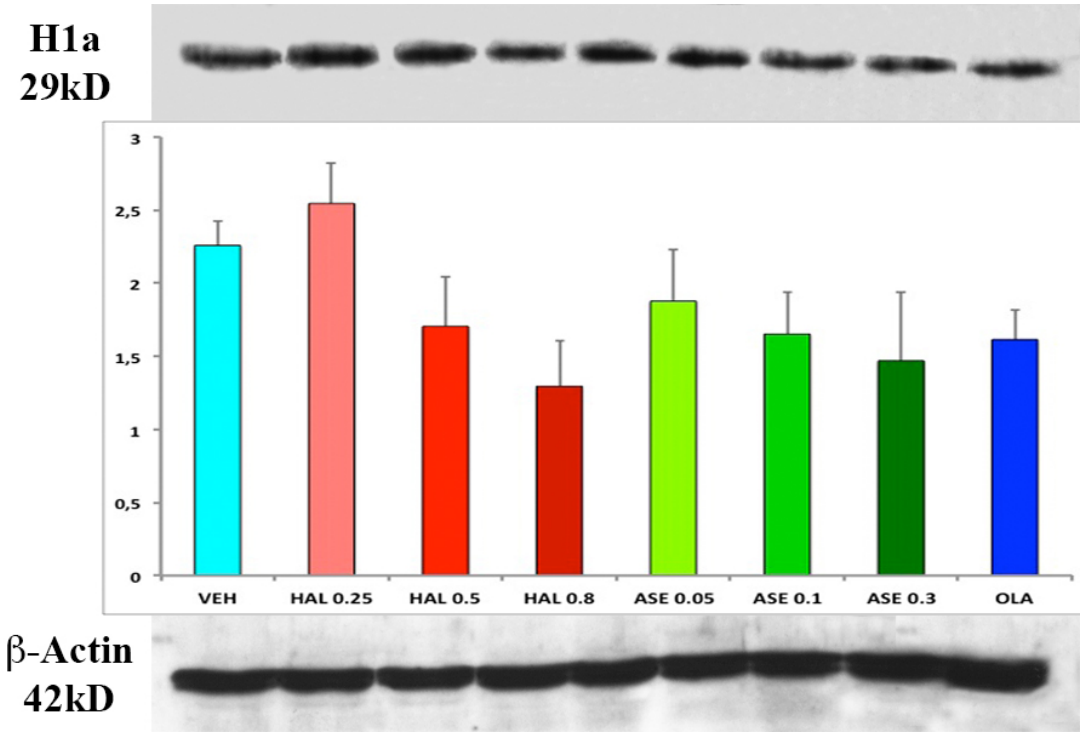

Figure 23. Homer1a protein expression in striatum following acute treatments. Vehicle (SAL), haloperidol 0.25mg/kg (HAL0.25), haloperidol 0.5mg/kg (HAL0.5), haloperidol 0.8mg/kg (HAL0.8), asenapine 0.05mg/kg (ASE0.05), asenapine 0.1mg/kg (ASE0.1), asenapine 0.3mg/kg (ASE0.3), olanzapine 2.5mg/kg (OLA). Data are reported in relative intensity as mean ± S.E.M.

Behavioral Activity Monitoring

ANOVA analysis on locomotor activity of rats from each experimental group (Figure 24) revealed a significant reduction of motion in rats administered with the three

dosages of haloperidol (HAL0.25, HAL0.5, HAL0.8) as well as with OLA ($F_{(7,23)}$=25.5140; p<0.0001). Oppositely, a trend in locomotor activity increase was recognized in asenapine-treated rats, although only ASE0.1 group showed a statistical significant locomotion enhancement after treatment ($F_{(7,23)}$=25.5140; p<0.0001).

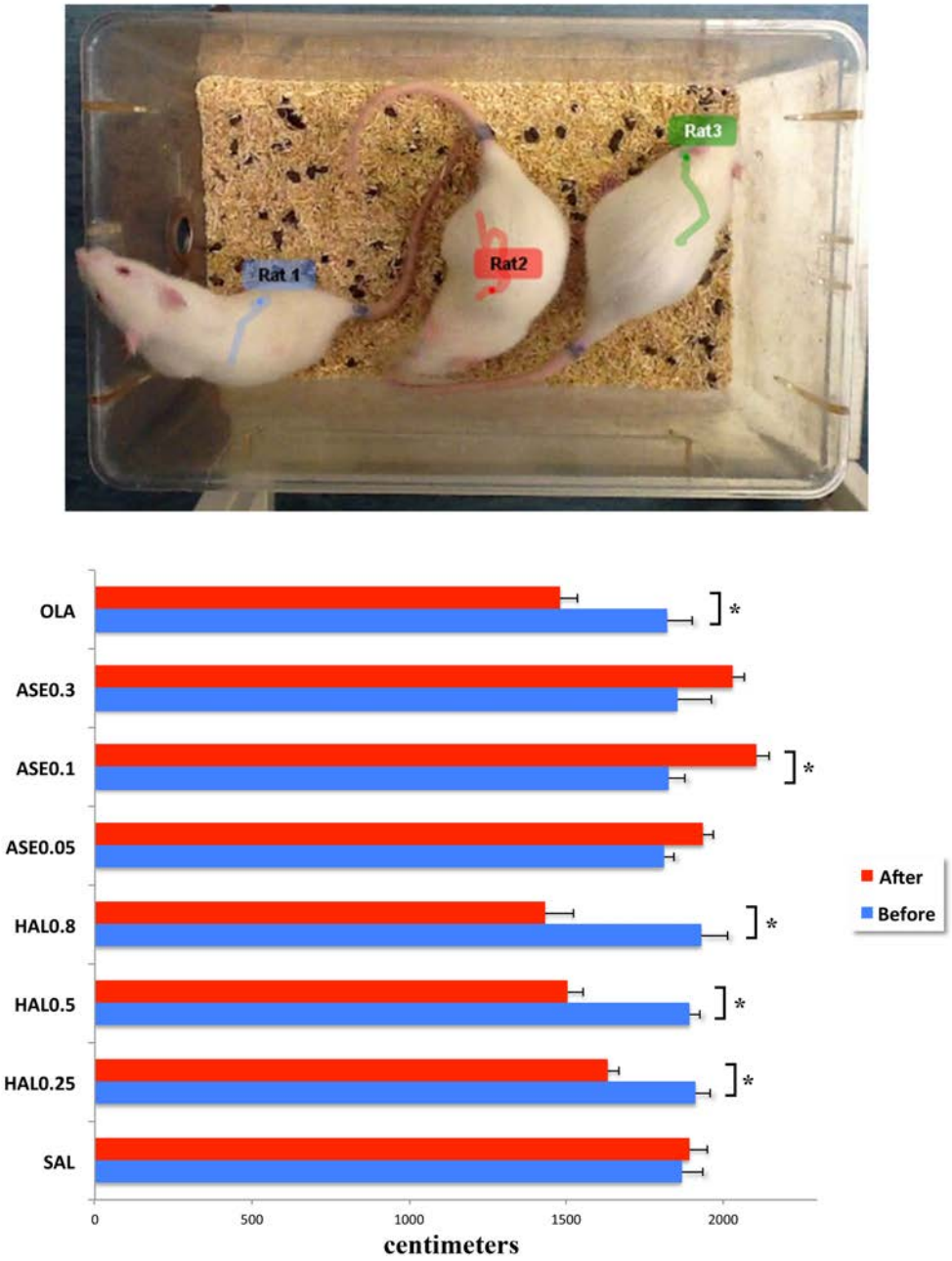

Figure 24. Behavior locomotor activity measurement following each treatment. Vehicle (SAL), haloperidol 0.25mg/kg (HAL0.25), haloperidol 0.5mg/kg (HAL0.5), haloperidol 0.8mg/kg (HAL0.8), asenapine 0.05mg/kg (ASE0.05), asenapine 0.1mg/kg (ASE0.1), asenapine 0.3mg/kg (ASE0.3), olanzapine 2.5mg/kg (OLA). Blue columns: distance walked before treatment administration. Red columns: distance walked after treatment administration. Data are reported in centimeters as mean ± S.E.M. Student-Neumann-Keuls's *post hoc* test: * = *vs.* before the corresponding treatment (p<0.05).

Discussion

Although being a relevant translational issue, the possibility that increasing dosages of the same antipsychotic may activate IEGs in progressively recruited brain areas (rather than increase signal intensity in the same regions) has been scarcely explored at present. Here we demonstrated for the first time that increasing doses of haloperidol may induce IEGs (but not constitutive genes) expression in different striatal areas, which are progressively recruited by incremental dosages with a dorsal-to-ventral gradient of expression. Particularly, our results demonstrated that a low dosage of haloperidol (0.25mg/kg) may specifically activate *Homer1a* gene expression program in the dorsal striatum. The progressive increase of haloperidol dosage seems to promote a gradual recruitment of ventral striatal subregions by *Homer1a* gene expression, until reaching the maximum signal at the highest dose of 0.8mg/kg, which activates *Homer1a* in the whole striatum and in the nucleus accumbens. Notably, no significant differences were noticed in *Homer1a* gene expression signal intensity in striatal subregions amongst the distinct dosages.

Similarly to *Homer1a*, all the other IEGs (*Arc, c-fos* and *Zif268*) analyzed displayed a progressive recruitment in striatal subregions by increasing dosages of haloperidol, even if with no specific dorsal-to-ventral gradient, as in the case of *Homer1a*. For instance, *Arc* expression was equally induced in the nucleus accumbens (both core and shell subregions) by all dosages of haloperidol. However, the progressive raising of doses seemed to recruit specifically caudate-putamen regions, starting from dorsal areas and gradually involving the dorsomedial subregion at the maximum haloperidol dose. Remarkably, only the lowest and the highest dosages of haloperidol, but not the intermediate one, promoted significant *Arc* expression decrease in the cortex.

C-fos expression was induced only in dorsolateral and ventromedial caudate-putamen, as well as in the nucleus accumbens shell, by the lowest haloperidol dosage. By

increasing the dose, *c-fos* expression was recruited in a "chessboard" fashion in striatal subregions, with haloperidol 0.5mg/kg inducing also ventrolateral caudate-putamen gene expression as compared to haloperidol 0.25mg/kg, and haloperidol 0.8mg/kg reaching the widest striatal *c-fos* induction, which was overexpressed in all the caudate-putamen and the nucleus accumbens.

Less sensitive than the other IEGs analyzed, *Zif268* showed a broad induction in the caudate-putamen by the lowest dose of haloperidol, and increasing doses only recruited gene expression specifically in the nucleus accumbens core.

A large amount of studies have demonstrated specific patterns of IEGs expression in response to haloperidol treatment [296,247,99,289,279,17,146]. Moreover, recent work from our laboratory has directly linked the peculiar striatal pattern of *Homer1a* gene expression by haloperidol to the selective dopamine D2 receptors blockade by this typical antipsychotic [20]. Present results further confirm our previous results on the differential impact on IEGs expression by typical antipsychotics, such as haloperidol, and atypical antipsychotics, such as olanzapine [21,99].

However, the abovementioned studies always used fixed doses of haloperidol, in order to achieve behavioral cut-offs (e.g. catalepsy), thereby comparing changes in animal behaviors obtained by haloperidol administration to the specific pattern of IEGs expression induced.

A recent work by Natesan et al. [351] tested increasing doses of haloperidol on multiple concurrent behavioral (i.e. locomotor activity, catalepsy, conditioned avoidance response) and biochemical (D2 dopamine and 5HT2a serotonin receptors occupancy, CFOS striatal expression) parameters, and compared haloperidol to risperidone and aripiprazole. The authors demonstrated that haloperidol may reach more than 80% of D2 receptors occupancy already at the dose of 0.1mg/kg. Increasing doses, till 1mg/kg, progressively achieved a D2 receptors occupancy plateau of about 90%. Oppositely,

even at maximum dosages, the occupancy of 5HT2 cortical receptors by haloperidol never reached values higher than 50%. However, behavioral tasks, in the same study, revealed that, although reaching the D2 receptors occupancy plateau at 0.1mg/kg, catalepsy gradually onsets between 0.1mg/kg and 1mg/kg. Similarly, locomotor activity is progressively reduced between 0.1mg/kg and 1mg/kg. Strikingly, with regards to CFOS striatal induction by haloperidol, it starts at the dose of 0.05mg/kg, but reaches a plateau of expression in the dorsal striatum at 0.5mg/kg, with no further variations by higher doses. Oppositely, nucleus accumbens CFOS expression seems to increase progressively with incremental doses of haloperidol. Remarkably, these findings tightly resemble our present gene expression results, even if Natesan et al. only analyzed two striatal macro-regions, compared to our subregions division of striatum. Moreover, our behavior locomotor activity analysis showed a progressive significant reduction in rat movements 20 minutes following haloperidol injection. To note, the higher is haloperidol dosage, the more this hypolocomotion is pronounced, even without reaching statistical significance amongst treatment groups.

Therefore, in the light of our results, we can hypothesize that the progressive reduction in locomotor behavior by incremental haloperidol dosages might depend on the gradual involvement of striatal subregions, as demonstrated by the progressive recruitment of IEGs expression in these areas, rather than an increase in dopamine D2 receptors blockade, which reaches a plateau already at doses lower than those used in the present study. Moreover, the lack of cortical IEGs induction by haloperidol is likely depending upon the scarce affinity to serotonergic receptors by this typical antipsychotic, as also suggested in our previous works [17].

We compared the effects of increasing doses of haloperidol on PSD genes expression to those of asenapine, a recently marketed antipsychotic with a broad multireceptor

profile, and of olanzapine, here used as a touchstone of atypical antipsychotic whose gene expression effects we have well studies in previous works [21,99].

As compared to the other atypical antipsychotics at present used in clinical practice, asenapine holds high affinity to multiple serotonin receptors (5HT1a-b, 5HT2a-c, 5HT5, 5HT6, 5HT7), to adrenaline receptors (alpha1, alpha2a-c) and to dopamine D1, D2, D3 and D4 receptors [236], with antagonist activity. Asenapine has been demonstrated to promote dopamine, serotonin and noradrenaline release in cortex and dopamine release in the nucleus accumbens at doses that have antipsychotic activity in animal behavioral studies [237]. Thanks to its unique multireceptorial profile, asenapine may differentially impact glutamatergic and dopaminergic systems in cortical and subcortical regions. Indeed, it enhances glutamate NMDA-mediated currents in pyramidal cortical neurons, while it decreases NMDA receptor activity in caudate-putamen and nucleus accumbens; moreover, the chronic treatment with asenapine potentiates AMPA receptor activity in hippocampus [241]. On the other hand, asenapine may specifically enhance the dopamine bursts from VTA to the medial prefrontal cortex and the nucleus accumbens, and of noradrenaline from locus coeruleus to the cortex [248].

Present results showed that asenapine may induce a peculiar pattern of PSD genes expression in both cortex and striatum. Paralleling the experiment with haloperidol, we used three incremental dosages of asenapine, based on previous studies analyzing biochemical and behavioral effects of this antipsychotic [352,353,239-241,354].

We found that *Homer1a* expression was strongly induced in both cortex and striatum (both caudate-putamen and nucleus accumbens) when animals were administered with low doses of asenapine (0.05 mg/kg and 0.1 mg/kg). Raising doses promoted a peculiar de-recruiting of *Homer1a* cortical gene expression and the maximum dosage of 0.3mg/kg showed a preferential striatal induction of the IEG. Moreover, differently

from haloperidol, incremental doses of asenapine induced a strong increase also in the signal intensity of *Homer1a* striatal gene expression, which resulted significantly higher in the dorsal striatum as compared to the ventral areas at the maximum dose we used. The other IEGs we analyzed displayed less sensitive response to asenapine treatment than *Homer1a*. However, increasing doses of the compound promoted differential patterns of gene expression. *C-fos* induction, for instance, was only apparent at the highest dose of asenapine, whereas the other dosages showed no impact on gene expression. Notably, the pattern of *c-fos* expression by asenapine 0.3mg/kg tightly resembled that by the highest dose of haloperidol (0.8mg/kg), causing *c-fos* transcript activation in the whole caudate-putamen and in the nucleus accumbens.

Arc gene expression was not impacted by the lowest dose of asenapine, but increasing dosages promoted a clearly different pattern of induction. Asenapine 0.1mg/kg, indeed, significantly induced *Arc* expression selectively in cingulate, motor and agranular cortex, whereas asenapine 0.3mg/kg had no impact on cortical gene expression but induced *Arc* in the dorsal caudate-putamen and in the nucleus accumbens core, with a pattern that was very similar to that promoted by haloperidol.

Zif268 displayed no variations in gene expression by increasing doses of asenapine. However, all the three dosages induced *Zif268* gene expression in the whole caudate-putamen and the nucleus accumbens shell, a pattern that resulted clearly similar to that described following haloperidol administration. Finally, asenapine administration resulted in a more pronounced impact on constitutive PSD genes expression as compared to haloperidol. *Homer1b/c*, indeed, was directly overexpressed in motor, agranular and cingulate cortices by the intermediate and the highest dosages of asenapine, as well as in the nucleus accumbens core. *PSD95*, in the other hand, was strongly upregulated by all the three doses of asenapine in both the cortex and the

striatum, with a pattern of gene modulation very similar to that induced by olanzapine, differently from haloperidol.

Although scarce data at present exist in literature on gene expression modulation by asenapine, our results seem consistent with a recent finding of FOS activation by asenapine 0.075mg/kg in medial prefrontal cortex lesioned rats [355], even in this study no modulation was induced in control animals.

As above mentioned, asenapine shows a broad multireceptor affinity for serotonin, adrenaline and dopamine receptors. Recent studies have demonstrated that asenapine, when administered at increasing doses as in our experiment, may progressively stimulate dopamine, noradrenaline and serotonin efflux in prefrontal cortex and nucleus accumbens [248]. These effects are strictly dependent on both 5HT2a serotonin receptors and alpha2 adrenoreceptors blockade by asenapine [353] and appear maximal at intermediate dose of 0.1mg/kg. This dose, indeed, may maximally elevate dopamine release in both prefrontal cortex and nucleus accumbens, as well as it increases cortical noradrenaline [248]. It appears that higher dosages than 0.1mg/kg may reach a plateau in stimulating monoamines efflux in cortical regions. However, only high dosages, such as 0.2mg/kg, specifically elicit cortical serotonin efflux, differently from lower doses [248]. Thus, it is possible that our findings of a differential impact on IEGs expression by increasing doses of asenapine may reflect their different effects on monoamines cortical and subcortical release. Indeed, we observed a wide *Homer1a* cortical expression when asenapine is administered at 0.1mg/kg, as well as *Arc* gene expression was only induced in cortical subregions by the same dose. These effects may putatively depend upon the maximal dopamine and serotonin efflux reached by asenapine at this dose. Moreover, the higher cortical activation achieved at this dose is probably mirrored by the significant increase in locomotor behavior we observed in rats treated with 0.1mg/kg asenapine.

The progressive de-recruitment of IEGs expression in cortical areas and the corresponding increase in striatal genes activation and signal intensity in striatum by incremental doses of asenapine might putatively be explained by a gradual increase in dopamine D2 receptors occupancy, which has been recently observed in a PET study on humans administered with increasing asenapine dosages [356]. A prominent role in these effects might be played by the balanced affinity, an probably occupancy, exerted by asenapine on dopamine D1 and D2 receptors, which tightly resembles that of clozapine, which we have previously demonstrated having no effects on cortical IEGs expression [17]. The increasing activity on dopamine D1 receptors at incremental doses by asenapine has been also recently correlated to a progressive improvement in phencyclidine-induced object recognition deficits in rats [354], as well as to a clozapine-like facilitation of NMDA receptors-mediated prefrontal cortical currents [352].

However, the remarkable differences in IEGs modulation in striatum by asenapine at high dosages (which shares large similarities with haloperidol) and clozapine might probably depend on the broad multireceptor affinity of asenapine as compared to clozapine, and need further specific investigations. Furthermore, asenapine has been demonstrated to have high affinity for both 5HT6 and 5HT7 serotonin receptors, which have been both correlated to pro-cognitive effects of novel antipsychotic compounds [357,358]. Our recent works identified a peculiar *Homer1a* gene cortical modulation as a pro-cognitive target in psychosis by compounds that have been proposed in add-on to antipsychotic therapies in schizophrenia, such as memantine [359]. It is possible that *Homer1a* peculiar cortical pattern of expression may reflect cognitive improving performances by asenapine due to its unique receptor profile.

In conclusion, our results demonstrated that antipsychotics may progressively recruit IEGs expression in cortical and subcortical areas when administered at incremental

doses. These effects may reflect a fine-tuned dose-dependent modulation of PSD genes by antipsychotics, which is strictly influenced by balancing in receptor affinities exerted at different dosages, thereby stimulating further investigation on postsynaptic mechanisms underlying antipsychotics clinical efficacy.

Concluding remarks

These studies represent a path following the logical thread of demonstrating that the PSD networks may specifically respond to multireceptorial stimuli. Indeed, our present findings not only confirm that PSD genes may differentially be induced by diverse antipsychotic drugs with regards to their degree of dopamine D2 receptors binding, but they shed light on the fact that these genes are differentially impacted by drug associations as compared to each drug when administered alone. Above all, *Homer1a*, which is induced in a IEG-like fashion withouth carrying a signaling *per se*, rapidly responds to multireceptorial stimuli with a specific topographic pattern in brain areas that have been implicated in the pathophysiology of psychotic disorders. Following the works by other laboratories, we have demonstrated that combined therapies substantially act on common intracellular pathways, elaborated and routed by PSD networks, and by which they can induce synergistic downstream messages to the nucleus. Homer family proteins, and related PSD proteins, represent a crucial signaling network for the integration and elaboration of multiple concurrent starting at diverse membrane receptors, such as dopamine, glutamate and serotonin, thereby acting as a functional protein crossroads. We also demonstrated that the increased efficacy of combined therapeutic strategies may putatively rely on the possibile synergistic intracellular effects on these common crossroads. For instance, mood stabilizers might act by facilitating the achievement of nuclear targets by downstream signaling activated

by antipsychotic that have been concurrently administered. Finally, multireceptorial agents seem a promising therapeutic strategy for psychosis. Our preclinical studies, indeed, demonstrated that they may induce peculiar IEG induction in cortical and subcortical areas that is highly different from that induced by common antipsychotics and include the progressive recruitment of brain areas depending on doses. All these experiments, although stating some concluding findings, aim at opening new avenues of investigation that will further deepen our knowledge on both antipsychotic mechanisms of action and the pathophysiology of psychotic disorders, thereby stimulating the future development of "molecular targeted" therapies that will increase efficacy and reduce side-effects in psychotic patients.

Acknowledgements

Ringraziare non è mai facile, soprattutto quando le persone da ringraziare sono tante e tutte care, e magari si corre il rischio di tralasciare qualcuno.

A mia moglie, innanzitutto e soprattutto, perché sopporta e vigila sui miei sogni, e li difende come se fossero suoi, anche se non li condivide. E, più di tutto, perché l'unico vero obiettivo della vita me l'ha insegnato lei, regalandomi il più bel sogno che si possa desiderare: mia figlia.

Ai miei genitori, perché credono che il loro figliolo sia il più bravo ed il più intelligente di tutti. Ed io glielo lascio credere, perché le illusioni sono il pane quotidiano della speranza e dei sogni, e la speranza e i sogni sono il motore di chi, come me, crede nella ricerca scientifica e nella cura delle persone.

Ai miei amici, perché c'erano, ci sono, ci saranno, qualunque sia la strada e dovunque mi porterà.

Ai miei colleghi, tutti, nessuno escluso, dai più grandi che mi hanno insegnato ai più piccoli a cui ho fatto sudare mani e camici in laboratorio. Perché da soli non si vince, è

la squadra che porta a casa il risultato. E, quanto più è unito e forte il gruppo, tanto meno amare saranno le delusioni e le sofferenze, e più importanti e salde le vittorie. E la nostra è una squadra vera.

Ai libri, perché in loro risiedono i miei sogni di bambino, di uomo, di medico e di ricercatore.

E infine, all'Università e all'Italia, perché mi hanno insegnato che niente è per sempre, se non i desideri; che nessuno è indispensabile, ma che devi sempre dimostrare di esserlo; che il potere, alla fine, logora solo chi ce l'ha; e che la ricerca scientifica, quella vera, si nutre del lavoro e dei sogni solo ed esclusivamente dei ricercatori appassionati. Tutti gli altri sono solo nomi su articoli scientifici.

References

1. Bennett MR (2011) Schizophrenia: susceptibility genes, dendritic-spine pathology and gray matter loss. Prog Neurobiol 95 (3):275-300

2. Balu DT, Coyle JT (2011) Neuroplasticity signaling pathways linked to the pathophysiology of schizophrenia. Neurosci Biobehav Rev 35 (3):848-870

3. Van Winkel R, Esquivel G, Kenis G, Wichers M, Collip D, Peerbooms O, Rutten B, Myin-Germeys I, Van Os J (2010) REVIEW: Genome-wide findings in schizophrenia and the role of gene-environment interplay. CNS Neurosci Ther 16 (5):e185-192

4. Lisman JE, Coyle JT, Green RW, Javitt DC, Benes FM, Heckers S, Grace AA (2008) Circuit-based framework for understanding neurotransmitter and risk gene interactions in schizophrenia. Trends Neurosci 31 (5):234-242

5. Zhang H, Etherington LA, Hafner AS, Belelli D, Coussen F, Delagrange P, Chaouloff F, Spedding M, Lambert JJ, Choquet D, Groc L (2013) Regulation of AMPA receptor surface trafficking and synaptic plasticity by a cognitive enhancer and antidepressant molecule. Mol Psychiatry 18 (4):471-484

6. Kennedy MB (2000) Signal-processing machines at the postsynaptic density. Science 290 (5492):750-754

7. de Bartolomeis A, Fiore G (2004) Postsynaptic density scaffolding proteins at excitatory synapse and disorders of synaptic plasticity: implications for human behavior pathologies. Int Rev Neurobiol 59:221-254

8. Murakoshi H, Yasuda R (2012) Postsynaptic signaling during plasticity of dendritic spines. Trends Neurosci 35 (2):135-143

9. Boeckers TM (2006) The postsynaptic density. Cell Tissue Res 326 (2):409-422

10. Bayes A, van de Lagemaat LN, Collins MO, Croning MD, Whittle IR, Choudhary JS, Grant SG (2011) Characterization of the proteome, diseases and evolution of the human postsynaptic density. Nat Neurosci 14 (1):19-21

11. Snyder MA, Gao WJ (2013) NMDA hypofunction as a convergence point for progression and symptoms of schizophrenia. Front Cell Neurosci 7:31

12. Coyle JT, Basu A, Benneyworth M, Balu D, Konopaske G (2012) Glutamatergic synaptic dysregulation in schizophrenia: therapeutic implications. Handb Exp Pharmacol (213):267-295

13. Clinton SM, Meador-Woodruff JH (2004) Abnormalities of the NMDA Receptor and Associated Intracellular Molecules in the Thalamus in Schizophrenia and Bipolar Disorder. Neuropsychopharmacology 29 (7):1353-1362

14. Clinton SM, Haroutunian V, Davis KL, Meador-Woodruff JH (2003) Altered transcript expression of NMDA receptor-associated postsynaptic proteins in the thalamus of subjects with schizophrenia. Am J Psychiatry 160 (6):1100-1109

15. Iasevoli F, Ambesi-Impiombato A, Fiore G, Panariello F, Muscettola G, de Bartolomeis A (2011) Pattern of acute induction of Homer1a gene is preserved after chronic treatment with first- and second-generation antipsychotics: effect of short-term drug discontinuation and comparison with Homer1a-interacting genes. J Psychopharmacol 25 (7):875-887

16. Moutsimilli L, Farley S, El Khoury MA, Chamot C, Sibarita JB, Racine V, El Mestikawy S, Mathieu F, Dumas S, Giros B, Tzavara ET (2008) Antipsychotics increase vesicular glutamate transporter 2 (VGLUT2) expression in thalamolimbic pathways. Neuropharmacology 54 (3):497-508

17. Tomasetti C, Dell'Aversano C, Iasevoli F, de Bartolomeis A (2007) Homer splice variants modulation within cortico-subcortical regions by dopamine D2 antagonists, a partial agonist, and an indirect agonist: implication for glutamatergic postsynaptic density in antipsychotics action. Neuroscience 150 (1):144-158

18. Brennand KJ, Simone A, Jou J, Gelboin-Burkhart C, Tran N, Sangar S, Li Y, Mu Y, Chen G, Yu D, McCarthy S, Sebat J, Gage FH (2011) Modelling schizophrenia using human induced pluripotent stem cells. Nature 473 (7346):221-225

19. Cahill ME, Xie Z, Day M, Photowala H, Barbolina MV, Miller CA, Weiss C, Radulovic J, Sweatt JD, Disterhoft JF, Surmeier DJ, Penzes P (2009) Kalirin regulates cortical spine morphogenesis and disease-related behavioral phenotypes. Proc Natl Acad Sci U S A 106 (31):13058-13063

20. Iasevoli F, Fiore G, Cicale M, Muscettola G, de Bartolomeis A (2010) Haloperidol induces higher Homer1a expression than risperidone, olanzapine and sulpiride in striatal sub-regions. Psychiatry Res 177 (1-2):255-260

21. Iasevoli F, Tomasetti C, Marmo F, Bravi D, Arnt J, de Bartolomeis A (2010) Divergent acute and chronic modulation of glutamatergic postsynaptic density genes expression by the antipsychotics haloperidol and sertindole. Psychopharmacology (Berl) 212 (3):329-344

22. Hashimoto R, Tankou S, Takeda M, Sawa A (2007) Postsynaptic density: a key convergent site for schizophrenia susceptibility factors and possible target for drug development. Drugs Today (Barc) 43 (9):645-654

23. Critchlow HM, Maycox PR, Skepper JN, Krylova O (2006) Clozapine and haloperidol differentially regulate dendritic spine formation and synaptogenesis in rat hippocampal neurons. Mol Cell Neurosci 32 (4):356-365

24. Meshul CK, Stallbaumer RK, Taylor B, Janowsky A (1994) Haloperidol-induced morphological changes in striatum are associated with glutamate synapses. Brain Res 648 (2):181-195

25. O'Connor JA, Muly EC, Arnold SE, Hemby SE (2007) AMPA receptor subunit and splice variant expression in the DLPFC of schizophrenic subjects and rhesus monkeys chronically administered antipsychotic drugs. Schizophr Res 90 (1-3):28-40

26. Fumagalli F, Frasca A, Racagni G, Riva MA (2008) Dynamic regulation of glutamatergic postsynaptic activity in rat prefrontal cortex by repeated administration of antipsychotic drugs. Mol Pharmacol 73 (5):1484-1490

27. Purkayastha S, Ford J, Kanjilal B, Diallo S, Del Rosario Inigo J, Neuwirth L, El Idrissi A, Ahmed Z, Wieraszko A, Azmitia EC, Banerjee P (2012) Clozapine functions through the prefrontal cortex serotonin 1A receptor to heighten neuronal activity via calmodulin kinase II-NMDA receptor interactions. J Neurochem 120 (3):396-407

28. Missale C, Nash SR, Robinson SW, Jaber M, Caron MG (1998) Dopamine receptors: from structure to function. Physiol Rev 78 (1):189-225

29. Traynelis SF, Wollmuth LP, McBain CJ, Menniti FS, Vance KM, Ogden KK, Hansen KB, Yuan H, Myers SJ, Dingledine R (2010) Glutamate receptor ion channels: structure, regulation, and function. Pharmacol Rev 62 (3):405-496

30. Conn PJ, Pin JP (1997) Pharmacology and functions of metabotropic glutamate receptors. Annu Rev Pharmacol Toxicol 37:205-237

31. Pin JP, Duvoisin R (1995) The metabotropic glutamate receptors: structure and functions. Neuropharmacology 34 (1):1-26

32. Nicoletti F, Bockaert J, Collingridge GL, Conn PJ, Ferraguti F, Schoepp DD, Wroblewski JT, Pin JP (2011) Metabotropic glutamate receptors: from the workbench to the bedside. Neuropharmacology 60 (7-8):1017-1041

33. Paoletti P (2011) Molecular basis of NMDA receptor functional diversity. Eur J Neurosci 33 (8):1351-1365

34. Yao WD, Spealman RD, Zhang J (2008) Dopaminergic signaling in dendritic spines. Biochem Pharmacol 75 (11):2055-2069

35. Oliveira AM, Bading H (2011) Calcium signaling in cognition and aging-dependent cognitive decline. Biofactors 37 (3):168-174

36. de Bartolomeis A, Iasevoli F (2003) The Homer family and the signal transduction system at glutamatergic postsynaptic density: potential role in behavior and pharmacotherapy. Psychopharmacol Bull 37 (3):51-83

37. Simeone A, Di Salvio M, Di Giovannantonio LG, Acampora D, Omodei D, Tomasetti C (2011) The role of otx2 in adult mesencephalic-diencephalic dopaminergic neurons. Mol Neurobiol 43 (2):107-113

38. Simeone A, Puelles E, Omodei D, Acampora D, Di Giovannantonio LG, Di Salvio M, Mancuso P, Tomasetti C (2011) Otx genes in neurogenesis of mesencephalic dopaminergic neurons. Dev Neurobiol 71 (8):665-679

39. Hoftman GD, Lewis DA (2011) Postnatal developmental trajectories of neural circuits in the primate prefrontal cortex: identifying sensitive periods for vulnerability to schizophrenia. Schizophr Bull 37 (3):493-503

40. Rao JS, Kellom M, Reese EA, Rapoport SI, Kim HW (2012) Dysregulated glutamate and dopamine transporters in postmortem frontal cortex from bipolar and schizophrenic patients. J Affect Disord 136 (1-2):63-71

41. Chen G, Henter ID, Manji HK (2010) Presynaptic glutamatergic dysfunction in bipolar disorder. Biol Psychiatry 67 (11):1007-1009

42. Tepper JM, Abercrombie ED, Bolam JP (2007) Basal ganglia macrocircuits. Prog Brain Res 160:3-7

43. Del Arco A, Mora F (2008) Prefrontal cortex-nucleus accumbens interaction: in vivo modulation by dopamine and glutamate in the prefrontal cortex. Pharmacol Biochem Behav 90 (2):226-235

44. Cousins DA, Butts K, Young AH (2009) The role of dopamine in bipolar disorder. Bipolar Disord 11 (8):787-806

45. Stone JM, Morrison PD, Pilowsky LS (2007) Glutamate and dopamine dysregulation in schizophrenia--a synthesis and selective review. J Psychopharmacol 21 (4):440-452

46. Zarate C, Jr., Machado-Vieira R, Henter I, Ibrahim L, Diazgranados N, Salvadore G (2010) Glutamatergic modulators: the future of treating mood disorders? Harv Rev Psychiatry 18 (5):293-303

47. Bondi C, Matthews M, Moghaddam B (2012) Glutamatergic Animal Models of Schizophrenia. Curr Pharm Des

48. Schwartz TL, Sachdeva S, Stahl SM (2012) 'Genetic data supporting the NMDA glutamate receptor hypothesis for schizophrenia'. Curr Pharm Des

49. Beaulieu JM, Sotnikova TD, Yao WD, Kockeritz L, Woodgett JR, Gainetdinov RR, Caron MG (2004) Lithium antagonizes dopamine-dependent behaviors mediated by an AKT/glycogen synthase kinase 3 signaling cascade. Proc Natl Acad Sci U S A 101 (14):5099-5104

50. Carr DB, Sesack SR (1996) Hippocampal afferents to the rat prefrontal cortex: synaptic targets and relation to dopamine terminals. J Comp Neurol 369 (1):1-15

51. Bergson C, Mrzljak L, Smiley JF, Pappy M, Levenson R, Goldman-Rakic PS (1995) Regional, cellular, and subcellular variations in the distribution of D1 and D5 dopamine receptors in primate brain. J Neurosci 15 (12):7821-7836

52. de Almeida J, Mengod G (2010) D2 and D4 dopamine receptor mRNA distribution in pyramidal neurons and GABAergic subpopulations in monkey prefrontal cortex: implications for schizophrenia treatment. Neuroscience 170 (4):1133-1139

53. Cepeda C, Andre VM, Jocoy EL, Levine MS (2009) NMDA and Dopamine: Diverse Mechanisms Applied to Interacting Receptor Systems.

54. Muly EC, Maddox M, Smith Y (2003) Distribution of mGluR1alpha and mGluR5 immunolabeling in primate prefrontal cortex. J Comp Neurol 467 (4):521-535

55. Tamaru Y, Nomura S, Mizuno N, Shigemoto R (2001) Distribution of metabotropic glutamate receptor mGluR3 in the mouse CNS: differential location relative to pre- and postsynaptic sites. Neuroscience 106 (3):481-503

56. Vinson PN, Conn PJ (2012) Metabotropic glutamate receptors as therapeutic targets for schizophrenia. Neuropharmacology 62 (3):1461-1472

57. Muly EC, 3rd, Szigeti K, Goldman-Rakic PS (1998) D1 receptor in interneurons of macaque prefrontal cortex: distribution and subcellular localization. J Neurosci 18 (24):10553-10565

58. Smith Y, Villalba R (2008) Striatal and extrastriatal dopamine in the basal ganglia: an overview of its anatomical organization in normal and Parkinsonian brains. Mov Disord 23 Suppl 3:S534-547

59. Tarazi FI, Baldessarini RJ (1999) Brain dopamine D(4) receptors: basic and clinical status. Int J Neuropsychopharmacol 2 (1):41-58

60. Tarazi FI, Baldessarini RJ (1999) Regional localization of dopamine and ionotropic glutamate receptor subtypes in striatolimbic brain regions. J Neurosci Res 55 (4):401-410

61. Tarazi FI, Campbell A, Yeghiayan SK, Baldessarini RJ (1998) Localization of dopamine receptor subtypes in corpus striatum and nucleus accumbens septi of rat brain: comparison of D1-, D2-, and D4-like receptors. Neuroscience 83 (1):169-176

62. Tarazi FI, Yeghiayan SK, Neumeyer JL, Baldessarini RJ (1998) Medial prefrontal cortical D2 and striatolimbic D4 dopamine receptors: common targets for typical and atypical antipsychotic drugs. Prog Neuropsychopharmacol Biol Psychiatry 22 (4):693-707

63. Paquet M, Smith Y (2003) Group I metabotropic glutamate receptors in the monkey striatum: subsynaptic association with glutamatergic and dopaminergic afferents. J Neurosci 23 (20):7659-7669

64. David HN, Ansseau M, Abraini JH (2005) Dopamine-glutamate reciprocal modulation of release and motor responses in the rat caudate-putamen and nucleus accumbens of "intact" animals. Brain Res Brain Res Rev 50 (2):336-360

65. Del Arco A, Mora F (2009) Neurotransmitters and prefrontal cortex-limbic system interactions: implications for plasticity and psychiatric disorders. J Neural Transm 116 (8):941-952

66. Wickens JR (2009) Synaptic plasticity in the basal ganglia. Behav Brain Res 199 (1):119-128

67. Beaulieu JM, Gainetdinov RR (2011) The physiology, signaling, and pharmacology of dopamine receptors. Pharmacol Rev 63 (1):182-217

68. Morgado-Bernal I (2011) Learning and memory consolidation: linking molecular and behavioral data. Neuroscience 176:12-19

69. Calabresi P, Picconi B, Tozzi A, Di Filippo M (2007) Dopamine-mediated regulation of corticostriatal synaptic plasticity. Trends Neurosci 30 (5):211-219

70. Shiflett MW, Balleine BW (2011) Molecular substrates of action control in cortico-striatal circuits. Prog Neurobiol 95 (1):1-13

71. Okabe S (2007) Molecular anatomy of the postsynaptic density. Mol Cell Neurosci 34 (4):503-518

72. Sheng M, Hoogenraad CC (2007) The postsynaptic architecture of excitatory synapses: a more quantitative view. Annu Rev Biochem 76:823-847

73. Foa L, Gasperini R (2009) Developmental roles for Homer: more than just a pretty scaffold. J Neurochem 108 (1):1-10

74. Zheng CY, Seabold GK, Horak M, Petralia RS (2011) MAGUKs, synaptic development, and synaptic plasticity. Neuroscientist 17 (5):493-512

75. Romero G, von Zastrow M, Friedman PA (2011) Role of PDZ proteins in regulating trafficking, signaling, and function of GPCRs: means, motif, and opportunity. Adv Pharmacol 62:279-314

76. Ciruela F, Canela L, Burgueno J, Soriguera A, Cabello N, Canela EI, Casado V, Cortes A, Mallol J, Woods AS, Ferre S, Lluis C, Franco R (2005) Heptaspanning membrane receptors and cytoskeletal/scaffolding proteins: focus on adenosine, dopamine, and metabotropic glutamate receptor function. J Mol Neurosci 26 (2-3):277-292

77. de Bartolomeis A, Fiore G, Iasevoli F (2005) Dopamine-glutamate interaction and antipsychotics mechanism of action: implication for new pharmacological strategies in psychosis. Curr Pharm Des 11 (27):3561-3594

78. Szumlinski KK, Dehoff MH, Kang SH, Frys KA, Lominac KD, Klugmann M, Rohrer J, Griffin W, 3rd, Toda S, Champtiaux NP, Berry T, Tu JC, Shealy SE, During MJ, Middaugh LD, Worley PF, Kalivas PW (2004) Homer proteins regulate sensitivity to cocaine. Neuron 43 (3):401-413

79. Szumlinski KK, Lominac KD, Kleschen MJ, Oleson EB, Dehoff MH, Schwarz MK, Seeburg PH, Worley PF, Kalivas PW (2005) Behavioral and neurochemical phenotyping of Homer1 mutant mice: possible relevance to schizophrenia. Genes Brain Behav 4 (5):273-288

80. Wyneken U, Marengo JJ, Orrego F (2004) Electrophysiology and plasticity in isolated postsynaptic densities. Brain Res Brain Res Rev 47 (1-3):54-70

81. Brakeman PR, Lanahan AA, O'Brien R, Roche K, Barnes CA, Huganir RL, Worley PF (1997) Homer: a protein that selectively binds metabotropic glutamate receptors. Nature 386 (6622):284-288

82. Kato A, Ozawa F, Saitoh Y, Fukazawa Y, Sugiyama H, Inokuchi K (1998) Novel members of the Vesl/Homer family of PDZ proteins that bind metabotropic glutamate receptors. J Biol Chem 273 (37):23969-23975

83. Xiao B, Tu JC, Petralia RS, Yuan JP, Doan A, Breder CD, Ruggiero A, Lanahan AA, Wenthold RJ, Worley PF (1998) Homer regulates the association of group 1 metabotropic glutamate receptors with multivalent complexes of homer-related, synaptic proteins. Neuron 21 (4):707-716

84. Sun J, Tadokoro S, Imanaka T, Murakami SD, Nakamura M, Kashiwada K, Ko J, Nishida W, Sobue K (1998) Isolation of PSD-Zip45, a novel Homer/vesl family protein containing leucine zipper motifs, from rat brain. FEBS Lett 437 (3):304-308

85. de Bartolomeis A, Aloj L, Ambesi-Impiombato A, Bravi D, Caraco C, Muscettola G, Barone P (2002) Acute administration of antipsychotics modulates Homer striatal gene expression differentially. Brain Res Mol Brain Res 98 (1-2):124-129

86. Bottai D, Guzowski JF, Schwarz MK, Kang SH, Xiao B, Lanahan A, Worley PF, Seeburg PH (2002) Synaptic activity-induced conversion of intronic to exonic sequence in Homer 1 immediate early gene expression. J Neurosci 22 (1):167-175

87. Hennou S, Kato A, Schneider EM, Lundstrom K, Gahwiler BH, Inokuchi K, Gerber U, Ehrengruber MU (2003) Homer-1a/Vesl-1S enhances hippocampal synaptic transmission. Eur J Neurosci 18 (4):811-819

88. Sala C, Roussignol G, Meldolesi J, Fagni L (2005) Key role of the postsynaptic density scaffold proteins Shank and Homer in the functional architecture of Ca2+ homeostasis at dendritic spines in hippocampal neurons. J Neurosci 25 (18):4587-4592

89. Xiao B, Tu JC, Worley PF (2000) Homer: a link between neural activity and glutamate receptor function. Curr Opin Neurobiol 10 (3):370-374

90. Hwang SY, Wei J, Westhoff JH, Duncan RS, Ozawa F, Volpe P, Inokuchi K, Koulen P (2003) Differential functional interaction of two Vesl/Homer protein isoforms with ryanodine receptor type 1: a novel mechanism for control of intracellular calcium signaling. Cell Calcium 34 (2):177-184

91. Kammermeier PJ, Xiao B, Tu JC, Worley PF, Ikeda SR (2000) Homer proteins regulate coupling of group I metabotropic glutamate receptors to N-type calcium and M-type potassium channels. J Neurosci 20 (19):7238-7245

92. Tu JC, Xiao B, Naisbitt S, Yuan JP, Petralia RS, Brakeman P, Doan A, Aakalu VK, Lanahan AA, Sheng M, Worley PF (1999) Coupling of mGluR/Homer and PSD-95 complexes by the Shank family of postsynaptic density proteins. Neuron 23 (3):583-592

93. Tu JC, Xiao B, Yuan JP, Lanahan AA, Leoffert K, Li M, Linden DJ, Worley PF (1998) Homer binds a novel proline-rich motif and links group 1 metabotropic glutamate receptors with IP3 receptors. Neuron 21 (4):717-726

94. Yuan JP, Kiselyov K, Shin DM, Chen J, Shcheynikov N, Kang SH, Dehoff MH, Schwarz MK, Seeburg PH, Muallem S, Worley PF (2003) Homer binds TRPC family channels and is required for gating of TRPC1 by IP3 receptors. Cell 114 (6):777-789

95. Abe H, Misaka T, Tateyama M, Kubo Y (2003) Effects of coexpression with Homer isoforms on the function of metabotropic glutamate receptor 1alpha. Mol Cell Neurosci 23 (2):157-168

96. Shiraishi Y, Mizutani A, Yuasa S, Mikoshiba K, Furuichi T (2003) Glutamate-induced declustering of post-synaptic adaptor protein Cupidin (Homer 2/vesl-2) in cultured cerebellar granule cells. J Neurochem 87 (2):364-376

97. Shiraishi Y, Mizutani A, Yuasa S, Mikoshiba K, Furuichi T (2004) Differential expression of Homer family proteins in the developing mouse brain. J Comp Neurol 473 (4):582-599

98. French PJ, O'Connor V, Jones MW, Davis S, Errington ML, Voss K, Truchet B, Wotjak C, Stean T, Doyere V, Maroun M, Laroche S, Bliss TV (2001) Subfield-specific immediate early gene expression associated with hippocampal long-term potentiation in vivo. Eur J Neurosci 13 (5):968-976

99. Polese D, de Serpis AA, Ambesi-Impiombato A, Muscettola G, de Bartolomeis A (2002) Homer 1a gene expression modulation by antipsychotic drugs: involvement of the glutamate metabotropic system and effects of D-cycloserine. Neuropsychopharmacology 27 (6):906-913

100. Worley PF, Zeng W, Huang G, Kim JY, Shin DM, Kim MS, Yuan JP, Kiselyov K, Muallem S (2007) Homer proteins in Ca2+ signaling by excitable and non-excitable cells. Cell Calcium 42 (4-5):363-371

101. Bertaso F, Roussignol G, Worley P, Bockaert J, Fagni L, Ango F (2010) Homer1a-dependent crosstalk between NMDA and metabotropic glutamate receptors in mouse neurons. PLoS One 5 (3):e9755

102. Huang G, Kim JY, Dehoff M, Mizuno Y, Kamm KE, Worley PF, Muallem S, Zeng W (2007) Ca2+ signaling in microdomains: Homer1 mediates the interaction between RyR2 and Cav1.2 to regulate excitation-contraction coupling. J Biol Chem 282 (19):14283-14290

103. Pouliquin P, Dulhunty AF (2009) Homer and the ryanodine receptor. Eur Biophys J 39 (1):91-102

104. Duncan RS, Hwang SY, Koulen P (2005) Effects of Vesl/Homer proteins on intracellular signaling. Exp Biol Med (Maywood) 230 (8):527-535

105. Yang L, Mao L, Tang Q, Samdani S, Liu Z, Wang JQ (2004) A novel Ca2+-independent signaling pathway to extracellular signal-regulated protein kinase by

coactivation of NMDA receptors and metabotropic glutamate receptor 5 in neurons. J Neurosci 24 (48):10846-10857

106. Romorini S, Piccoli G, Jiang M, Grossano P, Tonna N, Passafaro M, Zhang M, Sala C (2004) A functional role of postsynaptic density-95-guanylate kinase-associated protein complex in regulating Shank assembly and stability to synapses. J Neurosci 24 (42):9391-9404

107. Xu W (2011) PSD-95-like membrane associated guanylate kinases (PSD-MAGUKs) and synaptic plasticity. Curr Opin Neurobiol 21 (2):306-312

108. Sturgill JF, Steiner P, Czervionke BL, Sabatini BL (2009) Distinct domains within PSD-95 mediate synaptic incorporation, stabilization, and activity-dependent trafficking. J Neurosci 29 (41):12845-12854

109. Migaud M, Charlesworth P, Dempster M, Webster LC, Watabe AM, Makhinson M, He Y, Ramsay MF, Morris RG, Morrison JH, O'Dell TJ, Grant SG (1998) Enhanced long-term potentiation and impaired learning in mice with mutant postsynaptic density-95 protein. Nature 396 (6710):433-439

110. Schnell E, Sizemore M, Karimzadegan S, Chen L, Bredt DS, Nicoll RA (2002) Direct interactions between PSD-95 and stargazin control synaptic AMPA receptor number. Proc Natl Acad Sci U S A 99 (21):13902-13907

111. Colledge M, Dean RA, Scott GK, Langeberg LK, Huganir RL, Scott JD (2000) Targeting of PKA to glutamate receptors through a MAGUK-AKAP complex. Neuron 27 (1):107-119

112. El-Husseini Ael D, Schnell E, Dakoji S, Sweeney N, Zhou Q, Prange O, Gauthier-Campbell C, Aguilera-Moreno A, Nicoll RA, Bredt DS (2002) Synaptic strength regulated by palmitate cycling on PSD-95. Cell 108 (6):849-863

113. Xu J, Liu ZA, Pei DS, Xu TJ (2010) Calcium/calmodulin-dependent kinase II facilitated GluR6 subunit serine phosphorylation through GluR6-PSD95-CaMKII signaling module assembly in cerebral ischemia injury. Brain Res 1366:197-203

114. Ivenshitz M, Segal M (2010) Neuronal density determines network connectivity and spontaneous activity in cultured hippocampus. J Neurophysiol 104 (2):1052-1060

115. Nassirpour R, Bahima L, Lalive AL, Luscher C, Lujan R, Slesinger PA (2010) Morphine- and CaMKII-dependent enhancement of GIRK channel signaling in hippocampal neurons. J Neurosci 30 (40):13419-13430

116. Boeckers TM, Bockmann J, Kreutz MR, Gundelfinger ED (2002) ProSAP/Shank proteins - a family of higher order organizing molecules of the postsynaptic density with an emerging role in human neurological disease. J Neurochem 81 (5):903-910

117. Sala C, Piech V, Wilson NR, Passafaro M, Liu G, Sheng M (2001) Regulation of dendritic spine morphology and synaptic function by Shank and Homer. Neuron 31 (1):115-130

118. Baron MK, Boeckers TM, Vaida B, Faham S, Gingery M, Sawaya MR, Salyer D, Gundelfinger ED, Bowie JU (2006) An architectural framework that may lie at the core of the postsynaptic density. Science 311 (5760):531-535

119. Distelhorst CW, Bootman MD (2011) Bcl-2 interaction with the inositol 1,4,5-trisphosphate receptor: role in Ca(2+) signaling and disease. Cell Calcium 50 (3):234-241

120. Lidow MS (2003) Calcium signaling dysfunction in schizophrenia: a unifying approach. Brain Res Brain Res Rev 43 (1):70-84

121. Fujiyama K, Kajii Y, Hiraoka S, Nishikawa T (2003) Differential regulation by stimulants of neocortical expression of mrt1, arc, and homer1a mRNA in the rats treated with repeated methamphetamine. Synapse 49 (3):143-149

122. Fourgeaud L, Mato S, Bouchet D, Hemar A, Worley PF, Manzoni OJ (2004) A single in vivo exposure to cocaine abolishes endocannabinoid-mediated long-term depression in the nucleus accumbens. J Neurosci 24 (31):6939-6945

123. Cochran SM, Fujimura M, Morris BJ, Pratt JA (2002) Acute and delayed effects of phencyclidine upon mRNA levels of markers of glutamatergic and GABAergic neurotransmitter function in the rat brain. Synapse 46 (3):206-214

124. Iasevoli F, Polese D, Ambesi-Impiombato A, Muscettola G, de Bartolomeis A (2007) Ketamine-related expression of glutamatergic postsynaptic density genes: possible implications in psychosis. Neurosci Lett 416 (1):1-5

125. Chiba S, Hashimoto R, Hattori S, Yohda M, Lipska B, Weinberger DR, Kunugi H (2006) Effect of antipsychotic drugs on DISC1 and dysbindin expression in mouse frontal cortex and hippocampus. J Neural Transm 113 (9):1337-1346

126. Clapcote SJ, Lipina TV, Millar JK, Mackie S, Christie S, Ogawa F, Lerch JP, Trimble K, Uchiyama M, Sakuraba Y, Kaneda H, Shiroishi T, Houslay MD, Henkelman RM, Sled JG, Gondo Y, Porteous DJ, Roder JC (2007) Behavioral phenotypes of Disc1 missense mutations in mice. Neuron 54 (3):387-402

127. Hu JH, Park JM, Park S, Xiao B, Dehoff MH, Kim S, Hayashi T, Schwarz MK, Huganir RL, Seeburg PH, Linden DJ, Worley PF (2010) Homeostatic scaling requires group I mGluR activation mediated by Homer1a. Neuron 68 (6):1128-1142

128. Szumlinski KK, Abernathy KE, Oleson EB, Klugmann M, Lominac KD, He DY, Ron D, During M, Kalivas PW (2006) Homer isoforms differentially regulate cocaine-induced neuroplasticity. Neuropsychopharmacology 31 (4):768-777

129. Bae JS, Kim JY, Park BL, Cheong HS, Kim JH, Shin JG, Park CS, Kim BJ, Lee CS, Kim JW, Lee M, Choi WH, Shin TM, Hwang J, Shin HD, Woo SI (2013) Lack of association between DISC1 polymorphisms and risk of schizophrenia in a Korean population. Psychiatry Res

130. Jaubert PJ, Golub MS, Lo YY, Germann SL, Dehoff MH, Worley PF, Kang SH, Schwarz MK, Seeburg PH, Berman RF (2007) Complex, multimodal behavioral profile of the Homer1 knockout mouse. Genes Brain Behav 6 (2):141-154

131. Lominac KD, Oleson EB, Pava M, Klugmann M, Schwarz MK, Seeburg PH, During MJ, Worley PF, Kalivas PW, Szumlinski KK (2005) Distinct roles for different Homer1 isoforms in behaviors and associated prefrontal cortex function. J Neurosci 25 (50):11586-11594

132. Norton N, Williams HJ, Williams NM, Spurlock G, Zammit S, Jones G, Jones S, Owen R, O'Donovan MC, Owen MJ (2003) Mutation screening of the Homer gene family and association analysis in schizophrenia. Am J Med Genet B Neuropsychiatr Genet 120B (1):18-21

133. Spellmann I, Rujescu D, Musil R, Mayr A, Giegling I, Genius J, Zill P, Dehning S, Opgen-Rhein M, Cerovecki A, Hartmann AM, Schafer M, Bondy B, Muller N, Moller HJ, Riedel M (2011) Homer-1 polymorphisms are associated with psychopathology and response to treatment in schizophrenic patients. J Psychiatr Res 45 (2):234-241

134. Gilks WP, Allott EH, Donohoe G, Cummings E, Gill M, Corvin AP, Morris DW (2010) Replicated genetic evidence supports a role for HOMER2 in schizophrenia. Neurosci Lett 468 (3):229-233

135. Kelleher RJ, 3rd, Geigenmuller U, Hovhannisyan H, Trautman E, Pinard R, Rathmell B, Carpenter R, Margulies D (2012) High-throughput sequencing of mGluR signaling pathway genes reveals enrichment of rare variants in autism. PLoS One 7 (4):e35003

136. Giuffrida R, Musumeci S, D'Antoni S, Bonaccorso CM, Giuffrida-Stella AM, Oostra BA, Catania MV (2005) A reduced number of metabotropic glutamate subtype 5 receptors are associated with constitutive homer proteins in a mouse model of fragile X syndrome. J Neurosci 25 (39):8908-8916

137. Ronesi JA, Collins KA, Hays SA, Tsai NP, Guo W, Birnbaum SG, Hu JH, Worley PF, Gibson JR, Huber KM (2012) Disrupted Homer scaffolds mediate abnormal mGluR5 function in a mouse model of fragile X syndrome. Nat Neurosci 15 (3):431-440, S431

138. de Bartolomeis A, Tomasetti C (2012) Calcium-dependent networks in dopamine-glutamate interaction: the role of postsynaptic scaffolding proteins. Mol Neurobiol 46 (2):275-296

139. Zhang GC, Mao LM, Liu XY, Parelkar NK, Arora A, Yang L, Hains M, Fibuch EE, Wang JQ (2007) In vivo regulation of Homer1a expression in the striatum by cocaine. Mol Pharmacol 71 (4):1148-1158

140. Ambesi-Impiombato A, Panariello F, Dell'aversano C, Tomasetti C, Muscettola G, de Bartolomeis A (2007) Differential expression of Homer 1 gene by acute and chronic administration of antipsychotics and dopamine transporter inhibitors in the rat forebrain. Synapse 61 (6):429-439

141. Assie MB, Dominguez H, Consul-Denjean N, Newman-Tancredi A (2006) In vivo occupancy of dopamine D2 receptors by antipsychotic drugs and novel compounds in the mouse striatum and olfactory tubercles. Naunyn Schmiedebergs Arch Pharmacol 373 (6):441-450

142. Seeger TF, Seymour PA, Schmidt AW, Zorn SH, Schulz DW, Lebel LA, McLean S, Guanowsky V, Howard HR, Lowe JA, 3rd, et al. (1995) Ziprasidone (CP-88,059): a new antipsychotic with combined dopamine and serotonin receptor antagonist activity. J Pharmacol Exp Ther 275 (1):101-113

143. Iasevoli F, Tomasetti C, Ambesi-Impiombato A, Muscettola G, de Bartolomeis A (2009) Dopamine receptor subtypes contribution to Homer1a induction: insights into antipsychotic molecular action. Prog Neuropsychopharmacol Biol Psychiatry 33 (5):813-821

144. Robinet EA, Geurts M, Maloteaux JM, Pauwels PJ (2001) Chronic treatment with certain antipsychotic drugs preserves upregulation of regulator of G-protein signalling 2 mRNA in rat striatum as opposed to c-fos mRNA. Neurosci Lett 307 (1):45-48

145. Semba J, Sakai MW, Suhara T, Akanuma N (1999) Differential effects of acute and chronic treatment with typical and atypical neuroleptics on c-fos mRNA expression in rat forebrain regions using non-radioactive in situ hybridization. Neurochem Int 34 (4):269-277

146. Tomasetti C, Dell'Aversano C, Iasevoli F, Marmo F, de Bartolomeis A (2011) The acute and chronic effects of combined antipsychotic-mood stabilizing treatment on the expression of cortical and striatal postsynaptic density genes. Prog Neuropsychopharmacol Biol Psychiatry 35 (1):184-197

147. Silver H, Chertkow Y, Weinreb O, Danovich L, Youdim M (2009) Multifunctional pharmacotherapy: what can we learn from study of selective serotonin reuptake inhibitor augmentation of antipsychotics in negative-symptom schizophrenia? Neurotherapeutics 6 (1):86-93

148. Lindenmayer JP, Khan A (2004) Pharmacological treatment strategies for schizophrenia. Expert Rev Neurother 4 (4):705-723

149. Mojtabai R, Olfson M (2010) National trends in psychotropic medication polypharmacy in office-based psychiatry. Arch Gen Psychiatry 67 (1):26-36

150. Barnes TR, Paton C (2011) Antipsychotic polypharmacy in schizophrenia: benefits and risks. CNS Drugs 25 (5):383-399

151. Grunze H, Vieta E, Goodwin GM, Bowden C, Licht RW, Moller HJ, Kasper S (2009) The World Federation of Societies of Biological Psychiatry (WFSBP) guidelines for the biological treatment of bipolar disorders: update 2009 on the treatment of acute mania. World J Biol Psychiatry 10 (2):85-116

152. Gitlin M, Frye MA (2012) Maintenance therapies in bipolar disorders. Bipolar Disord 14 Suppl 2:51-65

153. Wright BM, Eiland EH, 3rd, Lorenz R (2013) Augmentation with atypical antipsychotics for depression: a review of evidence-based support from the medical literature. Pharmacotherapy 33 (3):344-359

154. Sepehry AA, Potvin S, Elie R, Stip E (2007) Selective serotonin reuptake inhibitor (SSRI) add-on therapy for the negative symptoms of schizophrenia: a meta-analysis. J Clin Psychiatry 68 (4):604-610

155. Buckley PF, Stahl SM (2007) Pharmacological treatment of negative symptoms of schizophrenia: therapeutic opportunity or cul-de-sac? Acta Psychiatr Scand 115 (2):93-100

156. Rummel C, Kissling W, Leucht S (2005) Antidepressants as add-on treatment to antipsychotics for people with schizophrenia and pronounced negative symptoms: a systematic review of randomized trials. Schizophr Res 80 (1):85-97

157. Singh SP, Singh V, Kar N, Chan K (2010) Efficacy of antidepressants in treating the negative symptoms of chronic schizophrenia: meta-analysis. Br J Psychiatry 197 (3):174-179

158. Akhondzadeh S, Malek-Hosseini M, Ghoreishi A, Raznahan M, Rezazadeh SA (2008) Effect of ritanserin, a 5HT2A/2C antagonist, on negative symptoms of schizophrenia: a double-blind randomized placebo-controlled study. Prog Neuropsychopharmacol Biol Psychiatry 32 (8):1879-1883

159. Berk M, Ichim C, Brook S (2001) Efficacy of mirtazapine add on therapy to haloperidol in the treatment of the negative symptoms of schizophrenia: a double-blind randomized placebo-controlled study. Int Clin Psychopharmacol 16 (2):87-92

160. Joffe G, Terevnikov V, Joffe M, Stenberg JH, Burkin M, Tiihonen J (2009) Add-on mirtazapine enhances antipsychotic effect of first generation antipsychotics in schizophrenia: a double-blind, randomized, placebo-controlled trial. Schizophr Res 108 (1-3):245-251

161. Abbasi SH, Behpournia H, Ghoreshi A, Salehi B, Raznahan M, Rezazadeh SA, Rezaei F, Akhondzadeh S (2010) The effect of mirtazapine add on therapy to

risperidone in the treatment of schizophrenia: a double-blind randomized placebo-controlled trial. Schizophr Res 116 (2-3):101-106

162. Zoccali R, Muscatello MR, Cedro C, Neri P, La Torre D, Spina E, Di Rosa AE, Meduri M (2004) The effect of mirtazapine augmentation of clozapine in the treatment of negative symptoms of schizophrenia: a double-blind, placebo-controlled study. Int Clin Psychopharmacol 19 (2):71-76

163. Hiemke C, Peled A, Jabarin M, Hadjez J, Weigmann H, Hartter S, Modai I, Ritsner M, Silver H (2002) Fluvoxamine augmentation of olanzapine in chronic schizophrenia: pharmacokinetic interactions and clinical effects. J Clin Psychopharmacol 22 (5):502-506

164. Legare N, Gregoire CA, De Benedictis L, Dumais A (2013) Increasing the clozapine: Norclozapine ratio with co-administration of fluvoxamine to enhance efficacy and minimize side effects of clozapine therapy. Med Hypotheses

165. Williams JW, Jr., Mulrow CD, Chiquette E, Noel PH, Aguilar C, Cornell J (2000) A systematic review of newer pharmacotherapies for depression in adults: evidence report summary. Ann Intern Med 132 (9):743-756

166. Nelson JC, Papakostas GI (2009) Atypical antipsychotic augmentation in major depressive disorder: a meta-analysis of placebo-controlled randomized trials. Am J Psychiatry 166 (9):980-991

167. Valenstein M, McCarthy JF, Austin KL, Greden JF, Young EA, Blow FC (2006) What happened to lithium? Antidepressant augmentation in clinical settings. Am J Psychiatry 163 (7):1219-1225

168. Spielmans GI, Berman MI, Linardatos E, Rosenlicht NZ, Perry A, Tsai AC (2013) Adjunctive atypical antipsychotic treatment for major depressive disorder: a meta-analysis of depression, quality of life, and safety outcomes. PLoS Med 10 (3):e1001403

169. Nadkarni A, Kalsekar I, You M, Forbes R, Hebden T (2013) Medical costs and utilization in patients with depression treated with adjunctive atypical antipsychotic therapy. Clinicoecon Outcomes Res 5:49-57

170. Shelton RC, Tollefson GD, Tohen M, Stahl S, Gannon KS, Jacobs TG, Buras WR, Bymaster FP, Zhang W, Spencer KA, Feldman PD, Meltzer HY (2001) A novel augmentation strategy for treating resistant major depression. Am J Psychiatry 158 (1):131-134

171. Shelton RC, Williamson DJ, Corya SA, Sanger TM, Van Campen LE, Case M, Briggs SD, Tollefson GD (2005) Olanzapine/fluoxetine combination for treatment-resistant depression: a controlled study of SSRI and nortriptyline resistance. J Clin Psychiatry 66 (10):1289-1297

172. Thase ME, Corya SA, Osuntokun O, Case M, Henley DB, Sanger TM, Watson SB, Dube S (2007) A randomized, double-blind comparison of olanzapine/fluoxetine combination, olanzapine, and fluoxetine in treatment-resistant major depressive disorder. J Clin Psychiatry 68 (2):224-236

173. Chen J, Gao K, Kemp DE (2011) Second-generation antipsychotics in major depressive disorder: update and clinical perspective. Curr Opin Psychiatry 24 (1):10-17

174. Corya SA, Andersen SW, Detke HC, Kelly LS, Van Campen LE, Sanger TM, Williamson DJ, Dube S (2003) Long-term antidepressant efficacy and safety of olanzapine/fluoxetine combination: a 76-week open-label study. J Clin Psychiatry 64 (11):1349-1356

175. Nelson JC, Thase ME, Bellocchio EE, Rollin LM, Eudicone JM, McQuade RD, Marcus RN, Berman RM, Baker RA (2012) Efficacy of adjunctive aripiprazole in patients with major depressive disorder who showed minimal response to initial antidepressant therapy. Int Clin Psychopharmacol 27 (3):125-133

176. Matthews JD, Siefert C, Dording C, Denninger JW, Park L, van Nieuwenhuizen AO, Sklarsky K, Hilliker S, Homberger C, Rooney K, Fava M (2009) An open study of aripiprazole and escitalopram for psychotic major depressive disorder. J Clin Psychopharmacol 29 (1):73-76

177. Lin CH, Lin SH, Jang FL (2011) Adjunctive low-dose aripiprazole with standard-dose sertraline in treating fresh major depressive disorder: a randomized, double-blind, controlled study. J Clin Psychopharmacol 31 (5):563-568

178. Grunze H, Vieta E, Goodwin GM, Bowden C, Licht RW, Moller HJ, Kasper S (2013) The World Federation of Societies of Biological Psychiatry (WFSBP) Guidelines for the Biological Treatment of Bipolar Disorders: Update 2012 on the long-term treatment of bipolar disorder. World J Biol Psychiatry 14 (3):154-219

179. Tohen M, Chengappa KN, Suppes T, Zarate CA, Jr., Calabrese JR, Bowden CL, Sachs GS, Kupfer DJ, Baker RW, Risser RC, Keeter EL, Feldman PD, Tollefson GD, Breier A (2002) Efficacy of olanzapine in combination with valproate or lithium in the treatment of mania in patients partially nonresponsive to valproate or lithium monotherapy. Arch Gen Psychiatry 59 (1):62-69

180. Delbello MP, Schwiers ML, Rosenberg HL, Strakowski SM (2002) A double-blind, randomized, placebo-controlled study of quetiapine as adjunctive treatment for adolescent mania. J Am Acad Child Adolesc Psychiatry 41 (10):1216-1223

181. Sachs G, Chengappa KN, Suppes T, Mullen JA, Brecher M, Devine NA, Sweitzer DE (2004) Quetiapine with lithium or divalproex for the treatment of bipolar mania: a randomized, double-blind, placebo-controlled study. Bipolar Disord 6 (3):213-223

182. Sachs GS, Grossman F, Ghaemi SN, Okamoto A, Bowden CL (2002) Combination of a mood stabilizer with risperidone or haloperidol for treatment of acute mania: a

double-blind, placebo-controlled comparison of efficacy and safety. Am J Psychiatry 159 (7):1146-1154

183. Fagiolini A, Nitti M, Forgione RN, Marra FS, Casamassima F (2011) Aripiprazole for the treatment of bipolar disorder: a review of current evidence. Expert Opin Pharmacother 12 (3):473-488

184. Fountoulakis KN, Vieta E, Siamouli M, Valenti M, Magiria S, Oral T, Fresno D, Giannakopoulos P, Kaprinis GS (2007) Treatment of bipolar disorder: a complex treatment for a multi-faceted disorder. Ann Gen Psychiatry 6:27

185. Gao K, Gajwani P, Elhaj O, Calabrese JR (2005) Typical and atypical antipsychotics in bipolar depression. J Clin Psychiatry 66 (11):1376-1385

186. Mazza M, Squillacioti MR, Pecora RD, Janiri L, Bria P (2008) Beneficial acute antidepressant effects of aripiprazole as an adjunctive treatment or monotherapy in bipolar patients unresponsive to mood stabilizers: results from a 16-week open-label trial. Expert Opin Pharmacother 9 (18):3145-3149

187. Bowden CL, Vieta E, Ice KS, Schwartz JH, Wang PP, Versavel M (2010) Ziprasidone plus a mood stabilizer in subjects with bipolar I disorder: a 6-month, randomized, placebo-controlled, double-blind trial. J Clin Psychiatry 71 (2):130-137

188. Suppes T, Vieta E, Liu S, Brecher M, Paulsson B (2009) Maintenance treatment for patients with bipolar I disorder: results from a north american study of quetiapine in combination with lithium or divalproex (trial 127). Am J Psychiatry 166 (4):476-488

189. Jones RM, Thompson C, Bitter I (2006) A systematic review of the efficacy and safety of second generation antipsychotics in the treatment of mania. Eur Psychiatry 21 (1):1-9

190. Leucht S, Kissling W, McGrath J (2007) Lithium for schizophrenia. Cochrane Database Syst Rev (3):CD003834

191. Wassef AA, Dott SG, Harris A, Brown A, O'Boyle M, Meyer WJ, 3rd, Rose RM (2000) Randomized, placebo-controlled pilot study of divalproex sodium in the treatment of acute exacerbations of chronic schizophrenia. J Clin Psychopharmacol 20 (3):357-361

192. Casey DE, Daniel DG, Wassef AA, Tracy KA, Wozniak P, Sommerville KW (2003) Effect of divalproex combined with olanzapine or risperidone in patients with an acute exacerbation of schizophrenia. Neuropsychopharmacology 28 (1):182-192

193. Casey DE, Daniel DG, Tamminga C, Kane JM, Tran-Johnson T, Wozniak P, Abi-Saab W, Baker J, Redden L, Greco N, Saltarelli M (2009) Divalproex ER combined with olanzapine or risperidone for treatment of acute exacerbations of schizophrenia. Neuropsychopharmacology 34 (5):1330-1338

194. Schwarz C, Volz A, Li C, Leucht S (2008) Valproate for schizophrenia. Cochrane Database Syst Rev (3):CD004028

195. Rajkumar RP (2012) Functional hallucinations in schizophrenia responding to adjunctive sodium valproate. Indian J Psychol Med 34 (1):76-78

196. Almeida J, Serrao EM, Almeida AT, Afonso JG (2011) Effective treatment with clozapine and valproate for refractory schizophrenia-like psychosis after cerebellar hemorrhage. Clin Neuropharmacol 34 (3):131-132

197. Gobbi G, Gaudreau PO, Leblanc N (2006) Efficacy of topiramate, valproate, and their combination on aggression/agitation behavior in patients with psychosis. J Clin Psychopharmacol 26 (5):467-473

198. Hodgson RE, Mendis S (2010) Lithium enabling use of clozapine in a patient with pre-existing neutropenia. Br J Hosp Med (Lond) 71 (9):535

199. Nykiel S, Henderson D, Bhide G, Freudenreich O (2010) Lithium to allow clozapine prescribing in benign ethnic neutropenia. Clin Schizophr Relat Psychoses 4 (2):138-140

200. Maher KN, Tan M, Tossell JW, Weisinger B, Gochman P, Miller R, Greenstein D, Overman GP, Rapoport JL, Gogtay N (2013) Risk factors for neutropenia in clozapine-treated children and adolescents with childhood-onset schizophrenia. J Child Adolesc Psychopharmacol 23 (2):110-116

201. Volz A, Khorsand V, Gillies D, Leucht S (2007) Benzodiazepines for schizophrenia. Cochrane Database Syst Rev (1):CD006391

202. Alexander J, Tharyan P, Adams C, John T, Mol C, Philip J (2004) Rapid tranquillisation of violent or agitated patients in a psychiatric emergency setting. Pragmatic randomised trial of intramuscular lorazepam v. haloperidol plus promethazine. Br J Psychiatry 185:63-69

203. Haw C, Stubbs J (2007) Benzodiazepines--a necessary evil? A survey of prescribing at a specialist UK psychiatric hospital. J Psychopharmacol 21 (6):645-649

204. Fazel S, Gulati G, Linsell L, Geddes JR, Grann M (2009) Schizophrenia and violence: systematic review and meta-analysis. PLoS Med 6 (8):e1000120

205. Bo S, Abu-Akel A, Kongerslev M, Haahr UH, Simonsen E (2011) Risk factors for violence among patients with schizophrenia. Clin Psychol Rev 31 (5):711-726

206. Bo S, Forth A, Kongerslev M, Haahr UH, Pedersen L, Simonsen E (2013) Subtypes of aggression in patients with schizophrenia: the role of personality disorders. Crim Behav Ment Health 23 (2):124-137

207. Dold M, Li C, Tardy M, Khorsand V, Gillies D, Leucht S (2012) Benzodiazepines for schizophrenia. Cochrane Database Syst Rev 11:CD006391

208. Hasan A, Falkai P, Wobrock T, Lieberman J, Glenthoj B, Gattaz WF, Thibaut F, Moller HJ (2013) World Federation of Societies of Biological Psychiatry (WFSBP) guidelines for biological treatment of schizophrenia, part 2: update 2012 on the long-term treatment of schizophrenia and management of antipsychotic-induced side effects. World J Biol Psychiatry 14 (1):2-44

209. Barbui C, Accordini S, Nose M, Stroup S, Purgato M, Girlanda F, Esposito E, Veronese A, Tansella M, Cipriani A (2011) Aripiprazole versus haloperidol in combination with clozapine for treatment-resistant schizophrenia in routine clinical care: a randomized, controlled trial. J Clin Psychopharmacol 31 (3):266-273

210. Gilmer TP, Dolder CR, Folsom DP, Mastin W, Jeste DV (2007) Antipsychotic polypharmacy trends among Medicaid beneficiaries with schizophrenia in San Diego County, 1999-2004. Psychiatr Serv 58 (7):1007-1010

211. Hoffer ZS, Roth RL, Mathews M (2009) Evidence for the partial dopamine-receptor agonist aripiprazole as a first-line treatment of psychosis in patients with iatrogenic or tumorogenic hyperprolactinemia. Psychosomatics 50 (4):317-324

212. Kane JM, Correll CU, Goff DC, Kirkpatrick B, Marder SR, Vester-Blokland E, Sun W, Carson WH, Pikalov A, Assuncao-Talbott S (2009) A multicenter, randomized, double-blind, placebo-controlled, 16-week study of adjunctive aripiprazole for schizophrenia or schizoaffective disorder inadequately treated with quetiapine or risperidone monotherapy. J Clin Psychiatry 70 (10):1348-1357

213. Shim JC, Shin JG, Kelly DL, Jung DU, Seo YS, Liu KH, Shon JH, Conley RR (2007) Adjunctive treatment with a dopamine partial agonist, aripiprazole, for antipsychotic-induced hyperprolactinemia: a placebo-controlled trial. Am J Psychiatry 164 (9):1404-1410

214. Langan J, Martin D, Shajahan P, Smith DJ (2012) Antipsychotic dose escalation as a trigger for Neuroleptic Malignant Syndrome (NMS): literature review and case series report. BMC Psychiatry 12:214

215. Taylor DM, Smith L, Gee SH, Nielsen J (2012) Augmentation of clozapine with a second antipsychotic - a meta-analysis. Acta Psychiatr Scand 125 (1):15-24

216. Freudenreich O, Goff DC (2002) Antipsychotic combination therapy in schizophrenia. A review of efficacy and risks of current combinations. Acta Psychiatr Scand 106 (5):323-330

217. Kontaxakis VP, Ferentinos PP, Havaki-Kontaxaki BJ, Roukas DK (2005) Randomized controlled augmentation trials in clozapine-resistant schizophrenic patients: a critical review. Eur Psychiatry 20 (5-6):409-415

218. Wang J, Omori IM, Fenton M, Soares B (2010) Sulpiride augmentation for schizophrenia. Cochrane Database Syst Rev (1):CD008125

219. Englisch S, Zink M (2012) Treatment-resistant Schizophrenia: Evidence-based Strategies. Mens Sana Monogr 10 (1):20-32

220. Fleischhacker WW, Heikkinen ME, Olie JP, Landsberg W, Dewaele P, McQuade RD, Loze JY, Hennicken D, Kerselaers W (2010) Effects of adjunctive treatment with aripiprazole on body weight and clinical efficacy in schizophrenia patients treated with clozapine: a randomized, double-blind, placebo-controlled trial. Int J Neuropsychopharmacol 13 (8):1115-1125

221. Henderson DC, Kunkel L, Nguyen DD, Borba CP, Daley TB, Louie PM, Freudenreich O, Cather C, Evins AE, Goff DC (2006) An exploratory open-label trial of aripiprazole as an adjuvant to clozapine therapy in chronic schizophrenia. Acta Psychiatr Scand 113 (2):142-147

222. Mossaheb N, Kaufmann RM (2012) Role of aripiprazole in treatment-resistant schizophrenia. Neuropsychiatr Dis Treat 8:235-244

223. Lerner V, Chudakova B, Kravets S, Polyakova I (2000) Combined use of risperidone and olanzapine in the treatment of patients with resistant schizophrenia: a preliminary case series report. Clin Neuropharmacol 23 (5):284-286

224. Raskin S, Durst R, Katz G, Zislin J (2000) Olanzapine and sulpiride: a preliminary study of combination/augmentation in patients with treatment-resistant schizophrenia. J Clin Psychopharmacol 20 (5):500-503

225. Chue P, Welch R, Snaterse M (2001) Combination risperidone and quetiapine therapy in refractory schizophrenia. Can J Psychiatry 46 (1):86-87

226. Englisch S, Enning F, Grosshans M, Marquardt L, Waltereit R, Zink M (2010) Quetiapine combined with amisulpride in schizophrenic patients with insufficient responses to quetiapine monotherapy. Clin Neuropharmacol 33 (5):227-229

227. Suzuki T, Uchida H, Watanabe K, Nakajima S, Nomura K, Takeuchi H, Tanabe A, Yagi G, Kashima H (2008) Effectiveness of antipsychotic polypharmacy for patients with treatment refractory schizophrenia: an open-label trial of olanzapine plus risperidone for those who failed to respond to a sequential treatment with olanzapine, quetiapine and risperidone. Hum Psychopharmacol 23 (6):455-463

228. Schonfelder S, Schirmbeck F, Waltereit R, Englisch S, Zink M (2011) Aripiprazole improves olanzapine-associated obsessive compulsive symptoms in schizophrenia. Clin Neuropharmacol 34 (6):256-257

229. Villari V, Frieri T, Fagiolini A (2011) Aripiprazole augmentation in clozapine-associated obsessive-compulsive symptoms. J Clin Psychopharmacol 31 (3):375-376

230. Roth BL, Hanizavareh SM, Blum AE (2004) Serotonin receptors represent highly favorable molecular targets for cognitive enhancement in schizophrenia and other disorders. Psychopharmacology (Berl) 174 (1):17-24

231. Roth BL, Sheffler DJ, Kroeze WK (2004) Magic shotguns versus magic bullets: selectively non-selective drugs for mood disorders and schizophrenia. Nat Rev Drug Discov 3 (4):353-359

232. Meltzer HY, Li Z, Kaneda Y, Ichikawa J (2003) Serotonin receptors: their key role in drugs to treat schizophrenia. Prog Neuropsychopharmacol Biol Psychiatry 27 (7):1159-1172

233. Moller HJ (2003) Management of the negative symptoms of schizophrenia: new treatment options. CNS Drugs 17 (11):793-823

234. Davis JM, Chen N, Glick ID (2003) A meta-analysis of the efficacy of second-generation antipsychotics. Arch Gen Psychiatry 60 (6):553-564

235. Newcomer JW (2004) Metabolic risk during antipsychotic treatment. Clin Ther 26 (12):1936-1946

236. Shahid M, Walker GB, Zorn SH, Wong EH (2009) Asenapine: a novel psychopharmacologic agent with a unique human receptor signature. J Psychopharmacol 23 (1):65-73

237. Franberg O, Wiker C, Marcus MM, Konradsson A, Jardemark K, Schilstrom B, Shahid M, Wong EH, Svensson TH (2008) Asenapine, a novel psychopharmacologic agent: preclinical evidence for clinical effects in schizophrenia. Psychopharmacology (Berl) 196 (3):417-429

238. Tarazi FI, Choi YK, Gardner M, Wong EH, Henry B, Shahid M (2009) Asenapine exerts distinctive regional effects on ionotropic glutamate receptor subtypes in rat brain. Synapse 63 (5):413-420

239. Tarazi FI, Moran-Gates T, Wong EH, Henry B, Shahid M (2008) Differential regional and dose-related effects of asenapine on dopamine receptor subtypes. Psychopharmacology (Berl) 198 (1):103-111

240. Tarazi FI, Moran-Gates T, Wong EH, Henry B, Shahid M (2010) Asenapine induces differential regional effects on serotonin receptor subtypes. J Psychopharmacol 24 (3):341-348

241. Tarazi FI, Shahid M (2009) Asenapine maleate: a new drug for the treatment of schizophrenia and bipolar mania. Drugs Today (Barc) 45 (12):865-876

242. Cortese L, Bressan RA, Castle DJ, Mosolov SN (2013) Management of schizophrenia: clinical experience with asenapine. J Psychopharmacol 27 (4 Suppl):14-22

243. Young AH, Altamura AC, Gonzalez-Pinto AM, Millet B, Wiedemann K (2013) Use of asenapine in clinical practice for the management of bipolar mania. J Psychopharmacol 27 (4 Suppl):3-13

244. Leucht S, Cipriani A, Spineli L, Mavridis D, Orey D, Richter F, Samara M, Barbui C, Engel RR, Geddes JR, Kissling W, Stapf MP, Lassig B, Salanti G, Davis JM (2013) Comparative efficacy and tolerability of 15 antipsychotic drugs in schizophrenia: a multiple-treatments meta-analysis. Lancet 382 (9896):951-962

245. Awad AG, Voruganti LN (2013) The impact of newer atypical antipsychotics on patient-reported outcomes in schizophrenia. CNS Drugs 27 (8):625-636

246. Chertkow Y, Weinreb O, Youdim MB, Silver H (2009) Molecular mechanisms underlying synergistic effects of SSRI-antipsychotic augmentation in treatment of negative symptoms in schizophrenia. J Neural Transm 116 (11):1529-1541

247. Dell'aversano C, Tomasetti C, Iasevoli F, de Bartolomeis A (2009) Antipsychotic and antidepressant co-treatment: effects on transcripts of inducible postsynaptic density genes possibly implicated in behavioural disorders. Brain Res Bull 79 (2):123-129

248. Franberg O, Marcus MM, Ivanov V, Schilstrom B, Shahid M, Svensson TH (2009) Asenapine elevates cortical dopamine, noradrenaline and serotonin release. Evidence for activation of cortical and subcortical dopamine systems by different mechanisms. Psychopharmacology (Berl) 204 (2):251-264

249. Beaulieu JM, Gainetdinov RR, Caron MG (2009) Akt/GSK3 signaling in the action of psychotropic drugs. Annu Rev Pharmacol Toxicol 49:327-347

250. Weisler R, Joyce M, McGill L, Lazarus A, Szamosi J, Eriksson H (2009) Extended release quetiapine fumarate monotherapy for major depressive disorder: results of a double-blind, randomized, placebo-controlled study. CNS Spectr 14 (6):299-313

251. Gijsman HJ, Geddes JR, Rendell JM, Nolen WA, Goodwin GM (2004) Antidepressants for bipolar depression: a systematic review of randomized, controlled trials. Am J Psychiatry 161 (9):1537-1547

252. Yatham LN, Goldstein JM, Vieta E, Bowden CL, Grunze H, Post RM, Suppes T, Calabrese JR (2005) Atypical antipsychotics in bipolar depression: potential mechanisms of action. J Clin Psychiatry 66 Suppl 5:40-48

253. Shiraishi-Yamaguchi Y, Furuichi T (2007) The Homer family proteins. Genome Biol 8 (2):206

254. Ango F, Prezeau L, Muller T, Tu JC, Xiao B, Worley PF, Pin JP, Bockaert J, Fagni L (2001) Agonist-independent activation of metabotropic glutamate receptors by the intracellular protein Homer. Nature 411 (6840):962-965

255. Kammermeier PJ (2008) Endogenous homer proteins regulate metabotropic glutamate receptor signaling in neurons. J Neurosci 28 (34):8560-8567

256. Tappe A, Kuner R (2006) Regulation of motor performance and striatal function by synaptic scaffolding proteins of the Homer1 family. Proc Natl Acad Sci U S A 103 (3):774-779

257. Jope RS, Johnson GV (2004) The glamour and gloom of glycogen synthase kinase-3. Trends Biochem Sci 29 (2):95-102

258. Grimes CA, Jope RS (2001) CREB DNA binding activity is inhibited by glycogen synthase kinase-3 beta and facilitated by lithium. J Neurochem 78 (6):1219-1232

259. Gould TD, Manji HK (2005) Glycogen synthase kinase-3: a putative molecular target for lithium mimetic drugs. Neuropsychopharmacology 30 (7):1223-1237

260. Benedetti F, Serretti A, Pontiggia A, Bernasconi A, Lorenzi C, Colombo C, Smeraldi E (2005) Long-term response to lithium salts in bipolar illness is influenced by the glycogen synthase kinase 3-beta -50 T/C SNP. Neurosci Lett 376 (1):51-55

261. Benedetti F, Serretti A, Colombo C, Lorenzi C, Tubazio V, Smeraldi E (2004) A glycogen synthase kinase 3-beta promoter gene single nucleotide polymorphism is associated with age at onset and response to total sleep deprivation in bipolar depression. Neurosci Lett 368 (2):123-126

262. Kato T (2008) Molecular neurobiology of bipolar disorder: a disease of 'mood-stabilizing neurons'? Trends Neurosci 31 (10):495-503

263. Emamian ES, Hall D, Birnbaum MJ, Karayiorgou M, Gogos JA (2004) Convergent evidence for impaired AKT1-GSK3beta signaling in schizophrenia. Nat Genet 36 (2):131-137

264. Kang UG, Seo MS, Roh MS, Kim Y, Yoon SC, Kim YS (2004) The effects of clozapine on the GSK-3-mediated signaling pathway. FEBS Lett 560 (1-3):115-119

265. Alimohamad H, Rajakumar N, Seah YH, Rushlow W (2005) Antipsychotics alter the protein expression levels of beta-catenin and GSK-3 in the rat medial prefrontal cortex and striatum. Biol Psychiatry 57 (5):533-542

266. Roh MS, Eom TY, Zmijewska AA, De Sarno P, Roth KA, Jope RS (2005) Hypoxia activates glycogen synthase kinase-3 in mouse brain in vivo: protection by mood stabilizers and imipramine. Biol Psychiatry 57 (3):278-286

267. Li X, Zhu W, Roh MS, Friedman AB, Rosborough K, Jope RS (2004) In vivo regulation of glycogen synthase kinase-3beta (GSK3beta) by serotonergic activity in mouse brain. Neuropsychopharmacology 29 (8):1426-1431

268. Pouyssegur J, Volmat V, Lenormand P (2002) Fidelity and spatio-temporal control in MAP kinase (ERKs) signalling. Biochem Pharmacol 64 (5-6):755-763

269. Wang JQ, Tang Q, Parelkar NK, Liu Z, Samdani S, Choe ES, Yang L, Mao L (2004) Glutamate signaling to Ras-MAPK in striatal neurons: mechanisms for inducible gene expression and plasticity. Mol Neurobiol 29 (1):1-14

270. Sweatt JD (2001) The neuronal MAP kinase cascade: a biochemical signal integration system subserving synaptic plasticity and memory. J Neurochem 76 (1):1-10

271. Einat H, Yuan P, Gould TD, Li J, Du J, Zhang L, Manji HK, Chen G (2003) The role of the extracellular signal-regulated kinase signaling pathway in mood modulation. J Neurosci 23 (19):7311-7316

272. Hao Y, Creson T, Zhang L, Li P, Du F, Yuan P, Gould TD, Manji HK, Chen G (2004) Mood stabilizer valproate promotes ERK pathway-dependent cortical neuronal growth and neurogenesis. J Neurosci 24 (29):6590-6599

273. Fumagalli F, Molteni R, Calabrese F, Frasca A, Racagni G, Riva MA (2005) Chronic fluoxetine administration inhibits extracellular signal-regulated kinase 1/2 phosphorylation in rat brain. J Neurochem 93 (6):1551-1560

274. Browning JL, Patel T, Brandt PC, Young KA, Holcomb LA, Hicks PB (2005) Clozapine and the mitogen-activated protein kinase signal transduction pathway: implications for antipsychotic actions. Biol Psychiatry 57 (6):617-623

275. Yuan P, Zhou R, Wang Y, Li X, Li J, Chen G, Guitart X, Manji HK Altered levels of extracellular signal-regulated kinase signaling proteins in postmortem frontal cortex of individuals with mood disorders and schizophrenia. J Affect Disord 124 (1-2):164-169

276. Lewis DA, Lieberman JA (2000) Catching up on schizophrenia: natural history and neurobiology. Neuron 28 (2):325-334

277. Green MJ, Cahill CM, Malhi GS (2007) The cognitive and neurophysiological basis of emotion dysregulation in bipolar disorder. J Affect Disord 103 (1-3):29-42

278. Weis S, Llenos IC, Dulay JR, Verma N, Sabunciyan S, Yolken RH (2007) Changes in region- and cell type-specific expression patterns of neutral amino acid transporter 1 (ASCT-1) in the anterior cingulate cortex and hippocampus in schizophrenia, bipolar disorder and major depression. J Neural Transm 114 (2):261-271

279. Robertson GS, Matsumura H, Fibiger HC (1994) Induction patterns of Fos-like immunoreactivity in the forebrain as predictors of atypical antipsychotic activity. J Pharmacol Exp Ther 271 (2):1058-1066

280. Deutch AY, Duman RS (1996) The effects of antipsychotic drugs on Fos protein expression in the prefrontal cortex: cellular localization and pharmacological characterization. Neuroscience 70 (2):377-389

281. Chen B, Wang JF, Hill BC, Young LT (1999) Lithium and valproate differentially regulate brain regional expression of phosphorylated CREB and c-Fos. Brain Res Mol Brain Res 70 (1):45-53

282. Plant N, Barber P, Horner E, Cockburn CL, Gibson G, Bugelski P, Lord P (2002) Differential gene expression in rats following subacute exposure to the anticonvulsant sodium valproate. Toxicol Appl Pharmacol 183 (2):127-134

283. Kapur S, Wadenberg ML, Remington G (2000) Are animal studies of antipsychotics appropriately dosed? Lessons from the bedside to the bench. Can J Psychiatry 45 (3):241-246

284. Gallo A, Lapointe S, Stip E, Potvin S, Rompre PP Quetiapine blocks cocaine-induced enhancement of brain stimulation reward. Behav Brain Res 208 (1):163-168

285. Natesan S, Reckless GE, Barlow KB, Nobrega JN, Kapur S (2008) Amisulpride the 'atypical' atypical antipsychotic--comparison to haloperidol, risperidone and clozapine. Schizophr Res 105 (1-3):224-235

286. Pira L, Mongeau R, Pani L (2004) The atypical antipsychotic quetiapine increases both noradrenaline and dopamine release in the rat prefrontal cortex. Eur J Pharmacol 504 (1-2):61-64

287. Wadenberg ML, Soliman A, VanderSpek SC, Kapur S (2001) Dopamine D(2) receptor occupancy is a common mechanism underlying animal models of antipsychotics and their clinical effects. Neuropsychopharmacology 25 (5):633-641

288. Cochran SM, McKerchar CE, Morris BJ, Pratt JA (2002) Induction of differential patterns of local cerebral glucose metabolism and immediate-early genes by acute clozapine and haloperidol. Neuropharmacology 43 (3):394-407

289. Robertson GS, Fibiger HC (1992) Neuroleptics increase c-fos expression in the forebrain: contrasting effects of haloperidol and clozapine. Neuroscience 46 (2):315-328

290. Merchant KM, Dorsa DM (1993) Differential induction of neurotensin and c-fos gene expression by typical versus atypical antipsychotics. Proc Natl Acad Sci U S A 90 (8):3447-3451

291. Kapur S, VanderSpek SC, Brownlee BA, Nobrega JN (2003) Antipsychotic dosing in preclinical models is often unrepresentative of the clinical condition: a suggested solution based on in vivo occupancy. J Pharmacol Exp Ther 305 (2):625-631

292. Ichikawa J, Meltzer HY (1999) Relationship between dopaminergic and serotonergic neuronal activity in the frontal cortex and the action of typical and atypical antipsychotic drugs. Eur Arch Psychiatry Clin Neurosci 249 Suppl 4:90-98

293. Huang M, Ichiwaka J, Li Z, Dai J, Meltzer HY (2006) Augmentation by citalopram of risperidone-induced monoamine release in rat prefrontal cortex. Psychopharmacology (Berl) 185 (3):274-281

294. Invernizzi R, Velasco C, Bramante M, Longo A, Samanin R (1997) Effect of 5-HT1A receptor antagonists on citalopram-induced increase in extracellular serotonin in the frontal cortex, striatum and dorsal hippocampus. Neuropharmacology 36 (4-5):467-473

295. Paxinos G, Watson C (1997) The rat brain, in stereotaxic coordinates. Compact 3rd edn. Academic Press, San Diego

296. Ambesi-Impiombato A, D'Urso G, Muscettola G, de Bartolomeis A (2003) Method for quantitative in situ hybridization histochemistry and image analysis applied for Homer1a gene expression in rat brain. Brain Res Brain Res Protoc 11 (3):189-196

297. Willuhn I, Sun W, Steiner H (2003) Topography of cocaine-induced gene regulation in the rat striatum: relationship to cortical inputs and role of behavioural context. Eur J Neurosci 17 (5):1053-1066

298. Steiner H, Gerfen CR (1993) Cocaine-induced c-fos messenger RNA is inversely related to dynorphin expression in striatum. J Neurosci 13 (12):5066-5081

299. Hesslinger B, Normann C, Langosch JM, Klose P, Berger M, Walden J (1999) Effects of carbamazepine and valproate on haloperidol plasma levels and on psychopathologic outcome in schizophrenic patients. J Clin Psychopharmacol 19 (4):310-315

300. Dong E, Nelson M, Grayson DR, Costa E, Guidotti A (2008) Clozapine and sulpiride but not haloperidol or olanzapine activate brain DNA demethylation. Proc Natl Acad Sci U S A 105 (36):13614-13619

301. Guidotti A, Auta J, Chen Y, Davis JM, Dong E, Gavin DP, Grayson DR, Matrisciano F, Pinna G, Satta R, Sharma RP, Tremolizzo L, Tueting P (2011) Epigenetic GABAergic targets in schizophrenia and bipolar disorder. Neuropharmacology 60 (7-8):1007-1016

302. Pozzi L, Hakansson K, Usiello A, Borgkvist A, Lindskog M, Greengard P, Fisone G (2003) Opposite regulation by typical and atypical anti-psychotics of ERK1/2, CREB and Elk-1 phosphorylation in mouse dorsal striatum. J Neurochem 86 (2):451-459

303. Moghaddam B, Bunney BS (1990) Acute effects of typical and atypical antipsychotic drugs on the release of dopamine from prefrontal cortex, nucleus

accumbens, and striatum of the rat: an in vivo microdialysis study. J Neurochem 54 (5):1755-1760

304. Dragunow M, Williams M, Faull RL (1990) Haloperidol induces Fos and related molecules in intrastriatal grafts derived from fetal striatal primordia. Brain Res 530 (2):309-311

305. Yanahashi S, Hashimoto K, Hattori K, Yuasa S, Iyo M (2004) Role of NMDA receptor subtypes in the induction of catalepsy and increase in Fos protein expression after administration of haloperidol. Brain Res 1011 (1):84-93

306. Flores-Hernandez J, Cepeda C, Hernandez-Echeagaray E, Calvert CR, Jokel ES, Fienberg AA, Greengard P, Levine MS (2002) Dopamine enhancement of NMDA currents in dissociated medium-sized striatal neurons: role of D1 receptors and DARPP-32. J Neurophysiol 88 (6):3010-3020

307. Sarantis K, Matsokis N, Angelatou F (2009) Synergistic interactions of dopamine D1 and glutamate NMDA receptors in rat hippocampus and prefrontal cortex: involvement of ERK1/2 signaling. Neuroscience 163 (4):1135-1145

308. Kato A, Fukazawa Y, Ozawa F, Inokuchi K, Sugiyama H (2003) Activation of ERK cascade promotes accumulation of Vesl-1S/Homer-1a immunoreactivity at synapses. Brain Res Mol Brain Res 118 (1-2):33-44

309. Li YC, Xi D, Roman J, Huang YQ, Gao WJ (2009) Activation of glycogen synthase kinase-3 beta is required for hyperdopamine and D2 receptor-mediated inhibition of synaptic NMDA receptor function in the rat prefrontal cortex. J Neurosci 29 (49):15551-15563

310. Gould TD, Manji HK (2005) DARPP-32: A molecular switch at the nexus of reward pathway plasticity. Proc Natl Acad Sci U S A 102 (2):253-254

311. Aubry JM, Schwald M, Ballmann E, Karege F (2009) Early effects of mood stabilizers on the Akt/GSK-3beta signaling pathway and on cell survival and proliferation. Psychopharmacology (Berl) 205 (3):419-429

312. Chen G, Henter ID, Manji HK Translational research in bipolar disorder: emerging insights from genetically based models. Mol Psychiatry

313. Izumi T, Inoue T, Kitaichi Y, Nakagawa S, Koyama T (2006) Target brain sites of the anxiolytic effect of citalopram, a selective serotonin reuptake inhibitor. Eur J Pharmacol 534 (1-3):129-132

314. Richelson E, Souder T (2000) Binding of antipsychotic drugs to human brain receptors focus on newer generation compounds. Life Sci 68 (1):29-39

315. Yamamura S, Ohoyama K, Hamaguchi T, Kashimoto K, Nakagawa M, Kanehara S, Suzuki D, Matsumoto T, Motomura E, Shiroyama T, Okada M (2009) Effects of

quetiapine on monoamine, GABA, and glutamate release in rat prefrontal cortex. Psychopharmacology (Berl) 206 (2):243-258

316. Denys D, Klompmakers AA, Westenberg HG (2004) Synergistic dopamine increase in the rat prefrontal cortex with the combination of quetiapine and fluvoxamine. Psychopharmacology (Berl) 176 (2):195-203

317. Amargos-Bosch M, Adell A, Artigas F (2007) Antipsychotic drugs reverse the AMPA receptor-stimulated release of 5-HT in the medial prefrontal cortex. J Neurochem 102 (2):550-561

318. Zhang W, Perry KW, Wong DT, Potts BD, Bao J, Tollefson GD, Bymaster FP (2000) Synergistic effects of olanzapine and other antipsychotic agents in combination with fluoxetine on norepinephrine and dopamine release in rat prefrontal cortex. Neuropsychopharmacology 23 (3):250-262

319. Liegeois JF, Ichikawa J, Meltzer HY (2002) 5-HT(2A) receptor antagonism potentiates haloperidol-induced dopamine release in rat medial prefrontal cortex and inhibits that in the nucleus accumbens in a dose-dependent manner. Brain Res 947 (2):157-165

320. Orsetti M, Di Brisco F, Canonico PL, Genazzani AA, Ghi P (2008) Gene regulation in the frontal cortex of rats exposed to the chronic mild stress paradigm, an animal model of human depression. Eur J Neurosci 27 (8):2156-2164

321. Orsetti M, Di Brisco F, Rinaldi M, Dallorto D, Ghi P (2009) Some molecular effectors of antidepressant action of quetiapine revealed by DNA microarray in the frontal cortex of anhedonic rats. Pharmacogenet Genomics 19 (8):600-612

322. Shiraishi Y, Mizutani A, Mikoshiba K, Furuichi T (2003) Coincidence in dendritic clustering and synaptic targeting of homer proteins and NMDA receptor complex proteins NR2B and PSD95 during development of cultured hippocampal neurons. Mol Cell Neurosci 22 (2):188-201

323. Ghasemzadeh MB, Vasudevan P, Mueller C, Seubert C, Mantsch JR (2009) Neuroadaptations in the cellular and postsynaptic group 1 metabotropic glutamate receptor mGluR5 and Homer proteins following extinction of cocaine self-administration. Neurosci Lett 452 (2):167-171

324. Ghasemzadeh MB, Vasudevan P, Mueller C, Seubert C, Mantsch JR (2009) Region specific alterations in glutamate receptor expression and subcellular distribution following extinction of cocaine self-administration. Brain Res

325. Iasevoli F, Fiore G, Cicale M, Muscettola G, de Bartolomeis A Haloperidol induces higher Homer1a expression than risperidone, olanzapine and sulpiride in striatal sub-regions. Psychiatry Res 177 (1-2):255-260

326. Moore GJ, Bebchuk JM, Hasanat K, Chen G, Seraji-Bozorgzad N, Wilds IB, Faulk MW, Koch S, Glitz DA, Jolkovsky L, Manji HK (2000) Lithium increases N-acetyl-aspartate in the human brain: in vivo evidence in support of bcl-2's neurotrophic effects? Biol Psychiatry 48 (1):1-8

327. Du J, Quiroz J, Yuan P, Zarate C, Manji HK (2004) Bipolar disorder: involvement of signaling cascades and AMPA receptor trafficking at synapses. Neuron Glia Biol 1 (3):231-243

328. Rietschel M, Mattheisen M, Frank J, Treutlein J, Degenhardt F, Breuer R, Steffens M, Mier D, Esslinger C, Walter H, Kirsch P, Erk S, Schnell K, Herms S, Wichmann HE, Schreiber S, Jockel KH, Strohmaier J, Roeske D, Haenisch B, Gross M, Hoefels S, Lucae S, Binder EB, Wienker TF, Schulze TG, Schmal C, Zimmer A, Juraeva D, Brors B, Bettecken T, Meyer-Lindenberg A, Muller-Myhsok B, Maier W, Nothen MM, Cichon S (2010) Genome-wide association-, replication-, and neuroimaging study implicates HOMER1 in the etiology of major depression. Biol Psychiatry 68 (6):578-585

329. Mao LM, Zhang GC, Liu XY, Fibuch EE, Wang JQ (2008) Group I Metabotropic Glutamate Receptor-mediated Gene Expression in Striatal Neurons. Neurochem Res

330. Williams RS, Harwood AJ (2000) Lithium therapy and signal transduction. Trends Pharmacol Sci 21 (2):61-64

331. Tokuoka SM, Saiardi A, Nurrish SJ (2008) The Mood Stabilizer Valproate Inhibits both Inositol- and Diacylglycerol-signaling Pathways in Caenorhabditis elegans. Mol Biol Cell 19 (5):2241-2250

332. Ronesi JA, Huber KM (2008) Homer interactions are necessary for metabotropic glutamate receptor-induced long-term depression and translational activation. J Neurosci 28 (2):543-547

333. Manji HK, Chen G (2002) PKC, MAP kinases and the bcl-2 family of proteins as long-term targets for mood stabilizers. Mol Psychiatry 7 Suppl 1:S46-56

334. Wang JQ, Fibuch EE, Mao L (2007) Regulation of mitogen-activated protein kinases by glutamate receptors. J Neurochem 100 (1):1-11

335. Yuan PX, Huang LD, Jiang YM, Gutkind JS, Manji HK, Chen G (2001) The mood stabilizer valproic acid activates mitogen-activated protein kinases and promotes neurite growth. J Biol Chem 276 (34):31674-31683

336. Ramaprasad S, Ripp E, Pi J, Lyon M (2005) Pharmacokinetics of lithium in rat brain regions by spectroscopic imaging. Magn Reson Imaging 23 (8):859-863

337. Kammermeier PJ (2006) Surface clustering of metabotropic glutamate receptor 1 induced by long Homer proteins. BMC Neurosci 7:1

338. Mao L, Yang L, Tang Q, Samdani S, Zhang G, Wang JQ (2005) The scaffold protein Homer1b/c links metabotropic glutamate receptor 5 to extracellular signal-regulated protein kinase cascades in neurons. J Neurosci 25 (10):2741-2752

339. Hashimoto K, Sawa A, Iyo M (2007) Increased levels of glutamate in brains from patients with mood disorders. Biol Psychiatry 62 (11):1310-1316

340. Basselin M, Chang L, Bell JM, Rapoport SI (2006) Chronic lithium chloride administration attenuates brain NMDA receptor-initiated signaling via arachidonic acid in unanesthetized rats. Neuropsychopharmacology 31 (8):1659-1674

341. Basselin M, Chang L, Chen M, Bell JM, Rapoport SI (2008) Chronic Administration of Valproic Acid Reduces Brain NMDA Signaling via Arachidonic Acid in Unanesthetized Rats. Neurochem Res

342. Kim WY, Kim S, Kim JH (2008) Chronic microinjection of valproic acid into the nucleus accumbens attenuates amphetamine-induced locomotor activity. Neurosci Lett 432 (1):54-57

343. Umeda K, Suemaru K, Todo N, Egashira N, Mishima K, Iwasaki K, Fujiwara M, Araki H (2006) Effects of mood stabilizers on the disruption of prepulse inhibition induced by apomorphine or dizocilpine in mice. Eur J Pharmacol 553 (1-3):157-162

344. Ichikawa J, Chung YC, Dai J, Meltzer HY (2005) Valproic acid potentiates both typical and atypical antipsychotic-induced prefrontal cortical dopamine release. Brain Res 1052 (1):56-62

345. Sheng M, Kim E (2000) The Shank family of scaffold proteins. J Cell Sci 113 (Pt 11):1851-1856

346. O'Donnell KC, Gould TD (2007) The behavioral actions of lithium in rodent models: leads to develop novel therapeutics. Neurosci Biobehav Rev 31 (6):932-962

347. Jonathan Ryves W, Dalton EC, Harwood AJ, Williams RS (2005) GSK-3 activity in neocortical cells is inhibited by lithium but not carbamazepine or valproic acid. Bipolar Disord 7 (3):260-265

348. Robbins MJ, Critchlow HM, Lloyd A, Cilia J, Clarke JD, Bond B, Jones DN, Maycox PR (2008) Differential expression of IEG mRNA in rat brain following acute treatment with clozapine or haloperidol: a semi-quantitative RT-PCR study. J Psychopharmacol 22 (5):536-542

349. Lahti AC, Weiler MA, Holcomb HH, Tamminga CA, Cropsey KL (2009) Modulation of limbic circuitry predicts treatment response to antipsychotic medication: a functional imaging study in schizophrenia. Neuropsychopharmacology 34 (13):2675-2690

350. Gass N, Schwarz AJ, Sartorius A, Cleppien D, Zheng L, Schenker E, Risterucci C, Meyer-Lindenberg A, Weber-Fahr W (2013) Haloperidol modulates midbrain-prefrontal functional connectivity in the rat brain. Eur Neuropsychopharmacol 23 (10):1310-1319

351. Natesan S, Reckless GE, Nobrega JN, Fletcher PJ, Kapur S (2006) Dissociation between in vivo occupancy and functional antagonism of dopamine D2 receptors: comparing aripiprazole to other antipsychotics in animal models. Neuropsychopharmacology 31 (9):1854-1863

352. Jardemark K, Marcus MM, Shahid M, Svensson TH (2010) Effects of asenapine on prefrontal N-methyl-D-aspartate receptor-mediated transmission: involvement of dopamine D1 receptors. Synapse 64 (11):870-874

353. Franberg O, Marcus MM, Svensson TH (2012) Involvement of 5-HT2A receptor and alpha2-adrenoceptor blockade in the asenapine-induced elevation of prefrontal cortical monoamine outflow. Synapse 66 (7):650-660

354. Snigdha S, Idris N, Grayson B, Shahid M, Neill JC (2011) Asenapine improves phencyclidine-induced object recognition deficits in the rat: evidence for engagement of a dopamine D1 receptor mechanism. Psychopharmacology (Berl) 214 (4):843-853

355. Tait DS, Marston HM, Shahid M, Brown VJ (2009) Asenapine restores cognitive flexibility in rats with medial prefrontal cortex lesions. Psychopharmacology (Berl) 202 (1-3):295-306

356. de Greef R, Maloney A, Olsson-Gisleskog P, Schoemaker J, Panagides J (2011) Dopamine D2 occupancy as a biomarker for antipsychotics: quantifying the relationship with efficacy and extrapyramidal symptoms. AAPS J 13 (1):121-130

357. Morozova MA, Lepilkina TA, Rupchev GE, Beniashvily AG, Burminskiy DS, Potanin SS, Bondarenko EV, Kazey VI, Lavrovsky Y, Ivachtchenko AV (2013) Add-on clinical effects of selective antagonist of 5HT6 receptors AVN-211 (CD-008-0173) in patients with schizophrenia stabilized on antipsychotic treatment: pilot study. CNS Spectr:1-8

358. Suckling CJ, Murphy JA, Khalaf AI, Zhou SZ, Lizos DE, van Nhien AN, Yasumatsu H, McVie A, Young LC, McCraw C, Waterman PG, Morris BJ, Pratt JA, Harvey AL (2007) M4 agonists/5HT7 antagonists with potential as antischizophrenic drugs: serominic compounds. Bioorg Med Chem Lett 17 (9):2649-2655

359. de Bartolomeis A, Sarappa C, Buonaguro EF, Marmo F, Eramo A, Tomasetti C, Iasevoli F (2013) Different effects of the NMDA receptor antagonists ketamine, MK-801, and memantine on postsynaptic density transcripts and their topography: Role of Homer signaling, and implications for novel antipsychotic and pro-cognitive targets in psychosis. Prog Neuropsychopharmacol Biol Psychiatry 46:1-12